

## ABSTRACT

WREN, PATRICIA ANSLEY. SEDIMENT TRANSPORT MEASUREMENTS ON THE MID-CONTINENTAL SHELF IN ONSLOW BAY, NORTH CAROLINA. (under the direction of Lynn A. Leonard and Lonnie Leithold.)

Long-term in situ measurements have been made on the mid-continental shelf in Onslow Bay, NC to determine the frequency and direction of bottom sediment movement and the processes responsible for bottom sediment motion. As part of the Coastal Ocean Research and Monitoring Program (CORMP) at the University of North Carolina at Wilmington, a quadrapod frame with a downward looking Pulse-Coherent Acoustic Doppler Profiler (PC-ADP) and an upward looking Acoustic Doppler Current Profiler (ADCP) has been maintained on the continental shelf at approximately 30 m depth since May of 2000. The instruments are moored 27 nautical miles off the coast of Wilmington, North Carolina in Onslow Bay, adjacent to a productive marine hardbottom. Simultaneous measurements of flow velocities from the surface to the seabed, along with acoustic backscatter measurements, have been obtained. Measurements of seabed elevation, temperature, conductivity, and pressure were also collected at the site. Bed stresses due to wave-current interactions are calculated using a bottom boundary layer model (Styles and Glenn, 2002). Wave-current interactions resulted in shear stresses at the sediment-water interface that exceeded the critical threshold for sediment movement over 50% of the time during a climatological average year. Sediment transport was been shown to occur during four different types of events at the site: 1) small to moderate northerly wind events 2) Gulf Stream Intrusion events 3) strong southerly wind events associated with the passage of frontal systems 4) the passage of tropical storm systems. Over the course of a year the total net suspended sediment flux at 1 mab was in the positive along-shelf direction (southwest) and in the negative across-shelf direction (onshore), where there was several times more *net* transport in the onshore direction than the along-shelf direction. Three mechanisms leading to significant sediment transport on the mid-continental shelf have been indentified: 1) wave-current interactions 2) subtidal currents associated with sustained wind-driven flows and the intrusion of Gulf Stream water on the shelf 3) infragravity

waves. Subtidal currents played a key role in the sediment transport during all types of events. Wind driven subtidal currents were important in determining the magnitude and direction of sediment transport during storm events, while subtidal currents associated with a Gulf Stream intrusion event combined with fair-weather swell resulted in accretion at the site of 3 cm over a three week period. The results show that a moderate northeasterly wind event with sufficient duration to generate wind driven subtidal flows resulted in an order of magnitude more sediment transport ( $20,237 \text{ g cm}^{-2}$ ) than a similar northerly wind event and the southerly wind event without developed wind-driven flows. These two events resulted in similar amounts of sediment transport of  $3,600 \text{ g cm}^{-2}$  and  $3,061 \text{ g cm}^{-2}$ , respectively. The passage of a hurricane resulted in an order of magnitude more sediment transport than the moderate northeasterly wind event, on the order of  $240,000 \text{ g cm}^{-2}$ . Shear velocities during the passage of Hurricane Isabel resulted in the largest bed shear stresses ( $\sim 300 \text{ dynes cm}^{-2}$ ) on record. Field measurements in the bottom boundary layer were compared with the bblm generated current profiles during moderate wind events and Hurricane Isabel. In addition, the suspended sediment concentration profiles from the model were compared with the ABS profile measurements to verify shape and magnitude as the storms increased and waned. In general, there was good agreement between the measured and model derived current profiles, and between suspended sediment measurements and the model concentration profiles for both large and small-scale events that occurred at the site.

**SEDIMENT TRANSPORT MEASUREMENTS ON THE MID-CONTINENTAL  
SHELF IN ONSLOW BAY, NORTH CAROLINA**

by  
**PATRICIA ANSLEY WREN**

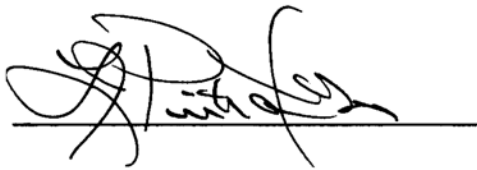
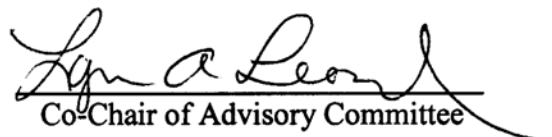
A dissertation submitted to the Graduate Faculty of  
North Carolina State University  
in partial fulfillment for the  
requirements for the Degree of  
Doctor of Philosophy

**MARINE SCIENCE**

Raleigh

2004

**APPROVED BY:**

A handwritten signature in black ink, appearing to read 'P. Ansley Wren', written over a horizontal line.A handwritten signature in black ink, appearing to read 'Stephen M. Bigner', written over a horizontal line.A handwritten signature in black ink, appearing to read 'Elena L. M. d.', written over a horizontal line.  
Co-chair of Advisory CommitteeA handwritten signature in black ink, appearing to read 'Lynn A. Leonard', written over a horizontal line.  
Co-Chair of Advisory Committee

*This dissertation is dedicated to my mother, Patricia P.Hollis, who taught me, through her words of wisdom and by the example of her life, the infinite value of education.*

## **BIOGRAPHY**

I was born in Columbia, South Carolina on September 28, 1973. I graduated from Spring Valley High School in Columbia in 1991. I attended the University of South Carolina and graduated with a Bachelor's of Science in civil engineering in 1996. I then moved to Raleigh, NC to begin a career in structural engineering at GKC Associates, but soon realized this was not my life long pursuit. I decided to pursue a field that I had always been interested in, and applied to the graduate program in Marine Science at NC State University. I was soon after accepted into the UNCW/NCSU Cooperative Ph.D. Program in Marine Science where I was able to conduct the research presented in this dissertation.

## **ACKNOWLEDGEMENTS**

I would like to thank my co-advisor at UNCW, Dr. Lynn Leonard, for making my time at UNCW a positive and memorable experience. I thank Lynn for all the opportunities she gave me while at UNCW which ranged from attending regional, national, and international conferences to becoming a certified scientific diver. Lynn was always there to give me positive encouragement and support whenever I needed it (especially during the writing of this dissertation), and has been a great role model and mentor to me over the past 41/2 years.

I thank my co-chair at NCSU, Dr. Lonnie Leithold, and my committee members, Dr. Len Pietrafesa, and Dr. Fred Bingham. I would also like to thank my previous advisor at NC State, Dr. Tom Drake, who is now at the Office of Naval Research. He graciously provided my first research opportunities at NC State at the USACE FRF in Duck, NC, and helped me to transfer into the UNCW/NCSU Cooperative Ph.D. Program.

I thank the UNCW Graduate School for employing me over the past four years while I have been at UNCW, and for helping me to attend numerous conferences. Donna, Alnita, and Nancy have made my life easier in so many ways, and they will be in some of my fondest memories of my graduate school experience at UNCW.

I would like to thank Heyward Key for his constant support and unconditional patience, kindness, and encouragement that he has shown to me through it all.

Finally, I thank my close friends and family. Mom, Bud, Carrie, and Joanna – thanks for always listening, for always encouraging, and believing in me. You have unwearingly helped me pursue my dream of studying the ocean.

## TABLE OF CONTENTS

List of Tables .....	viii
List of Figures .....	ix
Chapter 1 .....	1
1.1 Background .....	7
1.2 Physical processes in the bottom boundary layer .....	9
Chapter 2 .....	12
2.1 Introduction .....	12
2.2 Methods .....	15
2.2.1 Study site .....	15
2.2.2 Instrumentation .....	18
2.2.3 Bottom boundary layer model .....	20
2.2.4 Data analysis .....	26
2.3 Results .....	28
2.3.1 Atmospheric forcing .....	28
2.3.2 Tides and physical characteristics .....	29
2.3.3 Sediment Transport .....	31
2.4 Discussion .....	53
2.4.1 Sediment flux .....	53
2.4.2 Sediment-suspension event forcing .....	54
2.4.3 Mean circulation .....	59

2.5 Conclusions.....	62
Chapter 3 .....	64
3.1 Introduction.....	64
3.2 Field Experiment.....	66
3.2.1 Study site.....	66
3.2.2 Instrumentation and data collected .....	68
3.2.3 Data analysis .....	70
3.3 Results.....	72
3.3.1 Average wave, tidal, and physical properties .....	72
3.3.2 Currents.....	73
3.3.3 Sediment transport .....	76
3.3.4 Field measurements vs. model profiles.....	95
3.4 Discussion.....	108
3.4.1 Seabed altimetry and model predicted ripples .....	111
3.5 Conclusions.....	112
Chapter 4 .....	114
4.1 Introduction.....	114
4.2 Field Experiment.....	117
4.2.1 Instrumentation .....	117
4.3 Results.....	120
4.3.1 The hurricane .....	120



4.3.2 Bottom boundary layer dynamics .....	123
4.3.3 Spectral analysis.....	141
4.4 Discussion.....	147
4.4.1 Sediment transport .....	147
4.4.2 Seabed altimetry data.....	152
4.5 Conclusions.....	155
 Chapter 5 .....	 157
5.1 Conclusions.....	157
5.2 Future efforts.....	162
REFERENCES .....	163

## LIST OF TABLES

Table 1. Deployments .....	25
Table 2. Comparison of mean seasonal conditions for the year of record.....	33
Table 3. Apparent sediment flux at 1 mab.....	51
Table 4. Mean and maximum velocity magnitudes for the flow components.....	74
Table 5. Maximum measurements of atmospheric, hydrodynamic, and sediment mobilization characteristics during three wind events. Bottom orbital velocities ( $U_b$ ) and mean currents are reported at 1 meter above the bed.....	75

## LIST OF FIGURES

<b>Figure 1.</b> Onslow Bay is located on the southeastern coast of North Carolina and is bounded by Cape Lookout to the northeast, Cape Fear to the southwest, and by the Gulf Stream and continental slope to the east. OB27 marks the study site where the instrumentation frame is located. FPT (Frying Pan Tower) marks the NOAA C-Man station where the wind and wave data were collected. ....	5
<b>Figure 2 (a).</b> Elevation drawing of frame with instrumentation <b>(b).</b> Plan view drawing of frame with instrumentation.....	6
<b>Figure 3.</b> Underlying geology of the hardbottom reef at the study site .....	14
<b>Figure 4.</b> Comparison of seasonal wind direction from the year of study to the past 10 years. Winds during the study period agree with the climatology of the area. ....	30
<b>Figure 5.</b> Atmospheric pressure, wind velocity, low-pass filtered sea-level, and mean and subtidal along- and across-shelf currents from April 27 – May31, 2000. ....	34
<b>Figure 6.</b> April 27 – May31, 2000 mean current speed, bottom orbital velocities, wave-current shear velocities, measured ABS, and <i>relative</i> suspended sediment flux magnitude. The black dashed line in the third panel is the threshold for sediment movement, the green line represents the threshold for when sediments start to be suspended from the seabed, and the red is the threshold for full suspension transport. ....	35
<b>Figure 7.</b> April 27 – May31, 2000 seabed response during the spring deployment showing the bblm generated ripple height and steepness, measured seabed elevation, calculated bedload transport rates, and direction based on model calculated shear stresses.....	36
<b>Figure 8.</b> Atmospheric pressure, wind velocity, low-pass filtered sea-level, and mean and subtidal along- and across-shelf currents during the summer deployment.....	38
<b>Figure 9.</b> June 1 – August 31, 2000 mean current speed, bottom orbital velocities, wave-current shear velocities, measured ABS, and <i>relative</i> suspended sediment flux magnitude. The black dashed line in the third panel is the threshold for sediment movement, the green line represents the threshold for when sediments start to be suspended from the seabed, and the red is the threshold for full suspension transport .....	39
<b>Figure 10.</b> June 1 – August 31, 2000 - seabed response showing the bblm generated ripple height and steepness, measured seabed elevation, calculated bedload transport rates, and direction based on model calculated shear stresses.....	41

<b>Figure 11.</b> Atmospheric pressure, wind velocity, low-pass filtered sea-level, and mean and subtidal along- and across-shelf currents during the fall deployment.....	43
<b>Figure 12.</b> Autumn 2000 deployment - mean current speed, bottom orbital velocities, wave-current shear velocities, measured ABS, and <i>relative</i> suspended sediment flux magnitude. The black dashed line in the third panel is the threshold for sediment movement, the green line represents the threshold for when sediments start to be suspended from the seabed, and the red is the threshold for full suspension transport.....	44
<b>Figure 13.</b> Autumn 2000 deployment - seabed response showing the bblm generated ripple height and steepness, measured seabed elevation, calculated bedload transport rates, and direction based on model calculated shear stresses.....	46
<b>Figure 14.</b> Atmospheric pressure, wind velocity, low-pass filtered sea-level, and mean and subtidal along- and across-shelf currents during the winter deployment.....	48
<b>Figure 15.</b> Winter 2001 deployment - mean current speed, bottom orbital velocities, wave-current shear velocities, measured ABS, and <i>relative</i> suspended sediment flux magnitude. The black dashed line in the third panel is the threshold for sediment movement, the green line represents the threshold for when sediments start to be suspended from the seabed, and the red is the threshold for full suspension transport.....	49
<b>Figure 16.</b> Winter 2001 deployment - seabed response showing the bblm generated ripple height and steepness, measured seabed elevation, calculated bedload transport rates, and direction based on model calculated shear stresses.....	52
<b>Figure 17.</b> (a.) Along-shelf and (b.) across-shelf spectra for all data at 1 mab during the study .....	55
<b>Figure 18.</b> Spectra of the acoustic backscatter signal from the PC-ADP at 1 mab for all data during the study.....	57
<b>Figure 19.</b> (a.) Coherence between the along-shelf current and the acoustic backscatter signal at 1 mab. (b.) Coherence between the across-shelf current and the acoustic backscatter signal at 1 mab .....	58
<b>Figure 20.</b> May northerly wind event (a) mean current speed at 1 mab (b) bottom orbital velocities (c) wave-current and current bed shear stresses (d) acoustic backscatter signal (e) along and across-shelf subtidal currents .....	77
<b>Figure 21.</b> May northerly wind event: (a) model calculated ripple height and (b) ripple steepness (c) measured seafloor elevation (d) bedload transport rate.....	79

<b>Figure 22.</b> June 2 – 26, 2000: the 3 individual beams of the PCADP all show a gradual increase in seabed elevation during the Gulf Stream intrusion event.....	81
<b>Figure 23.</b> Pulse-coherent Acoustic Doppler Profiler bottom temperature record from May 12- June 26, 2000. The Gulf Stream intrusion event occurred from approximately June 3 – June 23, 2000.....	82
<b>Figure 24.</b> June 2 – 26, 2000 physical data. (a) wind velocity (b) significant wave height (c) dominant wave period (d) mean current velocity (e) subtidal flow speed .....	84
<b>Figure 25.</b> June 2 – June 26, 2000 (a) mean current speed at 1 mab (b) bottom orbital velocities (c) wave-current and current bed shear stresses (d) acoustic backscatter signal (e) along and across-shelf subtidal currents. The red line in the third panel represents the threshold for sediment movement.....	85
<b>Figure 26.</b> June 2 – June 26, 2000: (a) model calculated ripple height and (b) ripple steepness (c) measured seafloor elevation (d) bedload transport rate.....	87
<b>Figure 27.</b> September northerly wind event (a) mean current speed at 1 mab (b) bottom orbital velocities (c) wave-current and current bed shear stresses (d) acoustic backscatter signal (e) along and across-shelf subtidal currents .....	89
<b>Figure 28.</b> September northerly wind event: (a) model calculated ripple height and (b) ripple steepness (c) measured seafloor elevation (d) bedload transport rate .....	91
<b>Figure 29.</b> November southerly wind event (a) mean current speed at 1 mab (b) bottom orbital velocities (c) wave-current and current bed shear stresses (d) acoustic backscatter signal (e) along and across-shelf subtidal currents .....	93
<b>Figure 30.</b> November southerly wind: (a) model calculated ripple height and (b) ripple steepness (c) measured seafloor elevation (d) bedload transport rate.....	94
<b>Figure 31. (a.)</b> Burst 15 – Pre-storm conditions before September event <b>(b).</b> Burst 6 – Pre-storm conditions before November event .....	96
<b>Figure 32.</b> Burst 30 – Critical conditions are reached at the onset of September event. The measured and modeled current velocity profiles and a comparison between the sediment concentration profiles the ABS measurements are shown in the top three graphs. The bblm calculated sediment transport profile and suspended sediment grain sizes of are shown in the bottom two graphs .....	98
<b>Figure 33.</b> Burst 8 –Critical conditions are reached at the onset of November event. The measured and modeled current velocity profiles and a comparison between the sediment concentration profiles the ABS measurements are shown in the top three	

graphs. The bblm calculated sediment transport profile and suspended sediment grain sizes of are shown in the bottom two graphs .....	99
<b>Figure 34.</b> Burst 37 – Peak of September northerly wind event. The measured and modeled current velocity profiles and a comparison between the sediment concentration profiles the ABS measurements are shown in the top three graphs. The bblm calculated sediment transport profile and suspended sediment grain sizes of are shown in the bottom two graphs .....	101
<b>Figure 35.</b> Burst 10 – Peak of November southerly wind event. The measured and modeled current velocity profiles and a comparison between the sediment concentration profiles the ABS measurements are shown in the top three graphs. The bblm calculated sediment transport profile and suspended sediment grain sizes of are shown in the bottom two graphs .....	102
<b>Figure 36.</b> Burst 55 – Waning down of September event. The measured and modeled current velocity profiles and a comparison between the sediment concentration profiles the ABS measurements are shown in the top three graphs. The bblm calculated sediment transport profile and suspended sediment grain sizes of are shown in the bottom two graphs .....	104
<b>Figure 37.</b> Burst 18 - Waning down of November event. The measured and modeled current velocity profiles and a comparison between the sediment concentration profiles the ABS measurements are shown in the top three graphs. The bblm calculated sediment transport profile and suspended sediment grain sizes of are shown in the bottom two graphs .....	105
<b>Figure 38 (a.)</b> Burst 75 – Post-storm conditions after September event. The top graph shows the current profiles and the bottom graph indicates that there are still suspended sediments being measured in the lower water column. <b>(b.)</b> Burst 39 - Post-storm conditions after November event. The top graph shows the current profiles and the bottom graph indicates that there are less suspended sediments being measured in the lower water column than after the September event due to the low subtidal currents .....	106
<b>Figure 39.</b> Onslow Bay is located between Cape Lookout and Cape Fear, NC. OB27 marks the study site, 27 miles off the coast of directly east of Wilmington, NC. FPT is the location of the NOAA C-man station where wind and wave data were collected. Hurricane Isabel made landfall northeast of the study site.....	116
<b>Figure 40.</b> NOAA satellite imagery of Hurricane Isabel as the storm approached the NC coast on September 18 <sup>th</sup> . The red dot indicates the approximate location of the study site (for visual purposes only) .....	118

- Figure 41.** Hourly wind and wave data were obtained from the NOAA Frying Pan Tower C-Man station (<http://www.ndbc.noaa.gov/FSN7>) during Hurricane Isabel. The wave buoy failed during the peak storm conditions on September 18<sup>th</sup> .....122
- Figure 42.** The top two panels show the Acoustic Doppler Current Profiler velocity data. The bottom two panels show the burst-averaged currents from the Pulse-Coherent Acoustic Doppler Profiler .....125
- Figure 43.** Hurricane Isabel (a) mean current speed at 1 mab (b) bottom orbital velocities (c) wave-current and current bed shear stresses (d) acoustic backscatter signal (e) along and across-shelf subtidal currents .....126
- Figure 44.** Comparison of model calculated velocity profile with PCADP measured velocity profile in the bottom boundary layer. Burst 5 represents pre-storm conditions at 10:00 UTC on September 15<sup>th</sup> .....127
- Figure 45.** Hurricane Isabel: model calculated (a) ripple height and (b) ripple steepness (c) measured seabed altimetry data (d) calculated bedload transport rates .....128
- Figure 46.** Comparison of model calculated velocity profile with PCADP measured velocity profile in the bottom boundary layer. ABS and sediment concentrations are also shown along with the model calculated sediment transport profile. The bar graph shows what sediments comprise the total amount of the suspended sediments. Burst 9 is at 18:00 UTC on the 15<sup>th</sup> and is the first burst that model calculated sediment transport occurred.....130
- Figure 47.** Comparison of model calculated velocity profile with PCADP measured velocity profile in the bottom boundary layer. ABS and sediment concentrations are also shown along with the model calculated sediment transport profile. The bar graph shows sediments are mostly fine sands, with a small amount of medium sand being suspended. There is an order of magnitude more total suspended sediment in the bottom boundary layer at 20:00 UTC on the 16<sup>th</sup> than 1800 UTC on the September 15<sup>th</sup> .....131
- Figure 48.** Peak sediment transport conditions during burst 35 at 22:00 UTC on September 17<sup>th</sup>. Comparison of model calculated velocity profile with PCADP measured velocity profile in the bottom boundary layer. ABS and sediment concentrations are also shown along with the model calculated sediment transport profile. The bar graph shows sediments being suspended are mostly fine sand to medium sands.....135
- Figure 49.** Burst 50 occurred at 0400 UTC on September 19<sup>th</sup>. The bblm indicates no sediment transport is occurring at this time, although the ABS measurements still show elevated levels suggesting there are still suspended sediment in the bottom boundary layer .....138

<b>Figure 50.</b> Burst 60 was at 00:00 UTC on September 20 <sup>th</sup> . Both the model and measurements indicate that the sediment transport event is over at this time. Velocity profiles show good agreement with weak currents .....	140
<b>Figure 51.</b> Spectral analysis of raw PCADP data at 1 mab show high energy levels in the swell frequency bands before the storm and more energy in the local wind wave bands during the storm. Along-shelf subtidal flows generated when winds from hurricane directly impacted the site show up well in the along-shelf spectra during the storm.....	142
<b>Figure 52 (a.)</b> The raw PC-ADP across-shelf velocity data at 1 mab from a pre-storm burst of data on 15 September. Infragravity oscillations are shown in black. <b>b.)</b> The raw acoustic backscatter signal (in counts) during the same burst of data with infragravity waves shown in black.....	145
<b>Figure 53 (a.)</b> The raw PC-ADP across-shelf velocity data at 1 mab for from a burst of data collected during the storm at 0200 UTC on 18 September. Infragravity oscillations are shown in black. <b>(b.)</b> The raw acoustic backscatter signal (in counts) during the same burst of data with infragravity waves shown in black Another longer period oscillation due to wave group interactions can also be seen in the signal.....	146
<b>Figure 54.</b> Compass plot showing direction of suspended sediment flux that occurred at the site throughout sediment transport event .....	150
<b>Figure 55.</b> Pre- and post boxcores are aligned with the seabed elevation data. The storm layer is visible in the post-storm core and there was 1 cm of net erosion from pre- storm to post storm.....	151
<b>Figure 56.</b> A flow diagram showing the potential complex interactions that can occur on the mid-shelf in Onslow Bay, NC.....	158



# Chapter I

## Introduction

It is well documented that storm driven processes dominate sediment transport on many continental shelves and are an important factor in coastal change (Madsen *et al.*, 1993). The coastal response to these short-lived storm events is the most observable, and classical models describe these changes in terms of onshore-offshore sediment exchange between the intertidal beach and outer regions of the surf zone. The surf zone-beach realm, however, is rarely a closed system (Wright, 1995). Surf zones and beaches constitute the vertically thin and narrow edge of a much deeper and wider shelf system. To understand long-term and large-scale coastal changes, the physical processes that dominate the entire shelf system must be understood. In areas experiencing intense coastal development, such as southeastern North Carolina, an understanding of the physical and geological processes controlling offshore sediment movement is fundamental to predicting shoreline stability.

As part of the Coastal Ocean Research and Monitoring Program (CORMP) at the University of North Carolina at Wilmington, an instrumented quadrapod frame has been maintained on the mid-continental shelf since April, 2000. This multidisciplinary study was initiated in 1999 and funded by the National Oceanic and Atmospheric Administration to monitor the physical, geological, chemical, and biological processes occurring on the continental shelf in the northern portion of the South Atlantic Bight during fair-weather and storm events. This specific part of the study focuses on the

hydrodynamics of the bottom boundary layer and the associated sediment transport on the mid-continental shelf. The study site is located at the transition between the inner and mid-continental shelf in Onslow Bay, North Carolina, approximately 27 miles offshore of Wrightsville Beach, NC at a depth of approximately 30 m (Fig. 1). Instrumentation attached to the frame includes a downward looking Sontek/YSI Pulse-Coherent Acoustic Doppler Profiler and an upward looking RDI Acoustic Doppler Current Profiler (Fig.2). Simultaneous measurements of flow velocities from the surface to the seabed, along with acoustic backscatter profiles and seabed altimetry data have been collected. The instrumented frame is located on an area of fine sands, where underlying these fine sands are coarse sands, which are exposed as coarse sand bodies around the fine sand areas. The coarse sand bodies are covered with ripples and exposed and re-covered as the fine sands move around them and create a definitive contrast between the two. This study identified the different mechanisms resulting in the transport of these two sand types. The frame was also adjacent to a biologically productive marine hardbottom area, thus this study provided preliminary data on the effect that the hardbottom may have on sediment transport. The study area has also been used for other geologic (Riggs *et al.*, 1996; 1998) and biological studies (Renaud *et al.* 1996; 1997), therefore, there are existing data about the underlying geology of the site and the hardbottom reef, and of the organisms that inhabit the area. These studies have shown that the sediment distribution of the fine sands on and around the hardbottom reef can influence the entire ecological community (Renaud, 1996; 1997). The study site is unique in the fact that it is exposed to frequent hurricanes during the late summer and early fall, as well as nor'easter storms that can occur in the late spring. Gulf Stream effects have also been shown to influence

the site during the summer months (Pietrafesa *et al.*, 1985) and therefore, the effects that the Gulf Stream has on the sediment transport at the site were examined, as well. The work presented here is based on data collected during this project spanning from April, 2000 to September, 2003.

Chapter 2 is a broad prospective of the sediment transport that occurred at the site over an annual cycle, examining the distinct seasonality of sediment transport at the site. The forcing mechanisms that caused sediment motion thresholds to be exceeded were determined, and the rates and direction of sediment transport at the mid-shelf site were determined for each season.

Chapter 3 identifies and quantifies the magnitude, frequency, and duration of physical forcing mechanisms resulting in sediment mobility at the study site from May – December, 2000. Three moderate wind events occurred resulting in measurable sediment transport at the site, along with a Gulf Stream intrusion event during the summer of 2000. Measured current and acoustic backscatter signal profiles in the bottom boundary layer were compared to predicted current and concentration profiles from a bottom boundary layer model (Styles and Glenn, 2000; 2002).

Chapter 4 focuses on sediment transport processes that occurred on the mid-shelf during the close passage of Hurricane Isabel. Large amounts of bedload and suspended sediment transport occurred over a four day period as the storm approached and passed by the site from September 15 – September 19<sup>th</sup>, 2003. Measured current and acoustic backscatter signal profiles in the bottom boundary layer are used to verify the current and concentration profiles produced by the bottom boundary layer model during an event of this magnitude. Seabed altimetry data, bbl model output, bedload transport calculations,

and boxcores are used to document changes in the seafloor associated with storm passage.

Lastly, Chapter 5 summarizes the sediment transport processes that occurred on the mid-shelf in Onslow Bay over the duration of the study. Future research efforts for sediment transport data collection are discussed.

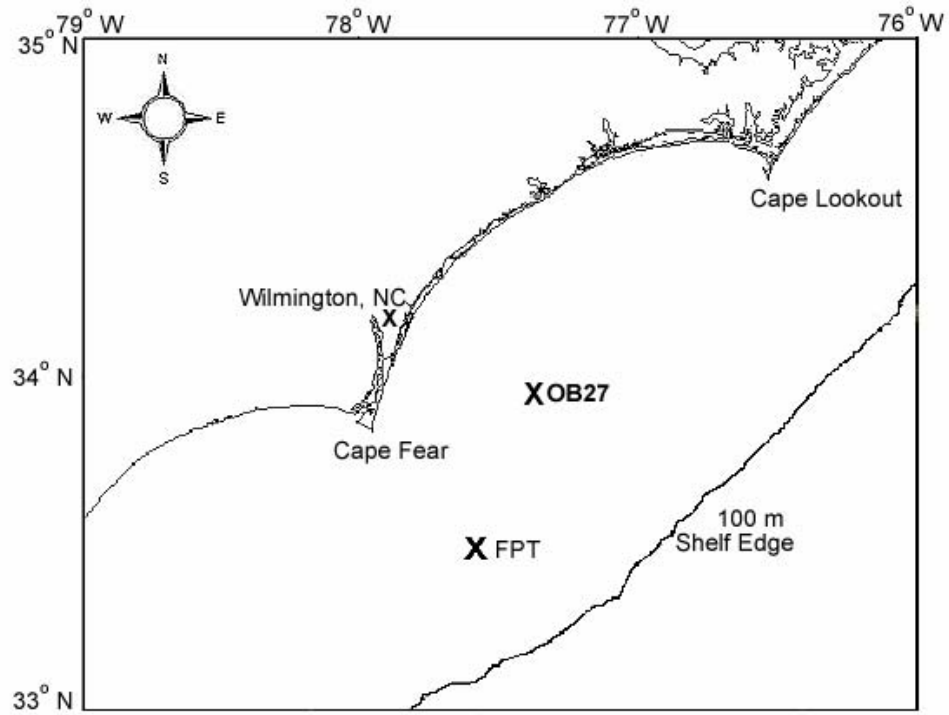


**Figure 1.** Onslow Bay is located on the southeastern coast of North Carolina and is bounded by Cape Lookout to the northeast, Cape Fear to the southwest, and by the Gulf Stream and continental slope to the east. OB27 marks the study site where the instrumentation frame is located. FPT (Frying Pan Tower) marks the NOAA C-Man station where the wind and wave data were collected.

a.)

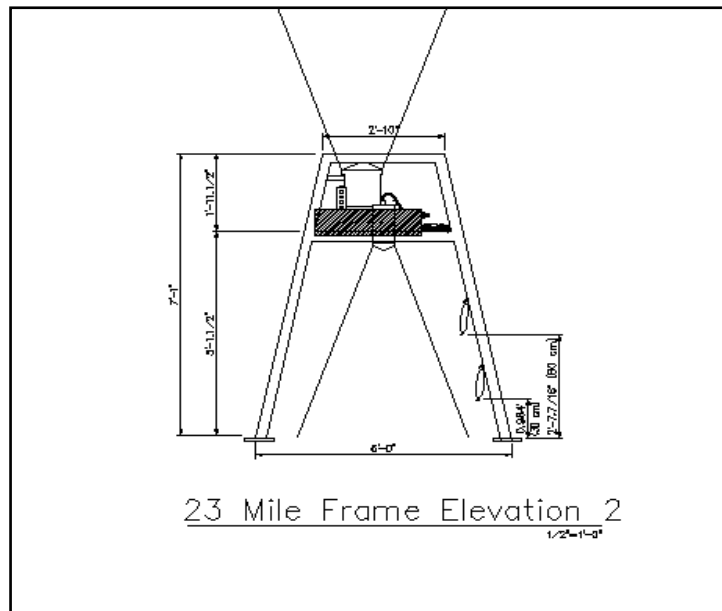


**Figure 2 (a.)** Elevation drawing of frame with instrumentation

b.)

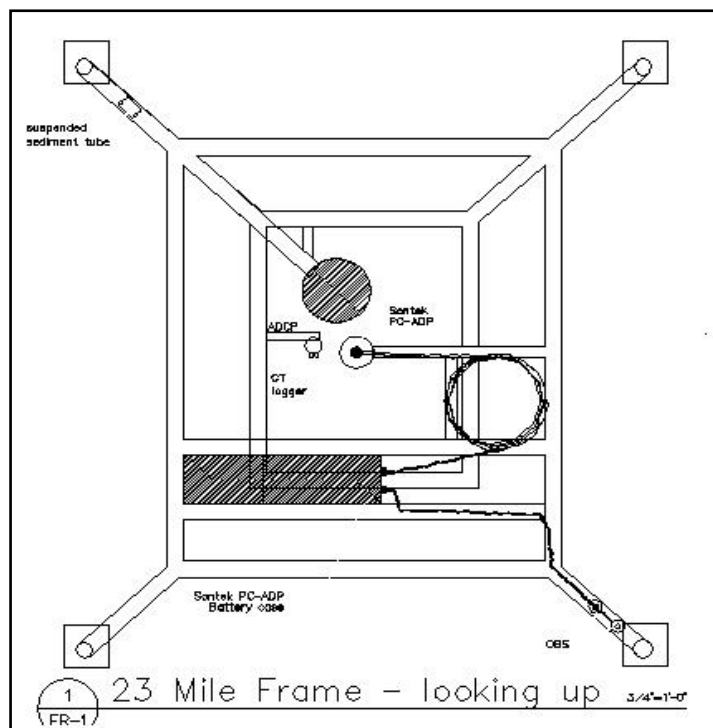


**Figure 2 (b.)** Plan view drawing of frame with instrumentation

## 1.2 Background

Knowledge of bottom boundary layer processes and how the hydrodynamics interact with the seabed has improved drastically over the past couple of decades. With improvements in technology, more accurate and precise instrumentation has become available for field measurements, and computer models are able to handle larger data sets and more complicated algorithms for predicting and simulating sediment transport. Field studies have been a critical component leading to an increased understanding of the processes that take place in this complicated environment. Many of these studies have been associated with large, multi-investigator programs such as Coastal Ocean Dynamics Experiment (CODE), Sediment Transport Events on Shelves and Slopes (STRESS), and the STRATAFORM project (STRATA FORMation on Margins), which took place on the Eel continental margin in Northern California (Cacchione *et al.*, 1999; Ogston and Sternberg, 1999; Wright *et al.*, 1999). Additional work has been undertaken on the U.S. mid-Atlantic shelf (Wright *et al.*, 1986; Wright *et al.*, 1991; Wright *et al.*, 1994; Madsen *et al.*, 1993), as well as on shelves off the coast of Washington and Oregon (Smith and Hopkins, 1972; Sternberg, 1986), New York (Niedoroda *et al.*, 1984; Swift *et al.*, 1985; Harris, 2003), Canada (Li and Amos, 1999) and Europe (Williams and Rose, 2001). These studies show that on many shelves the dominant mechanism for sediment transport are energetic waves interacting synergistically with wind-driven, slowly-varying currents. Bedforms and their interactions with boundary layer hydrodynamics also have been shown to be important in sediment transport processes (Wiberg and Harris, 1994; Wright, 1995; Li and Amos, 1999, Traykovski *et al.*, 1999). In addition, these types of studies

help to verify computer models and mathematical and physical theories, and also help scientists to observe “first hand” the processes that they are analyzing.

In Onslow Bay, NC, there have been several studies that have documented the physical oceanographic processes and circulation patterns on the shelf (Atkinson *et al.*, 1976; Blanton and Pietrafesa, 1978; Bane and Brooks, 1979; Pietrafesa and Janowitz, 1979; Janowitz and Pietrafesa, 1980; Pietrafesa and Janowitz, 1980; Singer *et al.*, 1980; Hoffman *et al.*, 1981; Pietrafesa, 1983; Pietrafesa *et al.*, 1985; Pietrafesa, 1989; Cione *et al.*, 1993; Xie *et al.*, 1997). These studies indicate that Onslow Bay is dominated by three principal forcing mechanisms: winds and related air-sea fluxes, tides, and the Gulf Stream, and that the magnitudes of these mechanisms change relative to the location of interest on the shelf. Other research efforts undertaken in Onslow Bay suggest that introduction of new sediment to this system is negligible due to limited fluvial inputs (Blackwelder *et al.* 1982). Milliman (1972) classified the Onslow Bay shelf sediment cover as residual; that is, derived from the erosion of underlying sediment and rocks. Additionally, a number of geophysical surveys have been conducted to describe the geologic framework of the inner to middle shelf of Onslow Bay (Cleary and Pilkey, 1968; Blackwelder *et al.*, 1982; Riggs *et al.*, 1998). These surveys have been coupled with descriptions of substrate characteristics and bedform morphologies, but little attempt has been made to measure bottom boundary layer hydrodynamics and associated sediment transport processes, with the exception of Gutierrez (2002) and Thielert *et al.* (2001). These studies have been useful in analyzing the dominant sediment transport processes on the inner portion of the shelf, and have shown that cross-shelf sediment transport is occurring and sediments are being moved from the shoreface to the inner



shelf region. The proposed study is located further offshore and will help to determine if there is a potential for sediments to be transported beyond the inner shelf.

## **1.2 Physical processes in the bottom boundary layer**

On the inner to mid-continental shelf, near-bottom flows are a combination of waves and slowly varying currents (Madsen, 1993). Due to friction with the seafloor and the “no-slip” condition, a constant shear bottom boundary layer is formed. The velocity profile in the bottom boundary layer is turbulent and varies logarithmically with depth. Due to the oscillatory nature of waves, the wave boundary layer has only a half of a wave period to develop, therefore this results in a thin boundary layer, on the order of a few cm. Within this boundary layer, the wave orbital velocity changes from the free stream velocity to zero at the boundary. The change in velocity with depth, or shear, is large within a thin boundary layer (such as for waves), and this large shear produces large shear stresses on the seabed. A slowly varying current, on the other hand, will develop a boundary layer on the order of several meters thick. In the thicker current boundary layer, the shear is much less throughout the several meters, and therefore currents will produce a smaller shear stress on the bottom than waves for the same magnitude of flow. In turbulent boundary layers, the shear velocity,  $u_*$ , is related to the shear stress on the seabed,  $\tau_b$ , by:

$$\rho u_*^2 = \tau_b$$

where  $\rho$  is water density. The shear velocity,  $u_*$ , can be calculated by measuring the flow,  $u(z)$  at any depth,  $z$ , within the logarithmic boundary layer by the equation known as “the law of the wall” where

$$u(z) = (u_* \ln(z/z_0)) / \kappa$$

and  $z_0$  is known as the hydraulic roughness length where  $u(z)$  equals zero, and is given by the vertical intercept in the extrapolated logarithmic velocity profile,  $\kappa$  is von Karman's constant (0.41) and  $z$  is the distance above the seabed. It is necessary to account for both waves and currents, and the interactions between the two, when calculating bed shear stresses. Waves and currents act synergistically in the bottom boundary layer, producing larger bottom stresses than if they were added together. There is still a limited understanding of how waves and current boundary layers interact, and how wave energies are dissipated within the small (mm thick) wave boundary layer. Theoretical models have been created for this purpose and computer models have been written and improved upon over the past several decades as the knowledge of the hydrodynamics in the bottom boundary layer (bbl) has increased (Smith, 1977; Grant and Madsen, 1979; Glenn and Grant, 1987; Madsen and Wikramanayake, 1991; Wiberg, 1995). There have been a limited number of field verification studies for these models, and one of the objectives in the Chapter 2 will be to address this issue. In order to use a bottom boundary layer model (bbm) to estimate shear stresses on the seabed, such as the Styles and Glenn (2002) bbm used in this study, bottom wave orbital velocities and currents in the bbl are needed. Bottom wave orbital velocities can be estimated from linear wave theory; however, bottom current velocities are slightly harder to obtain. In order to get quality current data within the current boundary layer, *in situ* current velocity measurements are needed. These types of measurements are becoming more common today with the improvements in technology and less intrusive instrumentation. The instrumentation used in this study measured a continuous profile of current velocity measurements throughout the bottom 1.5 meters of the boundary layer using a non-

intrusive acoustic signal. Wave parameters and a mean current at 1 mab were input into a process-oriented bottom boundary layer model which solves the turbulent closure model for the wave-current interactions, and calculates the wave-current shear velocities. These wave-current shear velocities on the bottom determine the magnitude of sediment resuspension. If the critical shear velocity for a sand grain is reached, the sand grain will start to move. The sediments in the seabed are first transported by bedload transport; however, as bed shear stresses increase, the turbulent eddies in the flow vertically mix the sediments in the water column and sediments begin to be picked up into the current flow and carried as suspended load.

## Chapter II

### **Long-term sediment transport measurements and modeling on the mid-continental shelf: Onslow Bay, North Carolina**

#### **2.1 Introduction**

A bottom quadrupod frame has been maintained on the mid-continental shelf since April of 2000 as part of the Coastal Ocean Research and Monitoring Program (CORMP) at the University of North Carolina at Wilmington (Fig 2). This multidisciplinary study was initiated to monitor the physical, geological, chemical, and biological processes occurring on the continental shelf in the South Atlantic Bight during fair-weather and storm events. This study focuses on the hydrodynamics of the bottom boundary layer and the associated sediment transport on the mid-shelf at the frame location. The frame is moored 27 nautical miles off the coast of Wilmington, North Carolina in Onslow Bay (Fig. 1) at a depth of approximately 30 meters, and was close to a biologically productive marine hardbottom.

It is well documented that storm driven processes dominate sediment transport on many continental shelves and are an important factor in coastal change (Madsen *et al.*, 1993). Understanding the geological processes, such as sediment resuspension and transport, caused by associated physical forcing mechanisms are important in Onslow Bay, NC for the management of fisheries habitats and because of the large amount of development along the coast. Several studies conducted in Onslow Bay, have documented the fluid forcing associated with low frequency currents and circulation

patterns (Atkinson *et al.*, 1976; Blanton and Pietrafesa., 1978; Bane and Brooks, 1979; Singer *et al.*, 1980; Hoffman *et al.*, 1981; Pietrafesa, 1989; Xie *et al.*, 1997). These studies have shown that Onslow Bay is dominated by three principal forcing mechanisms: (1) winds and related air-sea fluxes, (2) tides, and (3) the Gulf Stream.

Investigations of the geology of Onslow Bay have shown that the introduction of new sediment to this system is negligible due to limited fluvial inputs and minimal sediment exchange with adjacent shelf embayments (Blackwelder *et al.* 1982). Milliman (1972) classified the Onslow Bay shelf as a “sediment-starved” environment in which sediment cover is residual; i.e., derived from the erosion of underlying sediment and rocks. A number of geophysical surveys also have been conducted in Onslow Bay to describe the geologic framework of the inner to middle shelf of Onslow Bay (Cleary and Pilkey, 1968; Blackwelder *et al.*, 1982; Riggs *et al.*, 1998). A study of the geologic framework has been conducted of the hardbottom reef at the study site by Riggs *et al.* (1998). Their study showed the hardbottom reef is composed of a Pleistocene limestone overlying a Miocene muddy sandstone (Fig 3). In “sediment-starved” shelf environments these marine hardbottom areas have been shown to occupy a large percentage of the continental shelf and are critical for benthic habitats (Riggs *et al.*, 1996). Renaud *et al.* (1996, 1997) documented frequent changes in the distribution, orientation, and thickness of the fine sand bodies that overlie gravelly, coarse sands and adjacent hardbottom surfaces and scarps located at the site. These types of changes in distribution and thickness of the fine sands on and around the hardbottom during storms have been shown to alter the population, distribution, and type of benthic infauna and flora on the

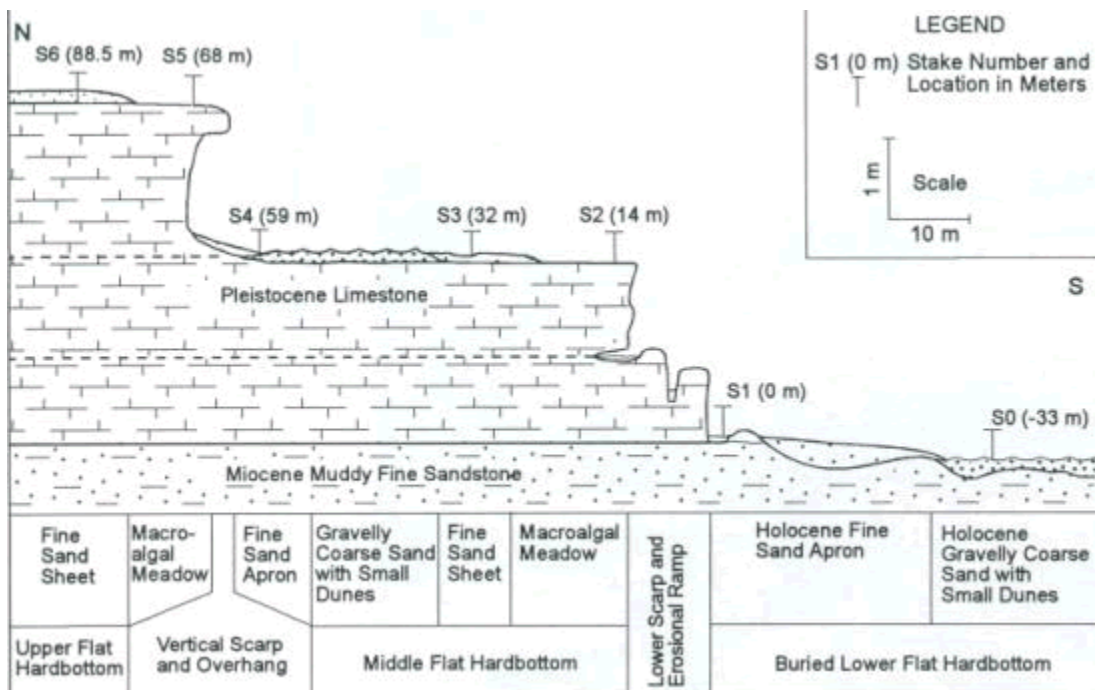


**Figure 3.** Underlying geology of the hardbottom reef at the study site (Riggs *et. al.*, 1998)

hardbottom and, therefore, the entire ecological community. These hardbottom sites in Onslow Bay form the framework for the highly productive “livebottom communities” that are important to commercial and recreational fisheries and thus are of major economic importance (*Riggs et. al*, 1998).

Although many of these previous investigations in Onslow Bay have included descriptions of substrate characteristics and bedform morphologies, little attempt has been made to quantify the bottom boundary layer hydrodynamics and associated sediment transport processes. Two exceptions are studies by Gutierrez and Volugaris (2002) and Thielor *et al.* (2001) who examined the dominant sediment transport processes on the inner portion of the shelf and observed sediment transport from the shoreface region to the inner shelf. Nonetheless, little is known about the physical forcing mechanisms and bottom boundary layer conditions that are responsible for mobilizing these sediment bodies adjacent to the marine hardbottoms. Thus, there is a need for quality physical data to be collected at the site. The purpose of this paper is to determine and constrain the forcing mechanisms that develop sufficient bottom stress to resuspend and transport sediments over an annual cycle, and to characterize the resulting sediment transport that occurs at this location on the shelf.

## **2.2 Methods**

### *2.2.1 Study site*

#### *2.2.1.1 Physical setting*

Onslow Bay is located off the southeastern coast of North Carolina in the northern region of the South Atlantic Bight (SAB). It is bounded to the northeast by Cape Lookout and to the southwest by Cape Fear, and by the shelf edge and Gulf Stream to the

east (Fig. 1). The mean tidal range in Onslow Bay is approximately 1.0 m and mainly consists of M2 frequency oscillations (Pietrafesa *et al.*, 1985). Average significant wave heights are 1.5 m with an average dominant period of 8.0 seconds (NOAA, FPSN7 C-Man station).

Onslow Bay has been included in several studies that focused on the physical oceanographic processes and climatology of the SAB region (Atkinson *et al.*, 1980; Chao and Pietrafesa, 1980; Pietrafesa and Janowitz, 1980; Weber and Blanton, 1980; Weisberg and Pietrafesa, 1983; Blanton *et al.*, 1985; Lee *et al.*, 1985; Pietrafesa *et al.*, 1994). These studies have shown that the physical processes of the region exhibit seasonal and synoptic (2 day - 2 week) variability. The synoptic variability is due largely to wind forcing and Gulf Stream frontal effects, while seasonal variability is caused by large-scale atmospheric events (Pietrafesa *et al.*, 1985). The dominant winds in Onslow Bay originate from either the Azores-Bermuda High, located in the North Atlantic, or the Ohio Valley High, a smaller-scale anticyclone centered over the Ohio Valley between August and January. Following Weisberg and Pietrafesa (1983), the four wind seasons can be defined as winter (from December - February), spring (March - May), summer (June-August), and fall (September – November) (Weisberg and Pietrafesa, 1983). Mean monthly winter winds are initially southwestward during December, then turn southward during January and are directed southeastward by late February. Spring is the transition month where the prominent influence of the Ohio Valley High is replaced by the Azores-Bermuda High. The wind stresses are directed towards the east during March and to the northeast by May. The northward flow of air strengthens in the summer as the Azores High shifts westward, and a northward wind stress is dominant. August is usually a



transition month where winds are weak with no dominant direction. During the fall, the flow of tropical air around the Azores-Bermuda High from the south rapidly collapses and is replaced by drier air from the Ohio Valley High. Strong southwestward wind stresses are exerted over the area during this time of the year (Pietrafesa *et al.*, 1994).

Atkinson (1980) described the hydrographic climatology of the region and concluded that the shelf can be broken up into three bathymetric zones according to the controlling physical processes. The outer shelf (41-60 m depth) is dominated by Gulf Stream incursions (Pietrafesa and Janowitz, 1980), the mid-shelf (21-40m depth) is an area of mixed response to wind forcing and Gulf Stream effects, and the inner shelf (0-20m) is strongly influenced by river runoff and atmospheric forcing (Lee *et al.*, 1985). The influence of the Gulf Stream on the shelf is more common during summer months due to the decreased density gradient between the shelf and Gulf Stream water (Pietrafesa *et al.*, 1985). Filaments, meandering eddies, and persistent southerly winds are all physical forcing mechanisms that transport the Gulf Stream (GS) water onto the shelf. Generally, water in Onslow Bay is more saline than that of the Middle Atlantic Bight to the north and the Georgia Bight to the south due to the proximity to the GS and relatively low river input along the Carolina Capes (Pietrafesa *et al.*, 1994).

#### *2.2.1.2 Geological setting*

Onslow Bay is a shallow, high energy, storm-dominated shelf environment bounded by the Cape Lookout and Frying Pan submerged shoals (Mearns, 1998). The “sediment-starved” continental shelf is characterized by a complex sequence of rocky outcrops with relief up to 10 m (Renaud *et al.*, 1997). The hardbottom habitats form extensive, irregular reef tracts due, in part, to the area being sediment starved. Although a thin and discon-

tinuous veneer of Holocene sediment exists, surface sediment is generally not accumulating on the shelf. The introduction of new sediment to this system is negligible due to limited fluvial inputs and minimal sediment exchange between adjacent shelf embayments (Blackwelder *et al.* 1982). The major sources of sediment for the inner and mid-shelf are shoreface bypassing of unconsolidated ancient sediment and bio-erosion of marine hard grounds on the inner shelf (Riggs *et al.*, 1998). More recent studies (Pierson and Riggs, 1981; Thielert *et al.*, 2001), however, suggest that beach nourishment projects are also an immediate source for sands on the inner shelf.

The upper hardbottom and lower sand flat sub-habitats are the major components of the Onslow Bay hardbottom system (Renaud *et al.*, 1997). The reef that is adjacent to the instrument frame is approximately 2 m in relief and is known as “23 Mile Rock”. Two types of sand bodies are dominant at the site: rippled, gravelly, coarse sand patches and fine sands. The fine sands are found on top of the hardbottom and in aprons adjacent to the reef. The coarser gravelly sands are only found on the lower sand flats and are not on the upper hardbottom surfaces. Major differences in distribution and thickness of the fine sands on the upper hardbottom have been observed (Renaud *et al.*, 1996; Riggs *et al.*, 1998) which suggests that these fine sands are mobile and readily suspended during sediment transport events.

### *2.2.2 Instrumentation and data collected*

In late April of 2000, a downward looking Sontek Pulse-Coherent Acoustic Doppler Profiler (PC-ADP) and an upward looking Acoustic Doppler Current Profiler (ADCP) were deployed on the mid-continental shelf (33° 59'N, 77° 21'W) approximately 25 to 100 m from “23 Mile Rock” (Fig. 1). The instruments were mounted on a 2 m tall frame

situated at approximately 29m depth (Fig. 2). The PC-ADP sampled in “burst mode” at 1 Hz for 17 minutes every 2 hours during the spring and summer and for 10 minutes during the winter. Secured 150 cm above the seabed, the downward looking 1.5 MHz PC-ADP measures velocity profiles of the bottom boundary layer in 10 cm bins. When examining bottom conditions and calculating bed shear stresses, the velocity time series at 1 mab was used as an arbitrary elevation above the bed.

The PC-ADP also measures temperature and pressure, and serves as a bottom altimeter. To monitor changes in seabed elevation, the 3 acoustic beams in the downward-looking transducer detect where the seabed is located under the frame once during each 17- minute burst. To measure changes in turbidity, the 1.5 MHz PCADP acoustic backscatter signal amplitude was used. This signal is useful for approximating relative changes in suspended particulate in the water column, similar to the Acoustic Backscatter Sensor, which has been shown to be especially successful with sands in sediment transport studies in the U.S. and the U.K. (Battisto, 2000; Williams and Rose, 2001).

The ADCP is an upward-looking 600 kHz RDI Workhorse Sentinel ADCP that profiles the overlying water column in 1m bins at 1 Hz. These data are averaged over a 60 second averaging interval and create a velocity profile of the upper water column every 5 minutes. In addition, a Microcat (Seabird SBE 37-SM) is attached to the frame and collects bottom conductivity, temperature, and pressure every 5 minutes in order to identify the different water masses occupying the site. Approximately 12 m from the frame, a mooring line equipped with a second Microcat collects conductivity and temperature data at approximately 15m below the surface, which enables identification of

the frequent stratification that occurs in Onslow Bay. Hourly averaged wind velocities and wave data were obtained from the nearby NOAA C-Man station at Frying Pan Tower (Fig. 1).

During this study, the PCADP and the ADCP were set up for 4 - 6 week deployments. They were then retrieved divers, brought into the lab for maintenance and data recovery, and redeployed. Deployments for this study began on April 27<sup>th</sup>, 2000 and lasted until November 30, 2000 (Table 1). The PC-ADP failed to power on during the winter deployment of 2000, therefore, the deployment of 2001 – 2002 was used to characterize sediment transport during the winter.

### *2.2.3 Bottom boundary layer model*

The bottom boundary layer model used in this study was the Styles and Glenn (2002) bblm. This model is an extension of the Glenn and Grant (1987) continental shelf bottom boundary layer model (bblm) for flow and suspended sediment concentration profiles in the constant stress layer over a non-cohesive sediment bed. Glenn and Grant (1987) adopted the turbulence closure scheme of Grant and Madsen (1979), and although they incorporated a number of important physical processes such as wave-current interaction and a moveable sediment bed, the discontinuous eddy viscosity profile they use leads to an artificial kink in the current and concentration profiles. The discontinuity will have a strong influence on the model's ability to predict accurately the current and concentration profiles, and therefore, the associated sediment transport. Styles and Glenn (2002) updated the Glenn and Grant model using a more realistic continuous eddy viscosity profile that removes the artificial kink in the current and concentration profiles. In order to predict the bottom roughness, the Styles and Glenn (2002) bblm modified the

simple model of Wikramanayake and Madsen (1991) to predict ripple height and wavelength primarily as a function of the wave excursion amplitude and wave orbital velocity. The Styles and Glenn bblm (2002) also includes a modification of the turbulent closure scheme of Grant and Madsen (1979) to account for rough conditions where turbulent transport associated with vortex ejection increases the wave boundary layer thickness.

The model is based on the following theoretical model where the Reynolds fluxes for sediment mass and fluid momentum are closed using a continuous, time-invariant linear eddy viscosity. The horizontal components of velocity ( $u, v$ ) are Reynolds averaged and then divided into independent wave ( $u_w, v_w$ ) and current ( $u_c, v_c$ ) components, i.e.,

$$u = u_c + u_w + u'$$

$$v = v_c + v_w + v'$$

where  $u'$  and  $v'$  are the turbulent velocity fluctuations. Assuming a time-independent eddy viscosity and using the usual bottom boundary layer and linear approximations, the momentum equation is averaged over a wave period to produce the following governing equation for the current:

$$\tau_c/\rho = K(\partial U/\partial z),$$

where  $\tau_c$  is the magnitude of the Reynolds stress averaged over a wave period evaluated at the bed,  $\rho$  is the fluid density,  $K$  is the time invariant eddy viscosity,  $U = (u_c^2 + v_c^2)^{1/2}$  is the magnitude of the current, and  $z$  is the vertical coordinate measured positive upward from the bed.

For suspended sediment it is customary to assume sediment concentrations are large enough to be treated as a continuum, yet small enough to neglect individual particle interactions. By similarly dividing up the sediment concentrations into mean ( $C_{nm}$ ), periodic ( $C_{np}$ ), and turbulent components ( $c'$ ),

$$C = C_{nm} + C_{np} + c',$$

for each size class  $n$ , and applying the conservation of mass to each class, the equation governing the mean concentration becomes:

$$w_{fn} (\partial C_{nm} / \partial z) + \partial / \partial z (K_s (\partial C_{nm} / \partial z)) = 0;$$

where  $w_{fn}$  is the particle settling velocity for each size class and  $K_s$  is the eddy diffusivity for suspended sediment. The above equation is the well-known relationship describing an equilibrium sediment concentration profile where the upward turbulent flux of the sediment is balanced by the gravitational settling.

In order to remove the discontinuity in the eddy viscosity profile, the following three-layer eddy viscosity profile is used that combines the formulation for the pure wave case with a combined wave and current boundary layer:

$$\begin{aligned} K &= k u_{*c} z, & z_2 < z, \\ K &= k u_{*cw} z_1, & z_1 \leq z \leq z_2, \\ K &= k u_{*cw} z, & z_0 \leq z \leq z_1, \end{aligned}$$

where  $k$  is von Karman's constant (0.4),  $z_0$  is the hydrodynamic roughness,  $z_1$  is an arbitrary scale that defines the lower boundary of the transition layer, and  $z_2 = z_1 u_{*cw} / k u_{*c}$ , which is determined by matching the eddy viscosities at  $z = z_2$ . Similar to the Grant and Madsen (1979) eddy viscosity model, the characteristic velocity scales within and above the wave boundary layer are  $u_{*cw}$  and  $u_{*c}$ . The three-layer eddy viscosity profile

was first proposed by Glenn (1983) and later revisited by Madsen and Wikramanayake (1991). Several field and laboratory studies have concluded that the improved eddy viscosity model is more accurate in predicting current and concentration profiles than the two-layer model developed by Grant and Madsen (1979, 1986) for unstratified flow conditions (Wikramanayake and Madsen, 1992; Wikramanayake, 1993; Lynch, 1997).

The equations used in the bblm to predict ripple height ( $\eta$ ) and wavelength ( $\lambda$ ) are taken from the empirical relationship similar to Madsen and Wikramanayake (1991) where:

$$\frac{\eta}{Ab} = 0.30X^{-0.39}; X \leq 2$$

$$\frac{\eta}{Ab} = 0.45X^{-0.99}; X \geq 2$$

$$\frac{\lambda}{Ab} = 1.96X^{-0.28}; X \leq 2$$

$$\frac{\lambda}{Ab} = 2.71X^{-0.75}; X \geq 2$$

where  $X$  is a non-dimensional wave and sediment parameter defined by

$$X = \frac{\theta_m}{S_*} = \frac{4\nu(A_b\omega)^2}{d[(s-1)gd]^{1.5}}.$$

$Ab$  is the bottom excursion amplitude,  $\nu$  is the kinematic viscosity of the water,  $s$  is the ratio of the sediment density to the fluid density, and  $g$  is the acceleration due to gravity. A comparison of the predicted ripple geometry using this relationship and ripple measurements by Traykovski *et al.* (1999) indicate that natural ripples exhibit characteristics that are similar to this simple model (Styles and Glenn, 2002).

The Styles and Glenn (2002) bblm, as described above, has been field verified with measurements from the LEO-15 site off the coast of New Jersey in which it produced

accurate estimates of the time averaged shear stress and apparent roughness during a moderate nor'easter event (Styles and Glenn, 2002). In the present study, the model was compared with field measurements collected on the mid-shelf in Onslow Bay, NC during common wind events and during a very close passage of a hurricane in order to determine if the model accurately predicts current velocity, suspended sediment profiles and associated sediment transport at the study site.

The input data that were used to run the model included: (1) time series data of the PC-ADP burst-averaged mean current ( $U_r$ ) measured at a 1 mab reference elevation ( $Z_r$ ) in the bottom boundary layer, (2) time series of near-bottom orbital velocities ( $U_b$ ) and near bottom wave excursion amplitude ( $A_b$ ), (3) a time series of the wave and current incidence angle ( $\Phi_{cw}$ ). Wave orbital velocities were calculated from the recorded hourly wave height and period data at FPSN7 using linear wave theory where:

$$U_b = \sqrt{2} * (a \omega / \sinh(kd))$$

and  $H_{rms} = H_s/\sqrt{2}$ ,  $a = H_{rms}/2$ ;  $\omega = 2\pi/T_{dom}$ , and  $k=2\pi/L$ . A comparison between wave data at FPSN7 and another bottom mounted ADCP, that collected wave data on the inner shelf in Onslow Bay at 17 m depth, indicated that wave conditions were similar at both sites.

Five grain sizes ( $d_{10}$ ,  $d_{25}$ ,  $d_{50}$ ,  $d_{75}$ ,  $d_{90}$ ) were used as input into the bblm based on the grain size distributions of surface sediment samples collected prior to each event. A default for ripple height and wavelength were also input into the bblm. All of the input parameters were obtained from current and wave measurements, sediment samples, and altimetry data. Diver observations were made of ripple characteristics during deployment



Table 1. Deployments

<b>Season</b>	<b>Deployment period</b>	<b>Instrumentation</b>	<b>Sampling scheme for PC-ADP</b>
Spring 2000	4/27 – 5/8; 5/12 – 5/31	PCADP, ADCP, ABS, altimeter	17 minute bursts at 1 Hz
Summer 2000	6/1 – 6/26; 7/12 – 8/7; 8/8 – 8/31	PCADP, ADCP, ABS, altimeter	17 minute bursts at 1 Hz
Fall 2000	9/1 – 9/21; 10/7 – 10/30; 11/2 – 11/30	PCADP, ADCP, ABS, altimeter	17 minute bursts at 1 Hz
Winter 2001- 2002	12/7 – 2/21	PCADP, ADCP, ABS, altimeter	10 minute bursts at 2 Hz

and retrieval of the instrumentation.

Time series of bed stresses due to currents and wave-current interactions were generated for each season. Critical shear stresses were calculated using the median grain size ( $d_{50}$ ) from surface sediment samples. The critical velocity for the initiation of sediment motion was determined by the bblm. A critical shear velocity for the transition between bedload and suspended transport was calculated for the median grain size of 0.0269 cm at the site using the Rouse parameter,  $P = (Ws/ku^*)$ . When the Rouse parameter is equal to or greater than 2.5 the critical velocity is equal to  $2.87 \text{ cm s}^{-1}$ , and this threshold is the point when sediments begin to be picked up from the bed and transported via suspended sediment transport. Times of full suspension sediment transport were defined as periods when the Rouse parameter was approximately equal to 1.0 (Wiberg and Harris, 1994). The critical shear velocity for full suspension using the median grain size was  $7.17 \text{ cm s}^{-1}$ .

#### 2.2.4 Data analysis

It has been shown (Pietrafesa *et al.*, 1985) that mid-shelf dynamics in Onslow Bay are strongly coupled with wind stress; therefore, in order to examine sediment transport at the site, synoptic variability in wind stress and the associated physical processes were evaluated. This paper focuses on the velocity measurements in the lower 1.5 meters of the water column and at a height of approximately 4 meters above the bed (mab). Available atmospheric and wave data from the NOAA C-Man station were used in conjunction with measured near-bottom (1mab) current velocity data to verify mean oceanographic circulation that has been shown to occur during each of the four climatological wind seasons (Pietrafesa *et al.*, 1985).

Mean current velocities at 1mab were calculated by taking the mean of the current speed measurements over one burst and the mean of the direction measurements for the corresponding burst. For example, the PC-ADP sampled at 1 Hz and the burst interval was 17 minutes so there were 1020 measurements of current speed and direction during each burst. The mean current speed was calculated for each burst by adding all of the 1020 measurements of current speed together and dividing by 1020. The direction component for the burst was calculated similarly. The resulting mean velocity consisted of the burst-averaged magnitude and direction.

Acoustic backscatter data collected in the bottom boundary layer, bottom altimetry data, and measurements of the physical properties of the water column such as temperature and salinity were also examined. Bed stresses due to wave-current interactions were calculated using the bottom boundary layer model and relative changes in the along- and across-shelf sediment flux were estimated using simultaneous measures of near-bottom flows and the acoustic backscatter signal.

Seasonal mean along- and across-shelf flows were determined for each of the four seasons to characterize the seasonality of flows and sediment transport at the site. When determining the seasonal mean flows, the mean of all of the burst-averaged along- and across-shelf current velocities was taken over the entire season; the result was the mean flow for that season in the along- and across-shelf direction. The along-shelf axis is taken at  $55.6^\circ$  east of north following Pietrafesa *et al.* (1994) and is positive towards the southwest in this paper; the across-shelf direction is positive in the offshore direction. Mean along- and across-shelf sediment fluxes were estimated for each season by multiplying the burst averaged along- or across-shelf velocity by the burst-averaged

acoustic backscatter signal at the specified elevation of the current. Because the instruments were not calibrated to convert the acoustic backscatter signal to suspended sediment concentrations, the data are used only for comparing *relative* differences in suspended sediment between seasons during this study. Mean along and across-shelf flows at 1 mab were input into the bblm in order to calculate shear velocities, bottom bedforms, and bedload transport rates and direction for each season. Critical shear velocities for bedload transport, combined transport of bedload and suspended load, and full suspension transport were determined for the median grain diameter at the site. The modes of sediment transport could then be identified and summarized for each season. Mean along- and across-shelf sediment fluxes were then estimated again for the times when the shear velocity exceeded the critical shear for combined suspended and bedload transport or full suspension transport for each season. A time series of bedload transport rates were determined using the Meyer-Peter-Muller bedload equation (Meyer-Peter and Muller, 1948) with the median grain size during each deployment. A time series of bedload direction was also determined using the formula  $\tan\Phi_{bl} = 2/3 \tan\Phi_{cw}$  (USACE, 2002), where the angle of the wave direction is estimated to be the angle of maximum variance in the raw PC-ADP velocity data at 1 mab.

## **2.3 Results**

### *2.3.1 Atmospheric forcing*

Previous studies (Pietrafesa *et. al.*, 1985) have documented that wind driven circulation plays an important role in the overall circulation patterns of Onslow Bay, and that wind is an especially important driving force for mean currents on the mid-shelf. In order to examine atmospheric forcing over the duration of the study, available wind,

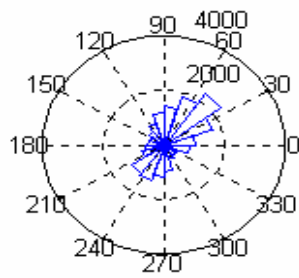
wave, and atmospheric data from a National Oceanic and Atmospheric Administration (NOAA) C-Man station located at the southern boundary of Onslow Bay were used (<http://www.ndbc.noaa.gov/FPSN7>). A climatological approach was used to characterize and estimate sediment transport at the site during the four wind seasons. Mean hourly wind directions during each of the four climatological seasons, as previously defined, were compared with the mean hourly data over last ten years in order to determine if the atmospheric forcing that occurred during the study period was consistent with the climatology. The comparison showed that mean hourly wind directions from the deployments agreed well with wind stresses from all four seasons over the past ten years (Fig. 4). Winds were dominantly between the south-southwest and east-northeast during the winter season and early spring, southwesterly during the late spring and summer months, and from the northeast during the fall season. These patterns are consistent with previous mean monthly wind directions reported for the area (Pietrafesa and Weisberg, 1983; Blanton *et al.*, 1985).

### 2.3.2. *Tides and physical characteristics*

The pressure time series shows that the maximum spring tidal range over the study period was 2.0 m. Spring tidal currents were typically  $15 \text{ cm s}^{-1}$  at the site and neap tidal currents were generally less than  $10 \text{ cm s}^{-1}$ . Harmonic analysis of the currents in the bottom boundary layer indicates that the semi-diurnal M2 tidal constituent dominated the tidal currents. This result is consistent with previous studies done of the upper water column which showed that the M2 tidal signal contained 80% of the tidal energy in Onslow Bay (Pietrafesa *et al.*, 1985). The major and minor axes of the M2 tidal ellipse

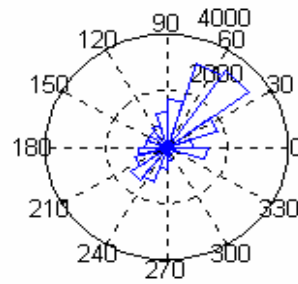
a.)

Spring wind direction 1990-1999

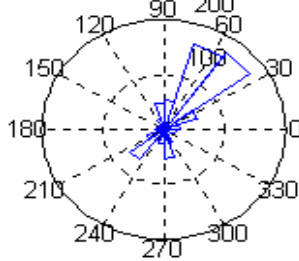


b.)

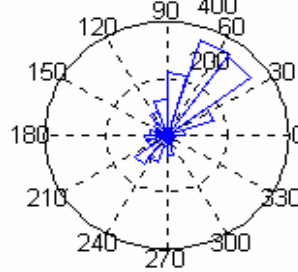
Summer wind direction 1990-1999



Spring wind direction yr. 2000

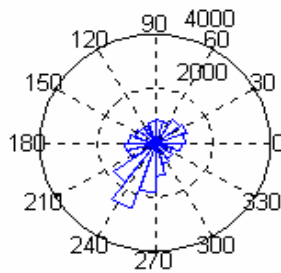


Summer wind direction yr. 2000



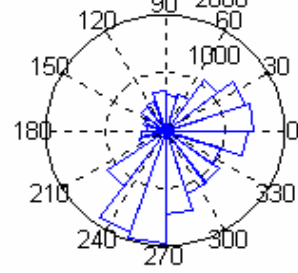
c.)

Fall wind direction 1990-1999

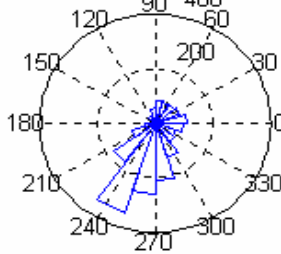


d.)

Winter wind direction 1990-1999



Fall wind direction yr. 2000



Winter wind direction yr. 2000

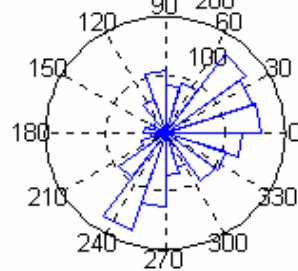


**Figure 4.** Comparison of seasonal wind direction from the year of study to the past 10 years. Winds during the study period agree with the climatology of the area.

were 4.6 and  $-2.25 \text{ cm s}^{-1}$ , respectively, with an orientation of 47.20 degrees west of north. The temperature of the near-bottom water on the shelf displayed a seasonal cycle and ranged from 12°C in mid-January to 27°C in September. Additionally, water temperatures and salinity measurements in the lower water column varied due to the presence of different water masses on the shelf and due to stratification of the overlying water column.

### *2.3.3 Sediment transport*

The mean along-and across-shelf velocities were calculated from the PC-ADP data at 1 mab and the ADCP data at 4 mab for each of the four seasons, respectively, and for all data during the study (Table 2). The mean flow velocities calculated for each season from both instruments were similar in magnitude and direction for all seasons except the winter. There was also no difference when the net flows of the entire data set were compared. During the winter, the ADCP data indicated a mean flow towards the positive along- and across-shelf directions, whereas the PC-ADP data indicated that mean flows were in the opposite direction. Additionally, during the winter deployment the PC-ADP data at 1mab indicated that the suspended sediment flux was also in the negative along-shelf direction (Table 3). This difference in flow direction from the ADCP, as well as the sediment flux direction, may be due to the effect of the hardbottom located to the north of the frame location. The PC-ADP measurements collected at 1 mab are below the height of the 1-2 meter ledge and may lie in a shadow zone produced by the ledge when flows are of high magnitude from the north and northeast (positive along-shelf). The ADCP at 4 mab is above the ledge and is, therefore not similarly affected. Furthermore, the reef located north of the site is a limited source of suspended sediments, whereas

extensive areas of fine sands lie to the south of the study site. However, for all the data over a year, the mean along- and across-shelf velocities from the two instruments reported similar results.

#### *2.3.3.1 Spring*

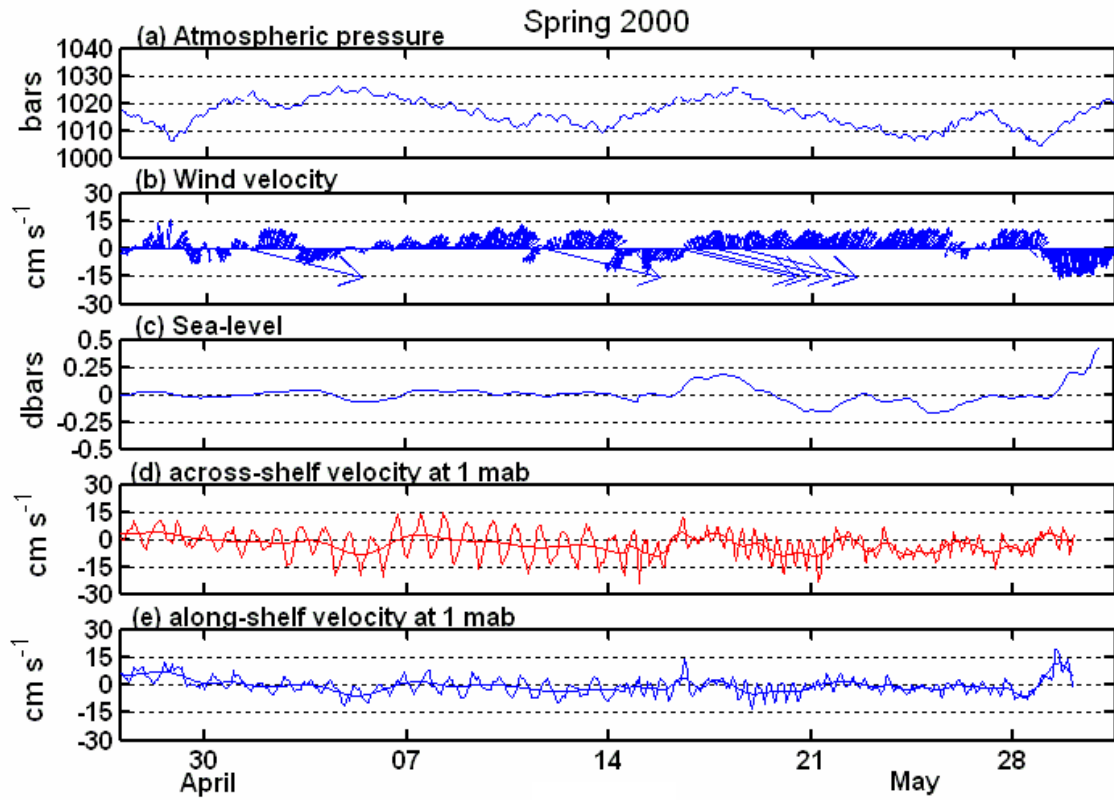
The spring deployment began on April 27th, 2000 and contained quality data from all instrumentation through the end of the spring season (Table 1). From late April through May, winds were predominantly from the southwest (Fig. 5). Wave periods were 5 – 12 seconds and bottom orbital velocities ranged from 0 to 64 cm s<sup>-1</sup> (Fig 6). Mean flow speeds at 1 mab were 0.4 – 25.0 cm s<sup>-1</sup> (Fig.6). Due to the southwest winds during this deployment, the across-shelf currents at 1 mab were stronger (0 – 20 cm s<sup>-1</sup>) than the along-shelf currents (0-10 cm s<sup>-1</sup>) (Fig. 6). However, during a period of northerly winds, the along-shelf current was larger than the across-shelf current, reaching magnitudes of 15 cm s<sup>-1</sup>. For all data collected during this deployment, the mean current speed at 1 mab in the across-shelf direction was -1.75 cm s<sup>-1</sup> and the mean along-shelf current speed was -0.9 cm s<sup>-1</sup> (Table 2).

During the spring deployment, wave-current combined shear velocities exceeded the critical shear threshold for movement of the median grain size for 61.2% of the time. Shear velocities ranged from 1 – 10 cm s<sup>-1</sup>, but were typically below 5 cm s<sup>-1</sup> (Fig. 6). Sediment transport occurred via bedload transport for 52% of this time, while combined bedload and suspended load occurred for 46% and full suspension transport for 2% of the total time that sediment transport was occurring. The mean along- and across-shelf flows at 1mab (Table 2) during periods of sediment suspension were -0.36 cm s<sup>-1</sup> (3.5 days positive/3.5 days negative) and -1.8 cm s<sup>-1</sup> (3.83 days positive/5.5 days negative),

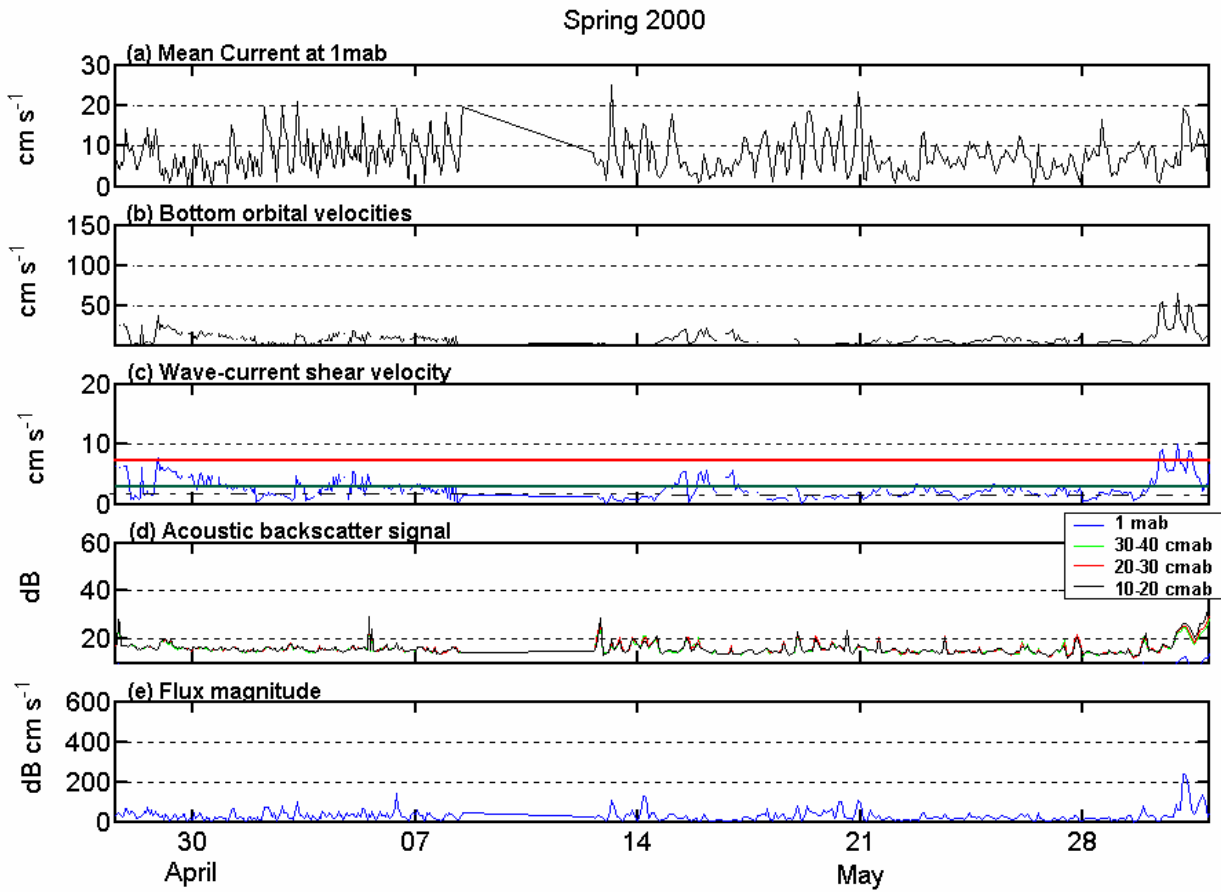


Table 2. Comparison of mean seasonal conditions for the year of record. The ADCP data is shaded in gray. Positive along-shelf is towards the southwest and positive across-shelf is directed offshore.

	Spring		Summer		Fall		Winter		All data	
Time period	4/27/00 – 5/31/00		6/01/00 – 8/31/00		9/1/000 – 11/30/00		12/1/01 – 2/28/02		4/27/00 -11/30/00; 3/1/01-3/31/01; 12/1/01-2/28/02	
$U_b$ ( $\text{cm s}^{-1}$ )	8.3		8.8		14.7		13.6		11.3	
No. days of data	33	33	75.5	90.3	75.5	75.5	70.5	70.5	254.5	295
Along-shelf velocity ( $\text{cm s}^{-1}$ )	-0.44	-0.51	-1.6	-2.9	-0.72	-0.91	-0.4	1.1	-0.9	-0.9
Across-shelf velocity ( $\text{cm s}^{-1}$ )	-2.7	-3.1	-3.4	-3.2	-0.76	-0.83	-0.45	.13	-1.75	-1.57
Mean ABS levels (dB)	3.8	8.6	3.1	6.7	6.1	9.5	5	8.4	5.66	8.1



**Figure 5.** Atmospheric pressure, wind velocity, low-pass filtered sea-level, and mean and subtidal across- and along-shelf currents from April 27 – May31, 2000.



**Figure 6.** April 27 – May31, 2000 mean current speed, bottom orbital velocities, wave-current shear velocities, measured ABS, and *relative* suspended sediment flux magnitude. The black dashed line in the third panel is the threshold for sediment movement, the green line represents the threshold for when sediments start to be suspended from the seabed, and the red is the threshold for full suspension transport.

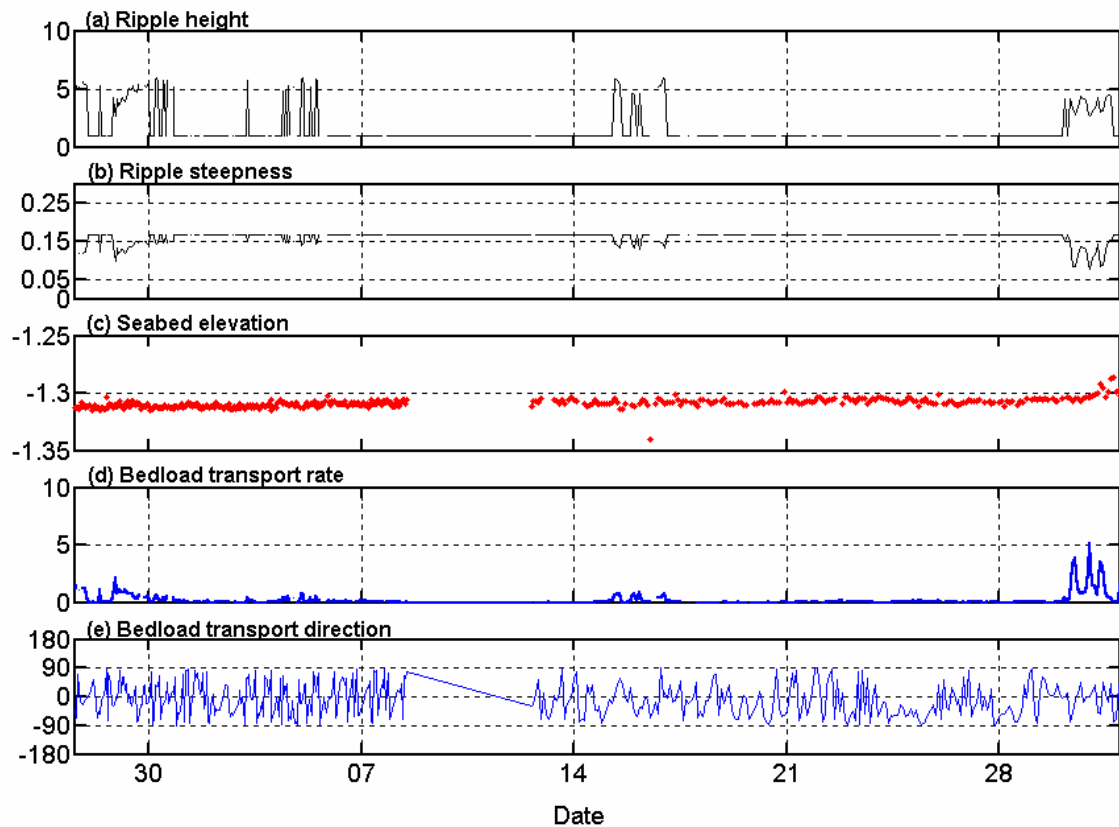


**Figure 7.** April 27 – May31, 2000 seabed response during the spring deployment showing the bblm generated ripple height and steepness, measured seabed elevation, calculated bedload transport rates, and direction based on model calculated shear stresses.

respectively. Along-shelf velocities ranged from  $-9.8$  to  $9.9 \text{ cm s}^{-1}$  and across-shelf velocities ranged between  $-20.7$  and  $14.8$  (Fig. 6). The net along- and across-shelf apparent fluxes at 1 mab during this time were  $-0.62 \text{ dB m s}^{-1}$  and  $-12.2 \text{ dB m s}^{-1}$ , respectively (Table 3).

The seabed was not very active during the late spring deployment according to both model predictions and the seabed altimetry data (Fig. 7). The model predicted the presence of ripples for approximately one third of the deployment. The seabed altimetry data are consistent with the bblm predictions and show fluctuations of  $1 - 2 \text{ cm}$  for the same periods that the model predicted ripples on the seafloor (Fig. 7). Bedload transport during this deployment occurred at rates of  $0 - 2 \text{ cm}^2 \text{ s}^{-1}$ , except during a wind event at the end of May when bedload rates increased to  $5 \text{ cm}^2 \text{ s}^{-1}$  (Fig. 7).

#### *2.3.3.2 Summer*

The summer months were characterized by fair weather conditions during which wave heights were generally around  $1.0 \text{ m}$  or less and winds were dominantly from the south and southwest and relatively calm ( $<10 \text{ m s}^{-1}$ ) (Fig. 8). Wave bottom orbital velocities were less than  $15 \text{ cm s}^{-1}$  during most of the summer (Fig. 9) with dominant wave periods of approximately 9 seconds, ranging from 5 to 16 seconds. Mean flow speed at 1 mab ranged from nearly zero to  $20 \text{ cm s}^{-1}$  (Fig. 8). Subtidal flows were primarily directed in the negative along and across- shelf direction (northeastward and onshore) at speeds of  $5 - 10 \text{ cm s}^{-1}$  throughout the summer (Fig. 8). The mean along-shelf velocity for the summer data was  $-2.9 \text{ cm s}^{-1}$  at 4 mab and  $-1.6 \text{ cm s}^{-1}$  at 1 mab (Table 2). The mean across-shelf velocity for all of the summer deployment was  $-3.2 \text{ cm s}^{-1}$  at 4 mab and  $-3.4 \text{ cm s}^{-1}$  at 1 mab.

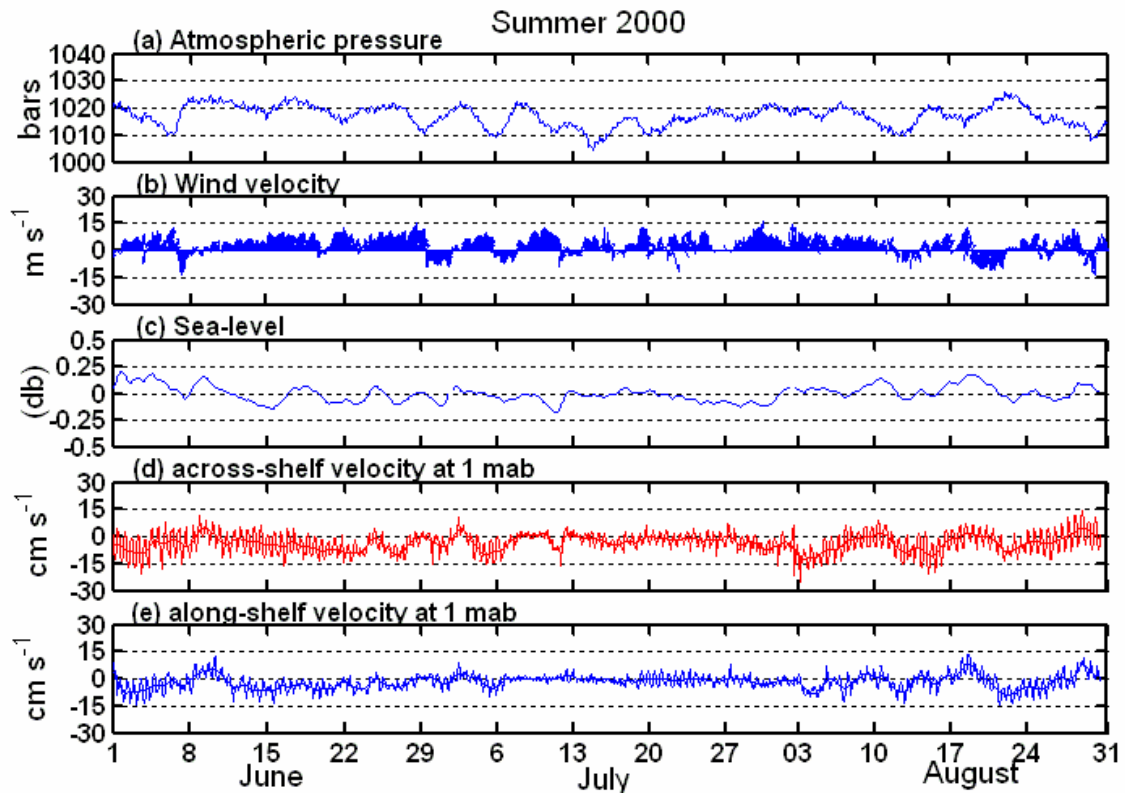


**Figure 8.** Atmospheric pressure, wind velocity, low-pass filtered sea-level, and mean and subtidal across- and along-shelf currents during the summer deployment.

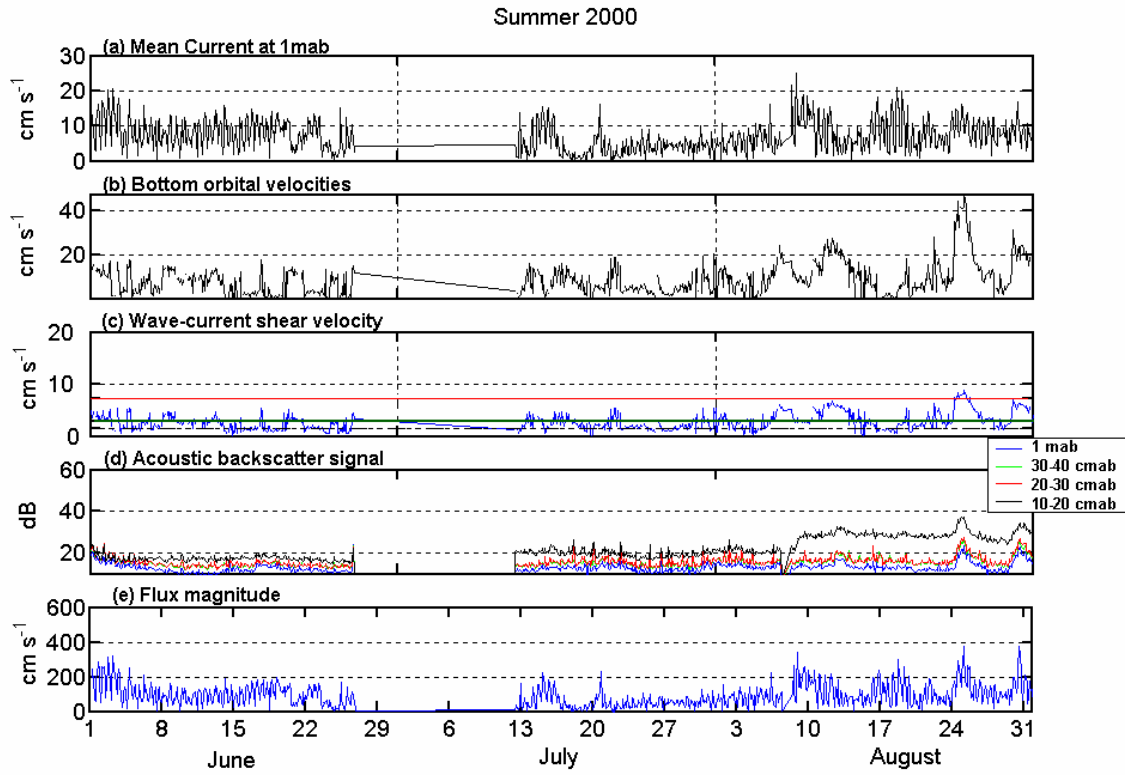


**Figure 9.** June 1 – August 31, 2000 mean current speed, bottom orbital velocities, wave-current shear velocities, measured ABS, and *relative* suspended sediment flux magnitude. The black dashed line in the third panel is the threshold for sediment movement, the green line represents the threshold for when sediments start to be suspended from the seabed, and the red is the threshold for full suspension transport.

Shear velocities due to wave-current interactions exceeded the critical shear stress for sediment movement for the median grain size ( $<0.0269\text{cm}$ ) at the site for 75% of the summer. The model calculated wave-current shear velocities were generally between  $2 - 5 \text{ cm s}^{-1}$  (Fig. 9), and skin friction bed stresses for this season were the lowest of the study ranging from approximately  $5 - 25 \text{ dynes cm}^{-2}$ . The model calculated wave-current shear velocities indicate that 49 % of the transport that occurred at the site during the summer was via bedload transport and 50% was by a combination of bedload and suspended sediment transport. Only 1 % of the sediment transport that occurred during the summer was fully suspended sediment transport based on the median grain size and bottom boundary layer conditions. The mean velocity in the along-shelf direction during periods of combined transport and full suspension transport was  $-1.9 \text{ cm s}^{-1}$ , with a range of  $-14.77$  to  $+13.85 \text{ cm s}^{-1}$ . The mean velocity in the across-shelf direction during periods of combined transport and full suspension transport was  $-3.09 \text{ cm s}^{-1}$  and ranged from  $-21.6$  to  $+14.1 \text{ cm s}^{-1}$ . Calculations of bedload transport indicate that transport occurred at a rate of  $0 - 3 \text{ cm}^2 \text{ s}^{-1}$  throughout most of the summer, but reached  $10 \text{ cm}^2 \text{ s}^{-1}$  due to long period swells ( $11.5 - 16.7 \text{ s}$ ) that moved across the shelf on August 25 (Fig. 10). The seabed altimetry data indicates that from June 2- June 23, a fairly significant amount of accretion occurred at the site. Upon closer examination of the temperature and salinity data, it appears that Gulf Stream (GS) water began to occupy the site during this time. Water temperature rapidly increased from  $23$  to  $25.5 \text{ }^{\circ}\text{C}$  in 72 hours, and temperatures remained elevated, between  $25 - 26 \text{ }^{\circ}\text{C}$ , for approximately three weeks. There was a concurrent rise in the near-bottom and mid-depth salinity measurements at the site, which is indicative of a Gulf Stream meander (Pietrafesa and Janowitz, 1980; Brooks and Bane,



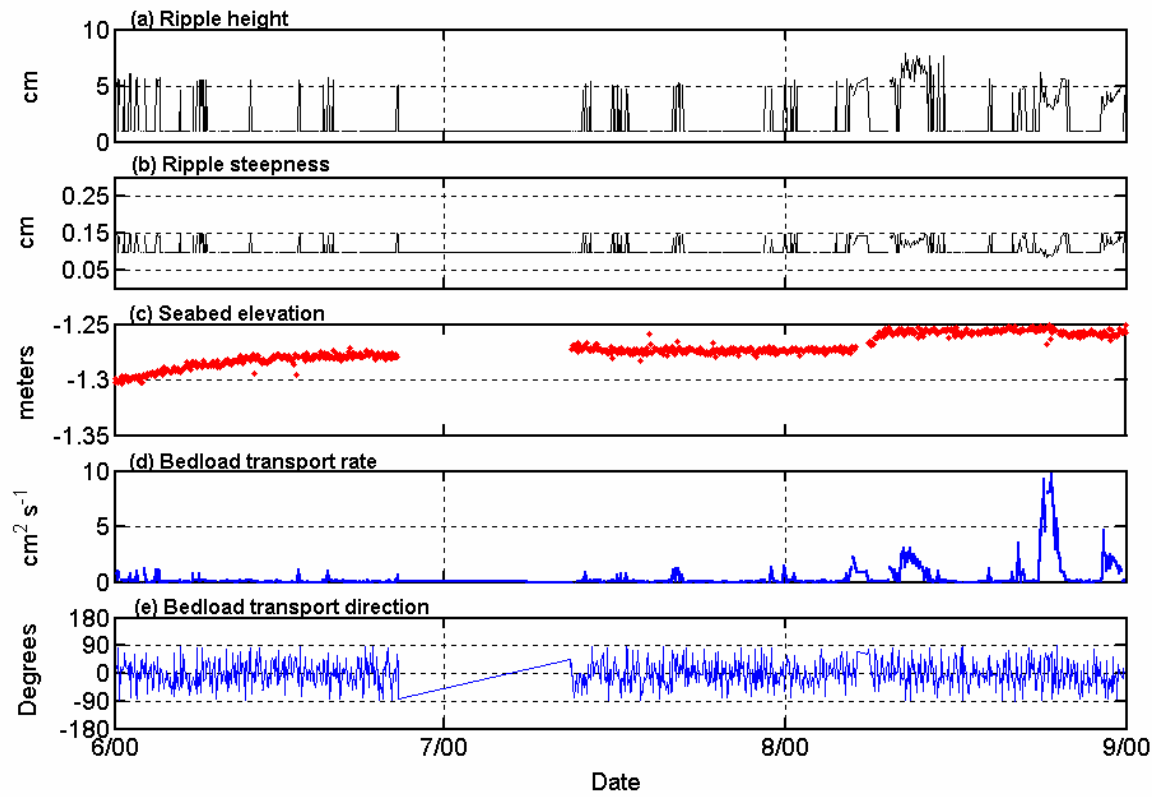


**Figure 10.** June 1 – August 31, 2000 - seabed response showing the bblm generated ripple height and steepness, measured seabed elevation, calculated bedload transport rates, and direction based on model calculated shear stresses.

1981). Temperature and salinity data recorded in the upper water column during this 3-week period indicate that the water column was well mixed. At the end of the 3-week period, the water column became stratified again and near-bottom temperatures and salinities returned to values typical for June (23°C, 35.5ppt). The presence of GS waters on the mid-shelf is corroborated by AVHRR satellite imagery taken during this time and was also reported by Quattrini (2002). During this time, subtidal currents towards the north, (creating negative along- and across-shelf flows) were persistent and are evident in the velocity time series (Fig. 8). This was a contributing factor to the large (negative) along- and across-shelf net fluxes that occurred during the summer months (Table 2 and 3). These types of Gulf Stream intrusion events have been shown to occur often during the summer months in Onslow Bay (Pietrafesa *et. al.*, 1985), and as shown, can play a role in sediment transport during this season when subtidal currents are combined with tidal currents and interact with bottom orbital velocities from fair weather swell.

#### 2.3.3.3 Fall

The hourly wind velocity time series collected during autumn of 2000 shows a transition from the gentle southwest winds typical of summer months, to stronger winds from the north and northeast (Fig. 11). The month of September was characterized by sudden changes in wind direction between these two dominant directions. Winds from a southerly direction ranged in magnitude from approximately 0 – 10 m s<sup>-1</sup>, and winds from a northerly direction ranged in magnitude from 5 – 20 m s<sup>-1</sup>. In October, the wind direction in Onslow Bay was predominantly from the north and northeast and ranged from approximately 5 – 15 m s<sup>-1</sup>. Winds relaxed slightly during the month of November and remained from the north and northeast. Mean bottom flow speeds during the fall

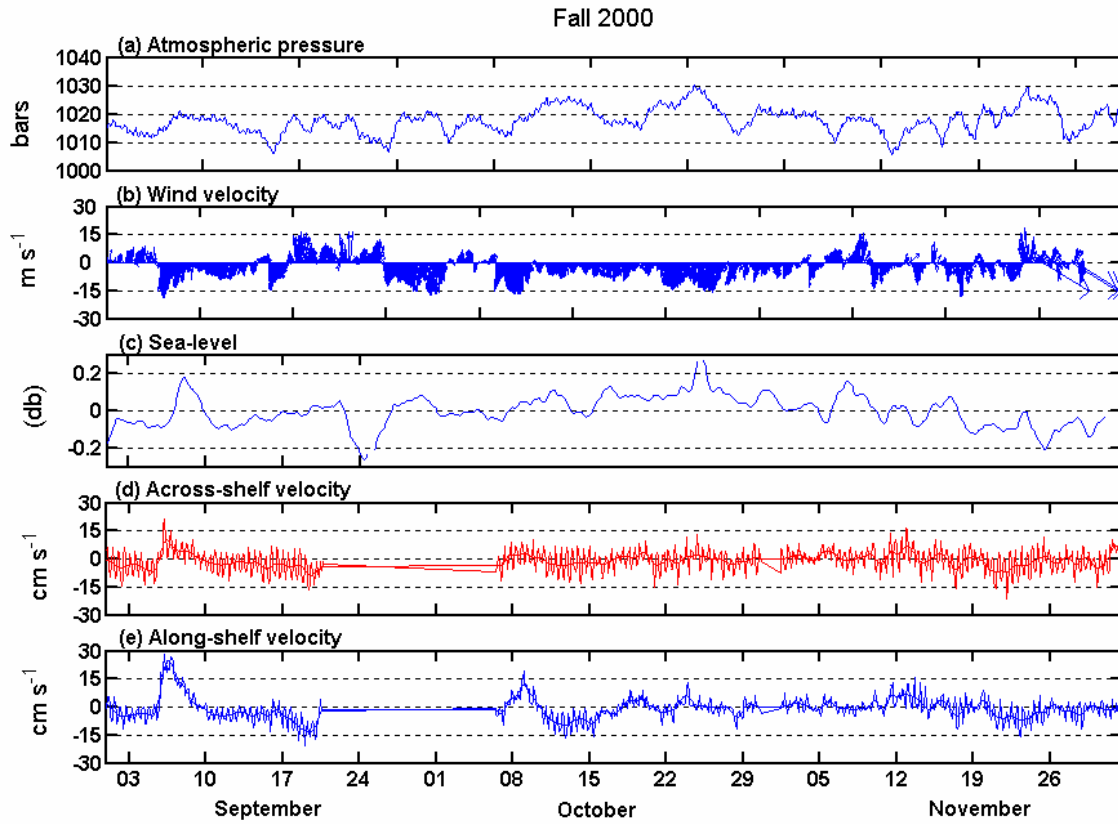


**Figure 11.** Atmospheric pressure, wind velocity, low-pass filtered sea-level, and mean and subtidal across- and along-shelf currents during the fall deployment.

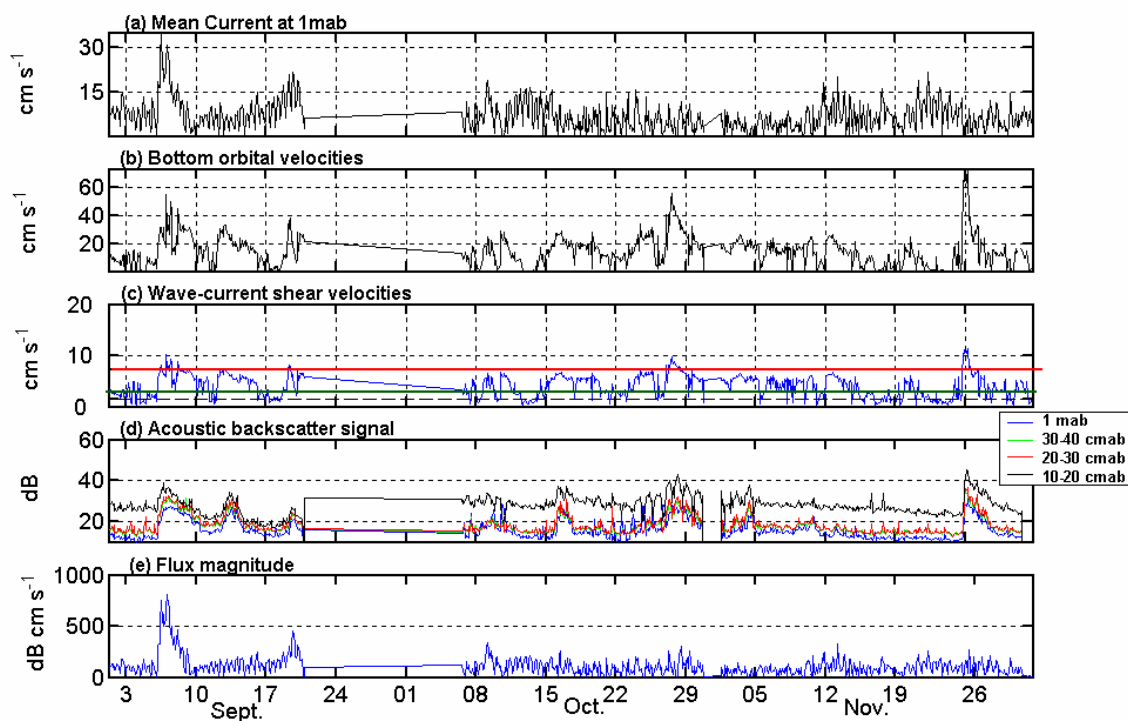


**Figure 12.** Autumn 2000 deployment - mean current speed, bottom orbital velocities, wave-current shear velocities, measured ABS, and *relative* suspended sediment flux magnitude. The black dashed line in the third panel is the threshold for sediment movement, the green line represents the threshold for when sediments start to be suspended from the seabed, and the red is the threshold for full suspension transport.

ranged from 0.04 - 35.1  $\text{cm s}^{-1}$  (Fig. 12) and bottom orbital velocities ranged from 0 – 73  $\text{cm s}^{-1}$  during the fall (Fig. 12). The dominant wave periods for the fall ranged from 5 – 12 seconds. There was no dominant current direction during the fall as these flows alternated throughout the season between positive and negative in both the along- and across-shelf directions (Fig. 11). Mean along and across-shelf flows were small (less than 1  $\text{cm s}^{-1}$ ) during the fall due to the constant alternating current directions corresponding to the transitioning winds (Table 2).

Model calculated shear velocities due to wave current interactions were higher during the fall than the spring and summer seasons and ranged from 0.5 – 12  $\text{cm s}^{-1}$ , but were generally between 2 – 6  $\text{cm s}^{-1}$  (Fig. 12). Sediment transport occurred for approximately 85% of the fall deployment of which bedload accounted for only 23 % of the sediment transport and combined transport accounted for 71% of the transport. Full suspension of the median grain size accounted for 6% of the total fall transport. The mean along-shelf velocity for this season was +0.08  $\text{cm s}^{-1}$  (southwest) and ranged from -28.88 to +27.97. There were 22.5 days that the flows were directed in the positive along-shelf direction and 26.5 days that flows were directed in the negative along-shelf direction. The mean velocity in the across-shelf direction was -0.24  $\text{cm s}^{-1}$ , but ranged between -16.75 to + 21.21. In the across-shelf direction the flows were directed in the positive along-shelf direction for 24.7 days and were directed in the negative along-shelf direction for 24.3 days. During the transition months of fall, the along-shelf and across-shelf components of the flows are comparable. Although, the mean currents were close in magnitude, the sediment flux during this time was in the along-shelf direction. The net flux in the along and across-shelf directions were +42.9  $\text{dB cm s}^{-1}$  and -2.4  $\text{dB cm s}^{-1}$ ,

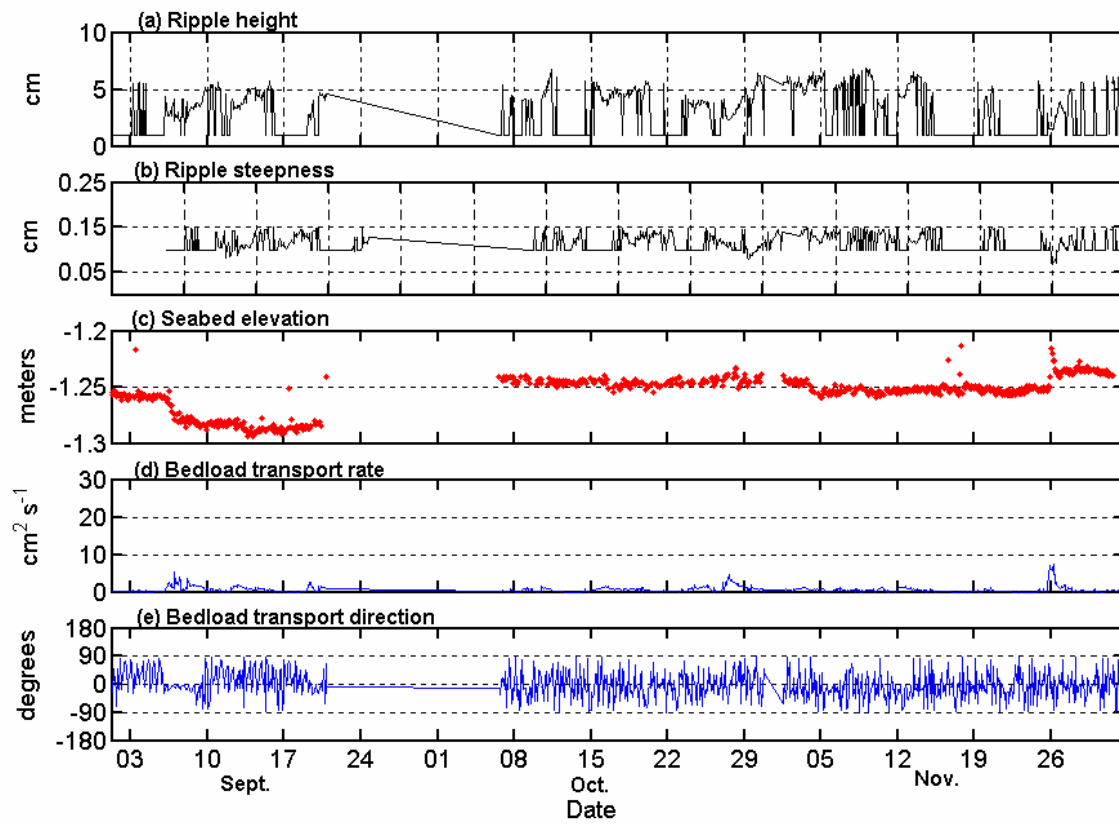


**Figure 13.** Autumn 2000 deployment - seabed response showing the bblm generated ripple height and steepness, measured seabed elevation, calculated bedload transport rates, and direction based on model calculated shear stresses.

respectively. Although currents were close to being equal in the positive and negative along-shelf directions, the wave activity was stronger when winds were from a northerly direction causing more sediment transport to occur in the positive along-shelf direction. The largest change in seabed elevation took place during the northerly wind event in early September when 3 cm of erosion occurred at the study site (Fig. 13). During the remainder of the season, small fluctuations are apparent in the seabed altimetry data during each of the subsequent events. The bblm output appeared to agree with the seabed altimetry data reasonably well and indicates ripples from 2-6 cm on the bed for over 50 % of the deployment.

#### *2.3.3.4 Winter*

Time series data of atmospheric pressure and wind velocity collected during the winter season exhibited a synoptic variability of 2-7 days associated with the passage of frontal systems. Winds velocities were generally directed along-shelf alternating between north and northeasterly to south and southwesterly, with the strongest winds from the northeasterly direction (Fig. 14). During the winter, bottom orbital velocities ranged from nearly zero to  $50 \text{ cm s}^{-1}$ , except during a southerly wind event in early January when bottom orbital velocities reached  $100 \text{ cm s}^{-1}$  (Fig. 15). Dominant wave periods were between 4 - 10 seconds, except during two days of longer period waves ranging from 12-14 seconds that occurred prior to the wind event at the beginning of January. Mean currents at 1 mab ranged from  $5 - 20 \text{ cm s}^{-1}$  during the winter (Figs.15). The across-shelf current velocities were less variable than the along-shelf currents and appear to be influenced strongly by the diurnal tidal signal, ranging from  $-15 - +15 \text{ cm s}^{-1}$  (Fig. 14). In contrast, along-shelf current velocities appear to be influenced more by the

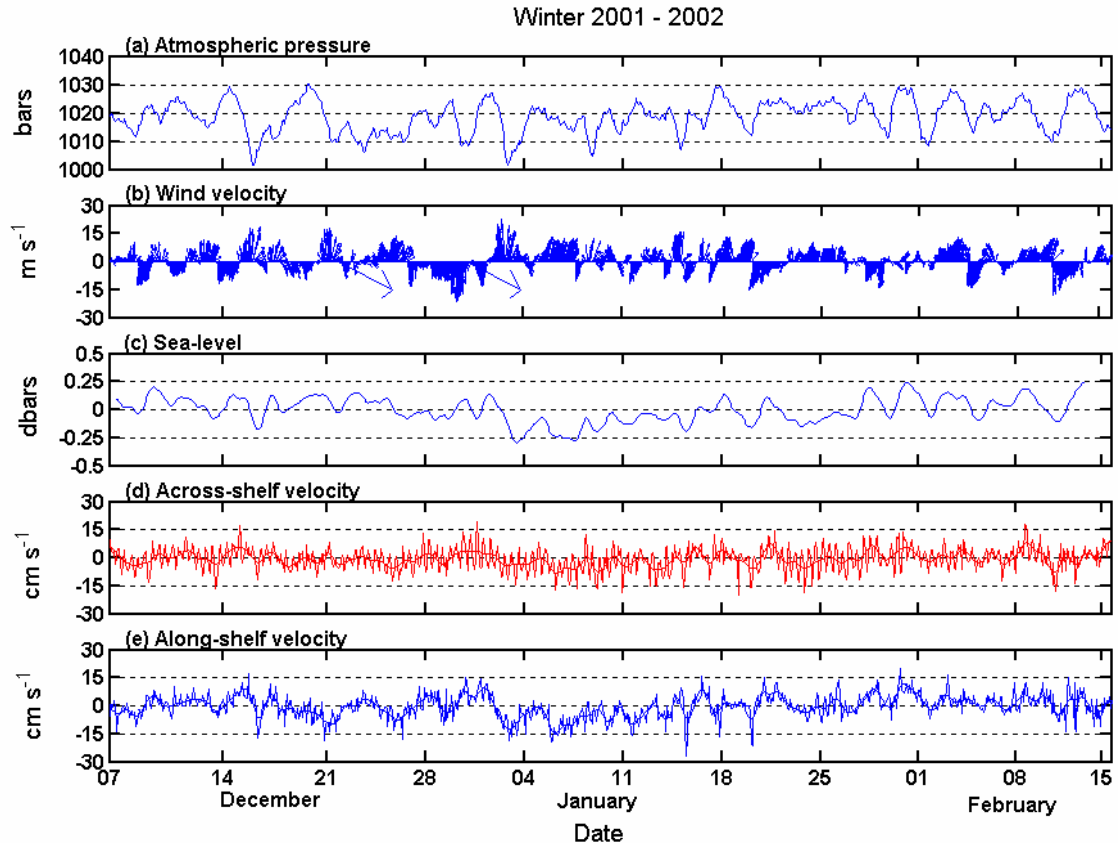


**Figure 14.** Atmospheric pressure, wind velocity, low-pass filtered sea-level, and mean and subtidal across-shelf and along-shelf currents during the winter deployment.



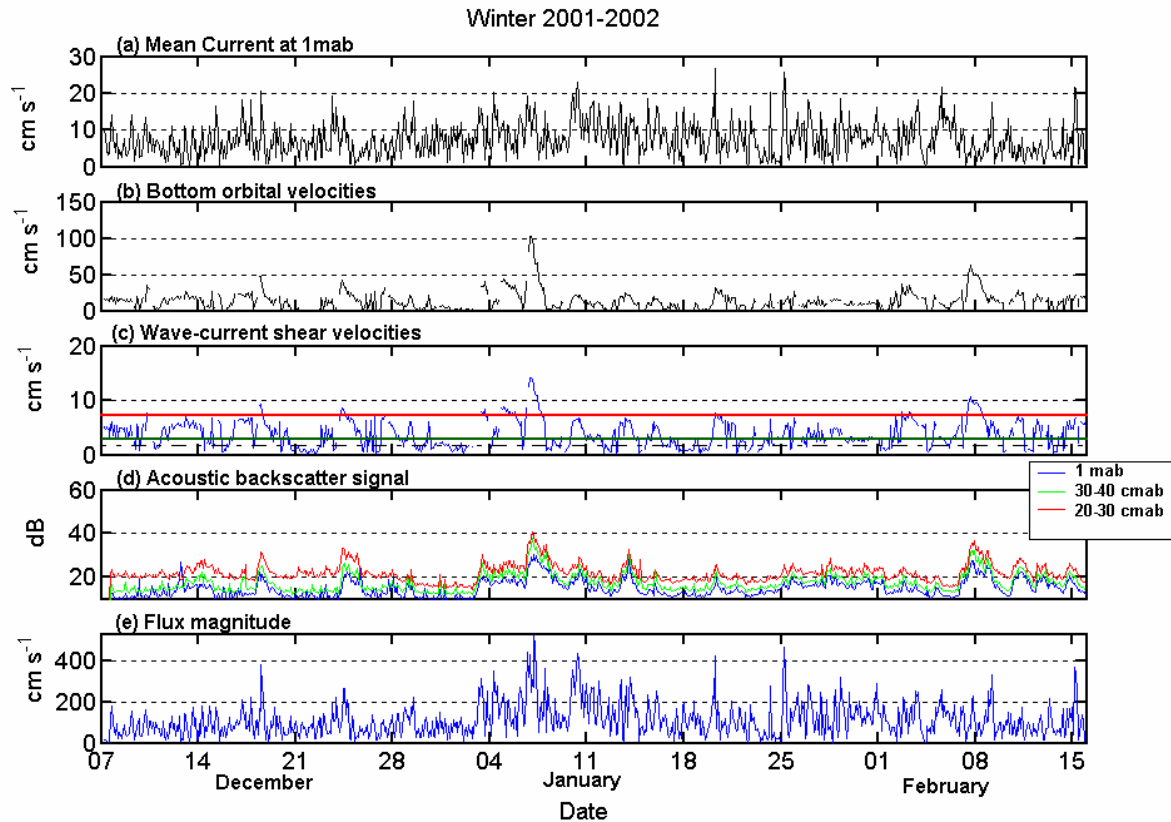


**Figure 15.** Winter 2001 deployment - mean current speed, bottom orbital velocities, wave-current shear velocities, measured ABS, and *relative* suspended sediment flux magnitude. The black dashed line in the third panel is the threshold for sediment movement, the green line represents the threshold for when sediments start to be suspended from the seabed, and the red is the threshold for full suspension transport.

local winds and ranged from  $-20$  to  $+20$   $\text{cm s}^{-1}$  (Fig.14). Subtidal currents also appear to be more variable and stronger in the along-shelf direction than in the across-shelf direction in the winter (Fig.14).

Calculated wave-current shear velocities ranged from  $1 - 11.34$   $\text{cm s}^{-1}$  (Fig. 15) throughout the winter months and were above the critical shear threshold for movement during 76% of the deployment. Of this time, 26% was purely bedload transport, 63% was a combination of bedload and suspended transport, and sediments were in full suspension 11% of the time. The mean flows at 1mab during the winter deployment were  $-0.17$  and  $-0.45$   $\text{cm s}^{-1}$  in the along-shelf and across-shelf directions, respectively (Table 2). The winter deployment was similar to the fall deployment in that the currents exhibited similar magnitudes in both the positive and negative directions for both the along and across-shelf flows. Currents were directed in the positive along-shelf direction for 20.5 days and in the opposite direction for 19.1 days. The across-shelf currents were directed onshore (negative) for 19.75 days and directed offshore 19.83 days during the winter. During the winter deployment, net sediment flux was towards the northeast, in the negative along-shelf direction, with a net transport of  $-41.9$   $\text{dB cm s}^{-1}$  and onshore with a net transport of  $49.6$   $\text{dB cm s}^{-1}$ .

The seabed altimetry data do not indicate appreciable change occurring in seafloor elevation over this season. Fluctuations of only 1-2 cm occurred during three events on record during this season (Fig. 16). The bblm time series of ripple height suggests that ripples of 1-8 cm were present on the bed for approximately 47% of the winter season (Fig. 16). The steepness of the ripples was predicted to range between zero

Table 3. Apparent suspended sediment flux at 1 mab

	<b>Spring</b>	<b>Summer</b>	<b>Fall</b>	<b>Winter</b>	<b>Cumulative</b>
Net along-shelf flux (dB m s <sup>-1</sup> )	-0.62	-28.8	42.9	-41.1	-27.6
Net across-shelf flux (dB m s <sup>-1</sup> )	-12.2	-42.6	2.4	-49.6	-102
Total flux (dB m s <sup>-1</sup> )	57.6	114.6	301.6	613.6	1087
Days of sediment suspension	9.3	28.9	49	39.7	126.9
Average flux per day (dB m s <sup>-1</sup> day <sup>-1</sup> )	6.0	4.0	6.2	15.5	8.6

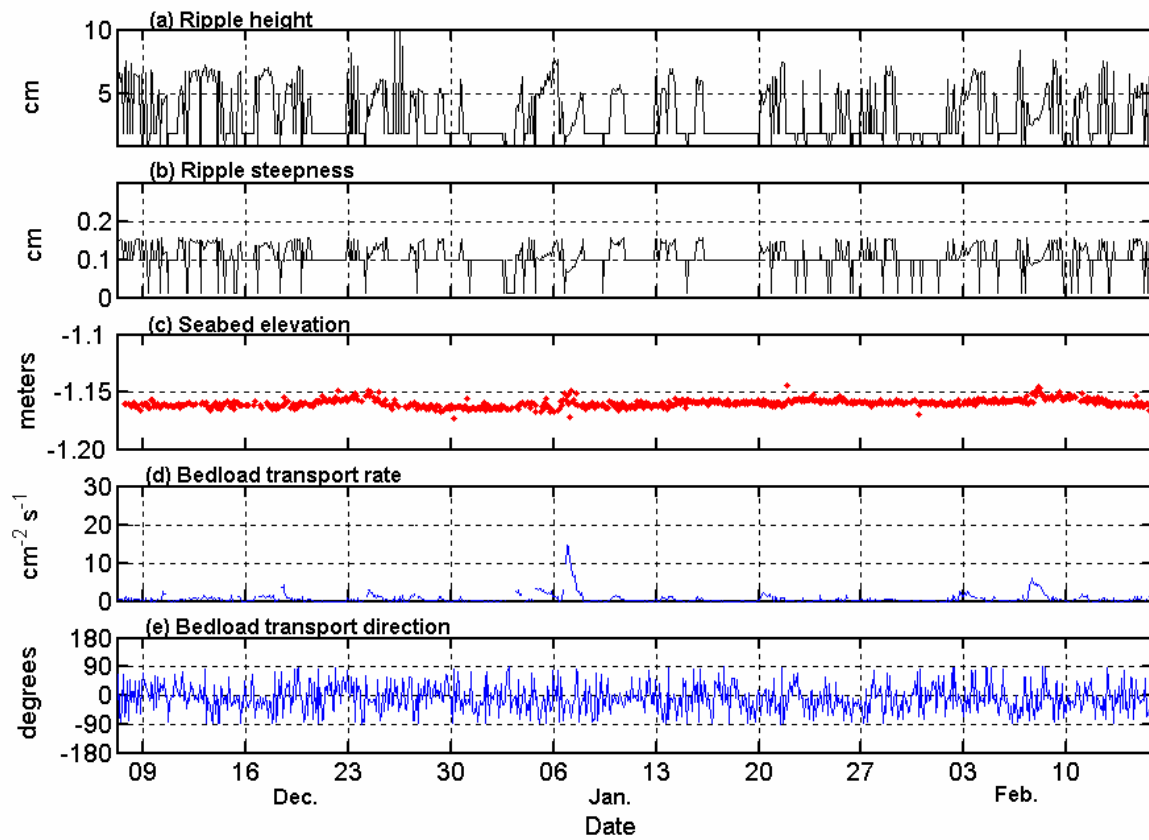


**Figure 16.** Winter 2001 deployment - seabed response showing the bblm generated ripple height and steepness, measured seabed elevation, calculated bedload transport rates, and direction based on model calculated shear stresses.

to 0.15, suggesting that bedforms varied throughout the winter from planar bed sheet flow conditions to anorbital and suborbital ripples (Fig. 16).

## **2.4 Discussion**

### *2.4.1 Net sediment flux*

Apparent sediment flux at 1 mab was toward the southwest, in the positive along-shelf direction, during the fall and toward the northeast in all other seasons (Table 3). More sediment transport took place during the winter than any other season. Fall was the second most active season for sediment transport where sediment flux at 1 mab was in the positive along-shelf direction (southwest) and in the negative across-shelf direction (onshore) (Table 3). During the year of record, net transport of sediment in the onshore direction was 3 times greater than net transport in the along-shelf direction. This result suggests that sand may be transported shoreward, beyond the hardbottom reef located shoreward of the site, if the sediments are suspended vertically higher in the water column than the height of the ledge (~1m), otherwise sediments will accumulate in the sand aprons found adjacent to the reef. It is also possible that in the absence of a ledge fine sediments from this mid-shelf location may traverse the inner shelf in the onshore direction and eventually join the beach/bar system. Many beaches along the coast of Onslow Bay are highly developed and actively eroding. The present thinking of the coastal engineering community is that once sand is lost to the shelf, it is lost from the beach system permanently. These data show that if the prevailing winds during a year are consistent with dominant wind patterns, significant potential exists to transport fine sands from the mid-shelf towards the coast.

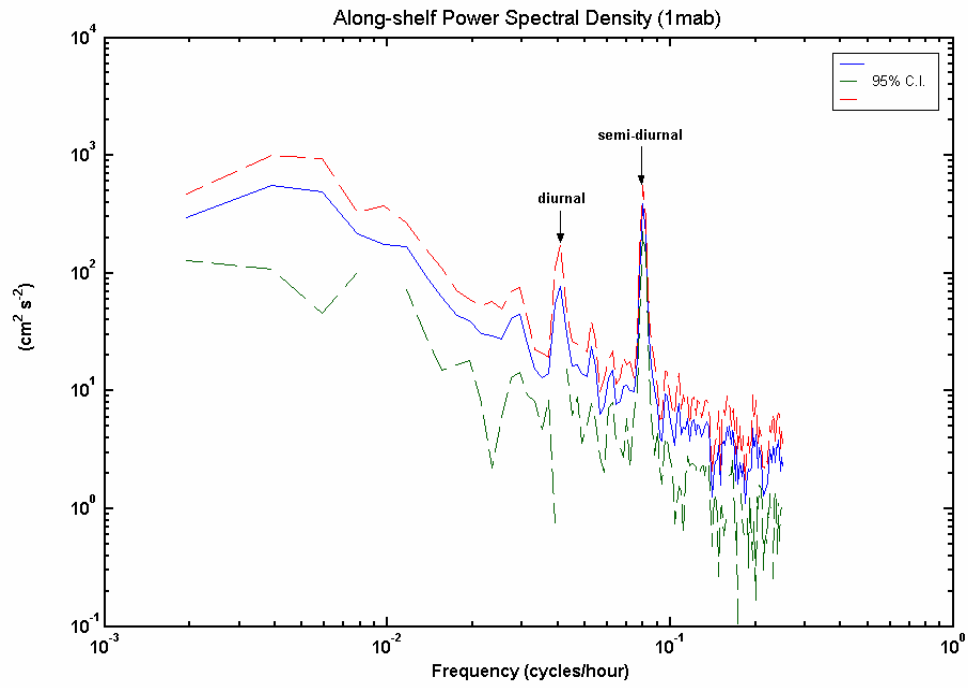
#### 2.4.2 Sediment-suspension event forcing

It is apparent from the analysis of sediment transport for the year-long record that multiple factors affect the resuspension and transport of sediment at the site. The energy spectra of along- and across-shelf currents (Fig.17) show significant peaks at the diurnal and semi-diurnal tidal frequencies. The spectra also show that a significant portion of the power is contained in the lower energy components. The following sections show examples of the major forcing mechanisms: waves, tidal currents, and low-frequency and mean currents.

##### 2.4.2.1 Waves

It has been shown that waves are an important factor in sediment transport on the shelf (Madsen *et al.*, 1993; Cacchione *et al.*,1999; Ogston and Sternberg,1999; Wright *et al.*,1999). Therefore, it is not unexpected that there was a high correlation between the bottom wave orbital velocities and the acoustic backscatter signal ( $R=0.60$ ) at 1mab for the entire data set. The importance of the waves was evident in the shear velocity time series data for all of the seasons. Further, when bottom orbital velocities decreased, there was a proportional decrease in the bed shear velocities. While the oscillatory motions of waves were incapable of transporting sediments across the shelf, they created high shear stresses on the seabed that acted to suspend sediments, and make them available for transport by currents in the bottom boundary layer.

a.)



b.)

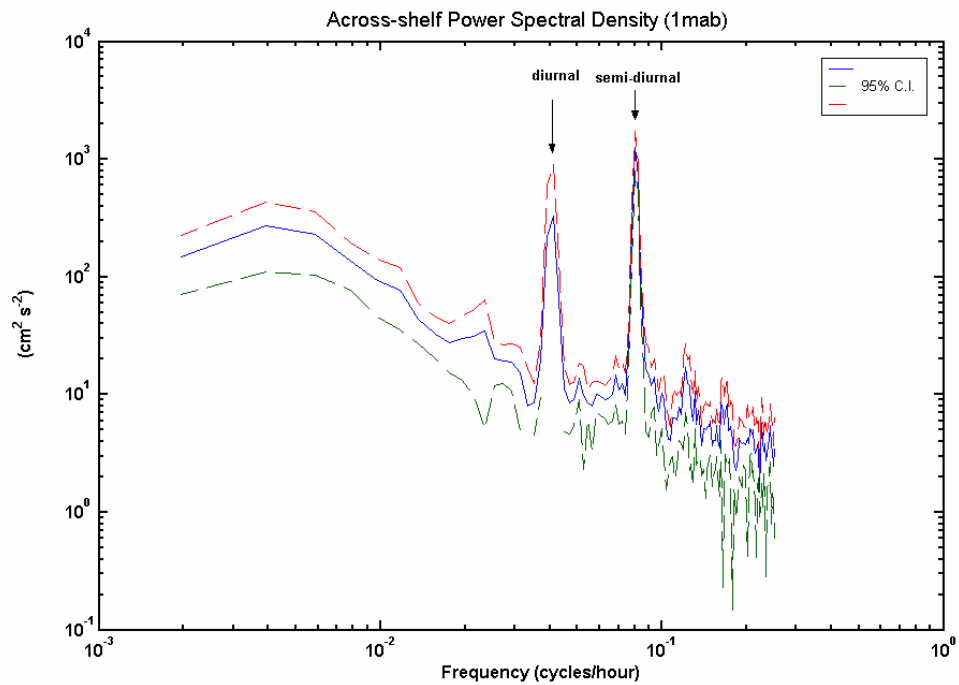


**Figure 17.** (a.) Along-shelf and (b.) across-shelf spectra for all data at 1mab during the study.

#### *2.4.2.2 Tidal currents*

Strong tidal currents associated with peak spring tide appear to have an effect on the retention of sediment in suspension following a wind event. As an example, large tidal currents associated with a spring tide reached  $20 \text{ cm s}^{-1}$  after the northerly wind event that occurred from May 29 – June 1<sup>st</sup>. While the shear velocities decreased to  $4 \text{ cm s}^{-1}$ , the ABS signal remained elevated over the next two days as it slowly decreased during the period spring tidal currents (Fig. 10). Shear velocities of this magnitude occurred again later in the summer where ABS levels did not increase at 1mab (Fig. 10). The calculated flux magnitude during the first days of June remained high due to the relatively higher tidal currents which caused the ABS levels to remain elevated (Fig. 10). The impact of the tidal currents on the suspension of sediment are also evident in the energy spectra for along- and across-shelf velocities (Fig. 17) and in the energy spectra of the PC-ADP ABS at 1 mab (Fig.18) where peaks at the semi-diurnal and diurnal frequencies occur for both velocity and suspended sediment. The coherence plots (Fig.19) of the along- and across-shelf velocity and the ABS at 1mab show that both the along- and across-shelf velocities are coherent at the semi-diurnal frequency, but show a low coherence at the diurnal frequency. Although tidal currents alone are not sufficient to suspend sediment at the site, the coherence between the spectra suggests that the semi-diurnal tides are important in maintaining the sediments in suspension.

#### *2.4.2.3 Low-frequency and mean currents*

Low frequency and mean currents appear to play an important role in determining the magnitude and direction of the sediment flux at the site. The along-shelf and across-



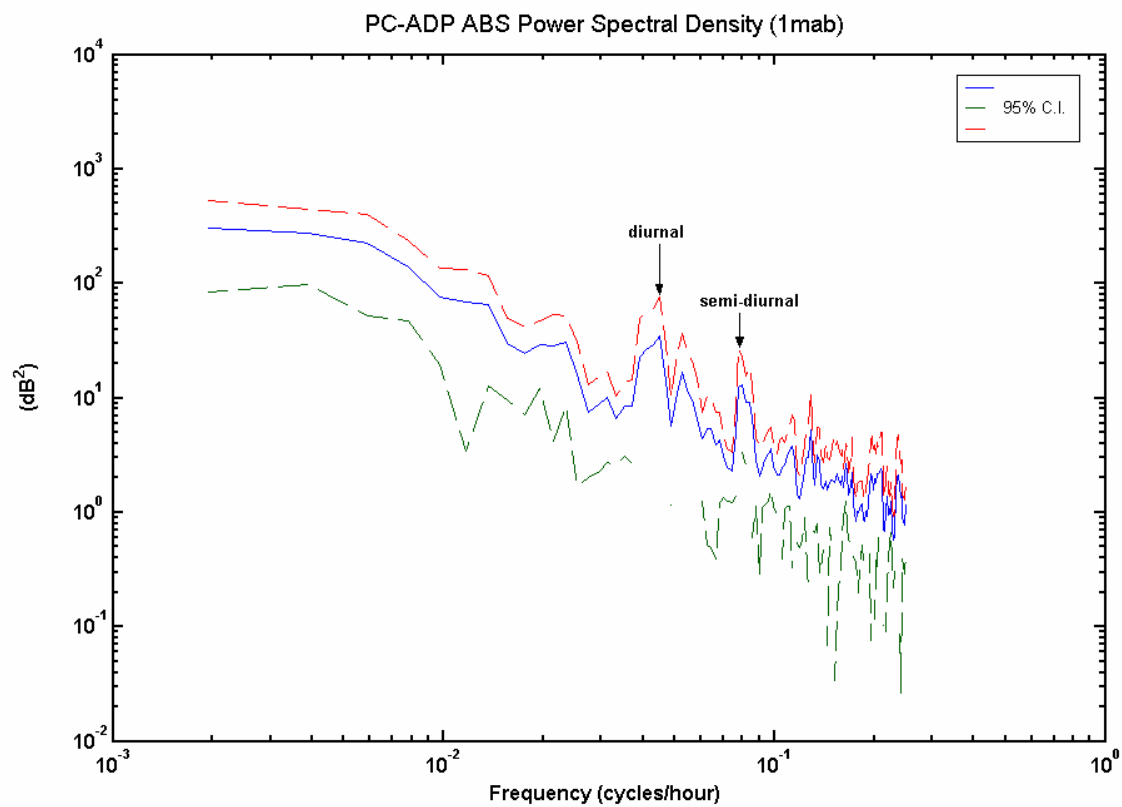
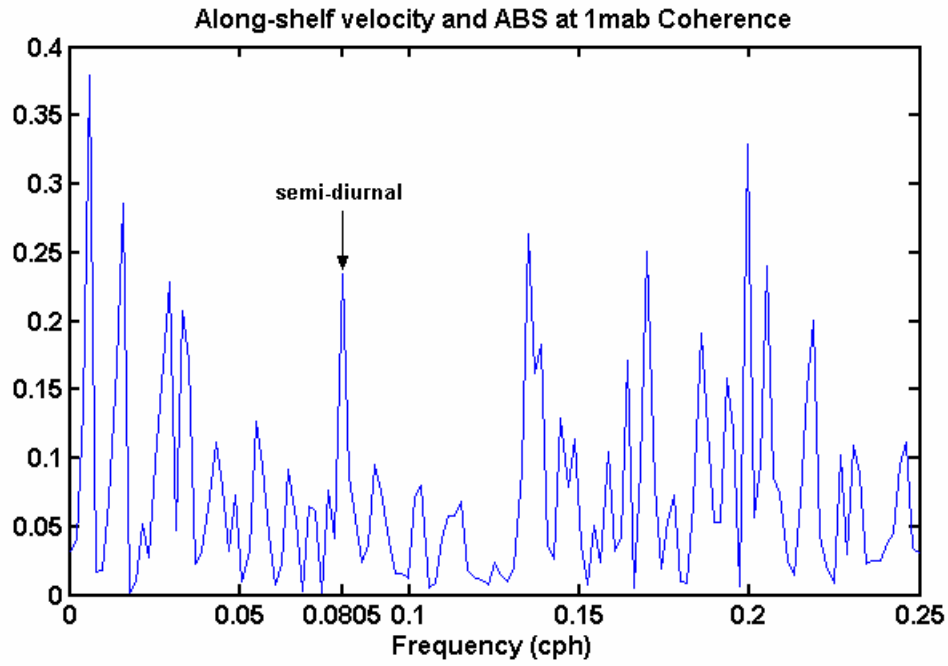


**Figure 18.** Spectra of the acoustic backscatter signal from the PC-ADP at 1 mab for all data during the study.

a.)



b.)

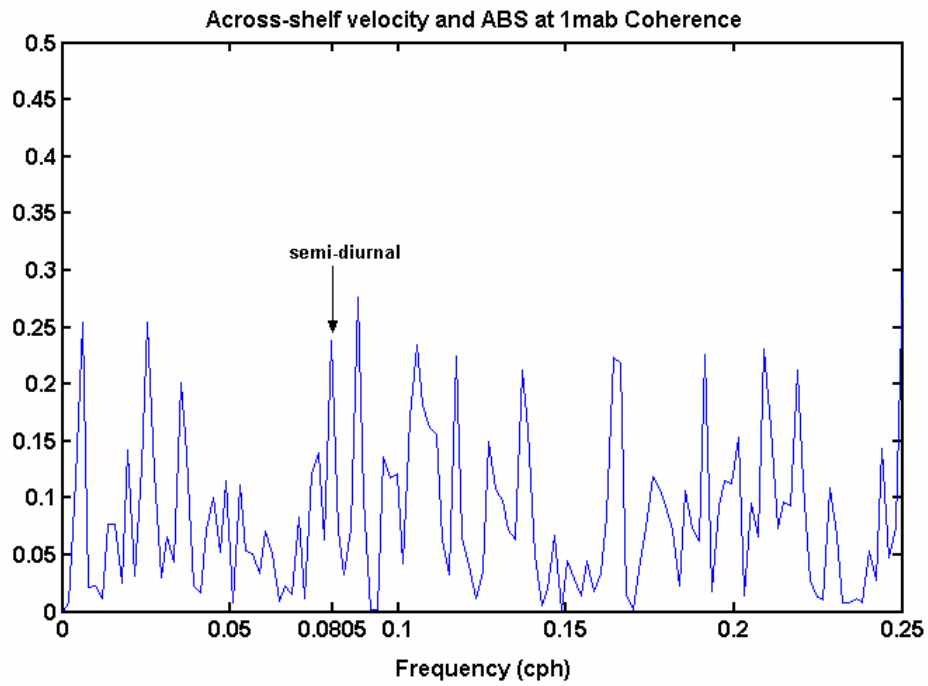


**Figure 19.** a.) Coherence between the along-shelf current and the acoustic backscatter signal at 1 mab. (b.) Coherence between the across-shelf current and the acoustic backscatter signal at 1 mab.

shelf velocity spectra (Fig.17) show a large amount of energy in the lower frequencies ( $0.001 - 0.01 \text{ hr}^{-1}$ ) as does the ABS spectra at 1mab (Fig.18). More energy occurs in the lower frequencies between  $0.004 - 0.006 \text{ hr}^{-1}$  (7 – 10 days) in the along-shelf current spectra than the across-shelf current spectra. This result suggests that the along- shelf currents respond more to the synoptic wind events than do the across-shelf flows. The coherence between the along-shelf current and the ABS at 1mab was higher at a synoptic event frequency ( $0.006 \text{ hr}^{-1}$ ) than at the tidal frequencies, while the across-shelf coherence was largest at the semi-diurnal tidal frequency. This suggests the important role of storm events in the transport of sediments in the along-shelf direction, as well as the importance of Gulf Stream events in the summer.

#### 2.4.3 Mean circulation

The previous calculations of shear velocities and sediment fluxes in the bottom boundary layer clearly show that sediment transport occurs throughout a majority of the year at this location on the mid-shelf. To understand the sediment transport that occurs on the shelf, knowledge of the regional mean shelf circulation of the bay can help to determine the movement, dispersal, and transport of sediments in the bottom boundary layer. *Re-suspension* of bottom material must be distinguished from the *transport* of material because processes that initiate sediment motion (waves) are not the same as those that transport sediments over significant distances (Butman *et al.*, 1979). The circulation patterns of mean flows that occur in the bay during different wind and wave directions must be known and related to the hydrodynamics of the bottom boundary layer. Fortunately, the circulation of Onslow Bay has been studied extensively (Chao and Pietrafesa, 1980; Weisberg and Pietrafesa, 1983; Pietrafesa and Janowitz, 1979; Xie *et al.*,

1996). The results of these studies, in conjunction with long-term boundary layer measurements, can be used to examine the relationship between the bottom boundary layer and the large-scale circulation and to characterize sediment transport.

Examination of the atmospheric pressure and the low-passed wind velocity data for each season indicates that northerly winds were generally associated with higher atmospheric pressure, and southerly winds were associated with lower atmospheric pressure throughout the study. Previous studies have shown that the currents associated with winds from the north and west cause a seaward sloping sea-level gradient throughout the water column due to coastal setup (Pietrafesa, 1985). This sea-level gradient results in a southwestward directed geostrophic flow. The 40-hour low-passed bottom pressure time series from the PCADP indicates that northerly winds are associated with an increase in sea level at the site. This increase in sea level was coincident in the time series data with positive along and across-shelf flows; the opposite was observed for southerly winds. This relationship existed for all of the seasons examined. The opposite setup of the bay was observed for winds from a southerly direction.

An example of this setup of circulation in the near-bottom flows can be seen in the Fall 2000 time series data during a northerly wind event that occurred from September 5<sup>th</sup> – 10<sup>th</sup> (Figs.12,13). An increase in atmospheric pressure is evident when the winds immediately switched from southerly to northerly and increased in magnitude. The sea-level time series shows a significant increase at this time due to the “pile up” of water along the coast resulting in the barotropic flow offshore. Currents in the positive along- and across-shelf responded rapidly at the site, resulting in a significant increase in

the along-shelf direction at 1mab. However, due to Ekman steering in the bottom friction layer, there was also a considerable increase in the positive across-shelf velocity (offshore) at 1mab. These data suggest that data collected during previous large-scale circulation studies of Onslow Bay can be useful in generally characterizing sediment transport on the shelf, when the Ekman steering effect in the bottom boundary layer is taken into account.

During this study, the mean velocities from 4mab and 1 mab calculated for all the data in both the along-shelf and across-shelf directions were very similar (Table 2). This result suggests that current data collected in large-scale circulation studies, if collected within the bottom several meters of the water column, can be used to characterize sediment transport patterns on the shelf. However, during this study, there was a slight difference in current velocity measurements from the two instruments that occurred during strong northeasterly and northerly winds when the measured velocity in the bottom 1 mab appeared to be in a shadow zone of the reef ledge. If sediment transport that occurs adjacent to a reef ledge were the topic of study, then measurements in the bottom 1 m of the boundary layer would be necessary. However, it is apparent that when net sediment transport on the mid-shelf is examined, current data collected in the lower 5 mab would be sufficient. If measurements of sediment concentration in the bottom 1mab were not collected, then current velocity measurements could be used as input into a bottom boundary layer model where concentration profiles could be generated.

## 2.5 Conclusions

During the four seasons included in the study, sediments were active at the site on the mid-shelf and shear velocities exceeded the critical threshold for sediment motion 75% of the period of record. Sediment flux at 1 mab was toward the northeast in the negative along-shelf direction during all seasons except autumn (Table 3). More than three times the *net* suspended sediment flux occurred in the across-shelf direction than the along-shelf direction, transporting sediments in the onshore direction during every season except the fall. More sediment transport per day took place during the winter than any other season. The forcing mechanisms for sediment transport on the mid-shelf in Onslow Bay appear to be a complex combination of: waves, tidal currents, and low-frequency and mean shelf currents. Wave orbital velocities were highly correlated with the ABS values at 1mab, suggesting a dominance of wave resuspension at the site. Power spectra of the current velocities and the ABS measurements both show peaks at the tidal frequencies, suggesting that the tides do play a role in transporting the suspended sediments on the shelf. Subtidal and mean current flows were one of the important processes in determining in what direction and what distance sediments will be transported on the mid-shelf. The coherence between the along-shelf current and the ABS at 1mab was higher at synoptic event frequency ( $\sim 7$  days) than at the tidal frequencies, while the across-shelf coherence was largest at the semi-diurnal tidal frequency.

During this study, the mean velocities from 4mab and 1 mab calculated for all the data in both the along-shelf and across-shelf directions were very similar. These data suggest that data collected during previous large-scale circulation studies of Onslow Bay

can be useful in generally characterizing sediment transport on the shelf, when the Ekman steering effect in the bottom boundary layer is taken into account. However, if one's interest lies in examining sediment transport next to reef ledges, due to the localized effects the reef may have on the hydrodynamics and the sediment supply, circulations patterns in these locations may vary.

## Chapter III

### **Physical forcing and sediment mobilization on the mid-continental shelf in Onslow Bay, North Carolina**

#### **3.1. Introduction**

It is well documented that storm driven processes dominate sediment transport on many continental shelves and are an important factor in coastal change (Madsen *et al.*, 1993). Geological processes, such as sediment resuspension and transport caused by associated physical forcing mechanisms, are important in Onslow Bay, North Carolina because of fisheries habitats and associated management and the increase of shoreline development. Several studies have been conducted in Onslow Bay that document the fluid forcing associated with low frequency currents and circulation patterns (Atkinson *et al.*, 1976; Blanton and Pietrafesa., 1978; Bane and Brooks, 1979; Singer *et al.*, 1980; Hoffman *et al.*, 1981; Pietrafesa, 1989; Xie *et al.*, 1997). These studies have shown that Onslow Bay is dominated by three principal forcing mechanisms: winds and related air-sea fluxes, tides, and the Gulf Stream. Studies conducted on the geology of Onslow Bay have shown that the introduction of new sediment to this system is negligible due to limited fluvial inputs and minimal sediment exchange between adjacent shelf embayments (Blackwelder, *et al.* 1982). Milliman (1972) classified the Onslow Bay shelf sediment cover as residual; that is derived from the erosion of underlying sediment and rocks. Additionally, a number of geophysical surveys have been conducted to describe the geologic framework of the inner to middle shelf of Onslow Bay (Cleary and Pilkey,



1968; Blackwelder *et al.*, 1982; Riggs *et al.*, 1998). These surveys have been coupled with descriptions of substrate characteristics and bedform morphologies, but little attempt has been made to combine hydrodynamic data with geological data to elucidate the mechanisms driving sediment transport on the shelf.

A quadrapod frame has been maintained on the mid-continental shelf since April of 2000 as part of the Coastal Ocean Research and Monitoring Program (CORMP) at the University of North Carolina at Wilmington. This multidisciplinary study was initiated to monitor the physical, geological, chemical, and biological processes occurring on the continental shelf in the northern portion of the South Atlantic Bight (SAB) during fair-weather and storm events. The frame is moored 27 nautical miles off the coast of Wilmington, NC in Onslow Bay at a depth of approximately 29 meters adjacent to a biologically productive marine hardbottom. In May of 2000, a downward looking Pulse-Coherent Acoustic Doppler Profiler and an upward looking Acoustic Doppler Current Profiler were deployed and attached to the frame. Acoustic backscatter data collected within the bottom boundary layer, seabed altimetry data, and measurements of the physical properties of the water column, such as temperature and salinity, are also examined. This paper focuses on the velocity measurements in the lower 1.5 meters of the water column and at a height of approximately 4 meters above the bed (mab). Measured velocity and suspended sediment profiles in the lower boundary layer were compared with profiles generated by a bottom boundary layer model (Styles and Glenn, 2000; 2002) and model predicted ripple heights and wavelengths are compared with seabed altimetry data. The bbl model was used to calculate wave-current combined bed shear stresses. The objective of this paper is to identify and quantify the magnitude,

frequency, and duration of physical forcing mechanisms resulting in sediment mobility at the study site and to quantify sediment transport that occurred during the study period, from May – December, 2000. Another objective of this study is also to verify bottom boundary layer model current profiles with measured current profiles, as well as compare the shape and relative changes in the acoustic backscatter profiles with suspended sediment concentration profiles.

### **3.2. Field Experiment**

#### *3.2.1 Study Site*

##### *3.2.1.1 Geological setting*

Onslow Bay is located off the southeastern coast of North Carolina and is bounded to the northeast and southwest by Cape Lookout and Cape Fear, respectively, and by the Gulf Stream at the shelf edge (Fig. 1). The inner to middle continental shelf of Onslow Bay is characterized by a complex sequence of rocky outcrops with relief up to 10 m (Renaud *et al.*, 1997). The hardbottom habitats form extensive, irregular reef tracts due, in part, to the area being sediment starved. Although a thin and discontinuous veneer of Holocene sediment exists, surface sediment is generally not accumulating on the shelf. The introduction of new sediment to this system is negligible due to limited fluvial inputs and minimal sediment exchange between adjacent shelf embayments (Blackwelder *et al.* 1982). The major sources of sediment for the inner and mid-shelf are shoreface bypassing of unconsolidated ancient sediment and bio-erosion of marine hard grounds on the inner shelf. The upper hardbottom and lower sand flat sub-habitats are the major components of the Onslow Bay hardbottom system (Renaud *et al.*, 1997).

The reef at the study site is approximately 2 m in relief and is known as “23 Mile Rock”. Two types of sand bodies are dominant at the site: rippled, gravelly, coarse sand patches and fine sands. The fine sands are found on top of the hardbottom and in aprons adjacent to the reef. The coarse, gravelly sands are only found on the lower sand flats and are not on the upper hardbottom surfaces. Major differences in the distribution and thickness of the fine sands on the upper hardbottom have been observed (Renauld *et al.*, 1996) suggesting that these fine sands are mobile and readily suspended during sediment transport events.

#### 3.2.1.2 Physical setting

The mean tidal range in Onslow Bay is approximately 1.0 m and mainly consists of M2 frequency oscillations (Pietrafesa *et al.*, 1985). Average significant wave heights are 1.5 m with an average dominant period of 8.0 seconds (NOAA, FPSN7 C-Man station). During the summer months, winds are generally out of the southwest and mild. Waves consist of longer period (9-10 second) fair weather swells moving across the shelf. The influence of the Gulf Stream on the shelf is more common during summer months due to the decreased density gradient between the shelf and Gulf Stream water (Pietrafesa *et al.*, 1985). Filaments, meandering eddies, and persistent southerly winds are all physical forcing mechanisms that transport the Gulf Stream (GS) water onto the shelf. Generally, water in Onslow Bay is more saline than that of the Middle Atlantic Bight to the north and the Georgia Bight to the south due to the proximity to the GS and relatively low river input along the Carolina Capes (Pietrafesa *et al.*, 1994).

During winter months, dominant winds are associated with weather fronts passing through the area on a 4-10 day period (Pietrafesa *et al.*, 1985). Winds blowing from the

north and northeast during the passage of these fronts generally are stronger than the gentle southwest winds in the summer. These north winds create steeper, smaller period waves with higher significant wave heights.

### *3.2.2 Instrumentation and data collected*

A downward looking Sontek Pulse-Coherent Acoustic Doppler Profiler (PC-ADP) and an upward looking Acoustic Doppler Current Profiler (ADCP) were deployed on the mid-continental shelf (33° 59'N, 77° 21'W) approximately 25 to 100 m from “23 Mile Rock” (Fig. 2). The instruments were mounted on a 2 m tall frame situated at approximately 29m depth. The PC-ADP samples in “burst mode” at 1 Hz for 17 minutes every 2 hours. Secured 150 cm above the seabed, the downward looking 1.5 MHz PC-ADP measures velocity profiles of the bottom boundary layer in 10 cm bins. When examining bottom conditions and calculating bed shear stresses, the velocity time series at 1 mab was used as an arbitrary elevation above the bed. The along-shelf axis is taken at 55.6° east of north following Pietrafesa *et al.* (1994) and is positive towards the southwest in this paper; the across-shelf direction is positive in the offshore direction.

The PC-ADP also measures temperature and pressure, and serves as a bottom altimeter to monitor changes in seabed elevation. The 3 acoustic beams in the downward-looking transducer detect where the seabed is located under the frame once during each 17 minute burst. These data can be averaged or examined individually to determine relative changes in seabed elevation. To measure changes in turbidity, the acoustic backscatter signal amplitude from the 1.5 MHz PCADP was used. The instrument uses Doppler shifting of the acoustic backscatter signal from the suspended particles in the water column to determine flow velocities, and therefore records the

amplitude of the backscatter signal. The amplitude of this signal can be used as a proxy for measuring relative changes in suspended sediments in the bottom boundary layer. This approach is similar to the Acoustic Backscatter Sensor, which has been shown to be especially successful with sands in sediment transport studies in the U.S. and the U.K. (Traykovski, 1999; Battisto, 2000; Williams and Rose, 2001).

Also mounted on the frame is an upward-looking 600 kHz RDI Workhorse Sentinel ADCP that profiles the overlying water column in 1m bins at 1 Hz. These data are averaged over a 60 second averaging interval and record a velocity profile of the upper water column every 5 minutes. In addition, a Microcat (Seabird SBE 37-SM) was attached to the frame and collects conductivity, temperature, and pressure once every 5 minutes in order to identify the different water masses occupying the site. Approximately 12 m from the frame, a mooring line equipped with a second Microcat at mid-depth collects conductivity and temperature at the same sampling rate which enables identification of the frequent stratification that occurs in Onslow Bay. Hourly averaged wind velocities and wave characteristics were obtained from the nearby NOAA C-Man station at Frying Pan Tower (Fig. 1).

Seabed altimetry and diver collected boxcores, pre- and post storm, were used to examine the depth of sediment reworking following storm disturbance. A sediment tube was also attached to the bottom of a leg of the frame to collect sediments that were suspended in the water column during the storm. Boxcores are sub-sampled at different depths and, along with suspended sediment samples, grain size distributions were determined using a Beckmann-Coulter LS 200 particle-sizer.

### 3.2.3 Data Analysis

Time series of velocity, acoustic backscatter, and seabed elevation data from the PC-ADP, along with available wind and wave data from a nearby NOAA C-Man station (FPSN7) were all used in concordance to identify and classify sediment transport events that occurred over the study period. A total of four events were documented (Table 1), although additional events did occur but were not sampled due to the equipment maintenance schedule. These events were easily identified in the ABS and seabed elevation time series data during each of the deployments.

A bottom boundary layer model (Styles and Glenn, 2002) was used to calculate shear velocities, as well as make bottom roughness predictions throughout the four events. This bottom boundary layer model (bbbm) is a modified version of the Grant-Madsen-Glenn model (Grant and Madsen, 1979; Grant and Glenn, 1986), which has been updated to incorporate changes in bottom roughness due to ripple migration. It also has been updated to use a more continuous 3-layer eddy diffusivity profile, which has been adjusted for the decay in turbulent kinetic energy that occurs at the top of the wave-boundary layer. This model has been calibrated in laboratory studies and verified in a limited number of field studies. The input data that were used to run the model included: (1) time series data of the PC-ADP burst-averaged mean current ( $U_r$ ) measured at a 1 mab reference elevation ( $Z_r$ ) in the bottom boundary layer, (2) time series of near-bottom orbital velocities ( $U_b$ ) and near bottom wave excursion amplitude ( $A_b$ ), (3) a time series of the wave and current incidence angle ( $\Phi_{cw}$ ). Wave direction was obtained by finding the angle of maximum variance using the raw PC-ADP data from 1 mab. Wave orbital

velocities were calculated from the recorded hourly wave height and period data at FPSN7 using linear wave theory where:

$$U_b = \sqrt{2} * (a \omega / \sinh(kd))$$

and  $H_{rms} = H_s/\sqrt{2}$ ,  $a = H_{rms}/2$ ;  $\omega = 2\pi/T_{dom}$ , and  $k=2\pi/L$ . A comparison between wave data at FPSN7 and another bottom mounted ADCP that collected wave data on the inner shelf in Onslow Bay indicated that wave conditions were similar at both sites.

Five grain sizes were used in the model calculations based on the grain size distributions of surface sediment samples collected prior to each event. A default for ripple height and wavelength were also input into the bblm. All of the input parameters were obtained from current and wave measurements, sediment samples, and altimetry data. In addition, diver observations were made of ripple characteristics while taking boxcores during deployment and retrieval of the instrumentation. Time series of shear velocities due to currents and wave-current interactions were generated for four events. Critical shear stresses were calculated based on the median grain size found in surficial sediment samples. Time series of the bedload transport rates were also determined using the Meyer-Peter-Muller equation for bedload (Meyer-Peter and Muller, 1948) with the model calculated shear stresses and the median grain diameter during each event.

In addition, the vertical profiles of current, suspended sediment concentration, and sediment transport were generated for selected individual bursts occurring pre, post, and during two events in order to compare the bblm generated current and concentration profiles with field measurements. The sediment transport profiles were vertically integrated and the weight of each grain size fraction that was in suspension has been determined.

Throughout the study, the ABS data were corrected for the effects of geometric spreading and absorption of the acoustic signal to allow for comparison of data from different elevations in the profile. Spreading and absorption cause decay in signal strength with increasing range from the transducer. This decay can be predicted by using the formula:

$$\text{DECAY} = -20 * \log_{10}(Z/\cos(15^\circ) - 2 * \alpha * (Z/\cos(15^\circ))),$$

where,  $\alpha = 0.68$  and is the sound absorption coefficient for 1.5 MHz and 35 ppt salinity, (Z) is the range bin in cm above the bed, and  $15^\circ$  is the angle of emission of the signal (Sontek, 2003). A measurement of approximately 20 dB was taken as the reference level, or “background level”, for the lower water column during fair-weather conditions; therefore, the ABS profile plots show the relative increase from this level. The bottom bin was also removed from the ABS profiles due to the reflection off of the seabed, which created a falsely high measurement in the lowest 10 cm.

### 3.3 Results

#### 3.3.1 Average wave, tidal, and physical properties

The maximum spring tidal range over the seven-month period was 2.0 m. The pressure time series shows a dominant semi-diurnal tidal signal, although a weaker diurnal signal was also present. Temperature of the near-bottom water on the shelf displayed a seasonal cycle and ranged from  $15^\circ\text{C}$  in late November to  $27^\circ\text{C}$  in September. Additionally, water temperatures and salinity measurements in the lower water column varied due to the presence of different water masses on the shelf and the vertical flow structure of the overlying water column. These fluctuations range in time



scale from a few days to 2 weeks and in temperature 2-5°C (Bingham, personal communication).

### 3.3.2 Currents

Throughout the duration of the study, the mean depth-averaged current in the lower 1.5 m was  $2.5 \text{ cm s}^{-1}$  directed towards the north. Bottom current data from the PCADP was dominated by wave oscillations superimposed on tidal and lower frequency flows. Analysis of current data show that near-bottom flows had the potential to include contributions from locally generated wind-waves, swells, infragravity oscillations, tidal, inertial, and subtidal flows (Table 4). In order to separate the relative contribution of each, bandpass and lowpass filters were used following Wright *et al.*, (1999) and Storlazzi and Jaffe (2002). Cut-off frequencies corresponding to periods of 10-16 hours and 20-28 hours were used for the semi-diurnal and diurnal components, respectively. Inertial motion, which has a frequency of approximately 21.5 hours, was not separated from the diurnal signal because of setup of the cutoff frequencies, with both of these frequencies in the 20-28 hour band. Infragravity oscillations (Table 4) were filtered using a cutoff frequency of 0.0333-0.00333 Hz ( $T=30\text{-}300\text{s}$ ). A 36-hour lowpass filter was used to separate the subtidal currents from the burst-averaged velocity time series.

The magnitude of the mean and maximum semi-diurnal tidal flows were two times the magnitude of the velocities due to inertial motion and diurnal tides. Mean and maximum subtidal flows, which were wind driven flows in most cases, were greater than the mean and maximum tidal flow velocities. The highest near-bottom velocities were recorded during wind events when wave oscillations and tidal currents were additive and superimposed on wind-driven subtidal flows.

Table 4. Mean and maximum velocity magnitudes for the flow components at 1 meter above the bed during the deployment period.

Component	Mean +/- 1 S.D. (cm s <sup>-1</sup> )	Max. (cm s <sup>-1</sup> )
Infragravity	1.6 +/- 2.1	22.5
Semi-diurnal	2.0	9.7
Diurnal and inertial	0.9	4.7
Subtidal	6.8	26.7

Table 5. Maximum measurements of atmospheric, hydrodynamic, and sediment mobilization characteristics during three wind events. Bottom orbital velocities ( $U_b$ ) and mean currents are reported at 1 meter above the bed.

Storm event	Winds ( $\text{m s}^{-1}$ )	Duration (Hours)	$T_{\text{dom}}$	Avg. $U_b$	Mean Currents ( $\text{cm s}^{-1}$ )	Acoustic Signal (dB)	Avg. $\Delta$ seabed (cm)
I	12-15 N-NE	48	5-8	30-40	20	20-35	-1
III	15-18 N-NE	60	5-8	35-50	30	35-40	-3
IV	16-21 SE	12	9-10	100	<10	30-40	+2

### 3.3.3 Sediment transport

During the deployment period, sediment mobilization occurred during 3 types of events: northerly wind events, a southerly wind event, and during fair weather. The 2 types of wind events are typical for the different seasons throughout the year. Events I and III (Table 5) were northerly wind events that generated significant wave heights on the order of 2.5 to 3.5 m, respectively, and hourly averaged wind speeds from 15-20 m s<sup>-1</sup>. Event IV (Table 5) was also a wind event that occurred at the end of November when winds were directed out of the south at approximately 20 m s<sup>-1</sup> and significant wave heights increased to over 5m. Sediment mobilization was associated with each of these wind events, but also was observed during a period of fair weather. Over a three-week period in June 2000, persistent and relatively strong subtidal currents were measured in the velocity time series and T-S values suggested that Gulf Stream water was present at the site. Coincident with this recorded Gulf Stream event, the seabed altimetry data exhibited a gradual increase in elevation under the frame. This period of sediment movement was identified as Event II.

#### 3.3.3.1 Event I - May 29-June 1, 2000

Event I was a northerly wind event that occurred during late spring at the study site from May 29 – June 1, 2000 (Table 5). Preceding the event, moderate southeasterly winds were dominant for several days before suddenly switching to northeasterly on May 29<sup>th</sup>. This type of rapid wind shift is typical of the spring season in this area because winds are in transition from a winter to a summer regime; therefore, Event I is classified as a “spring northerly wind event”. After the shift in wind direction, significant wave

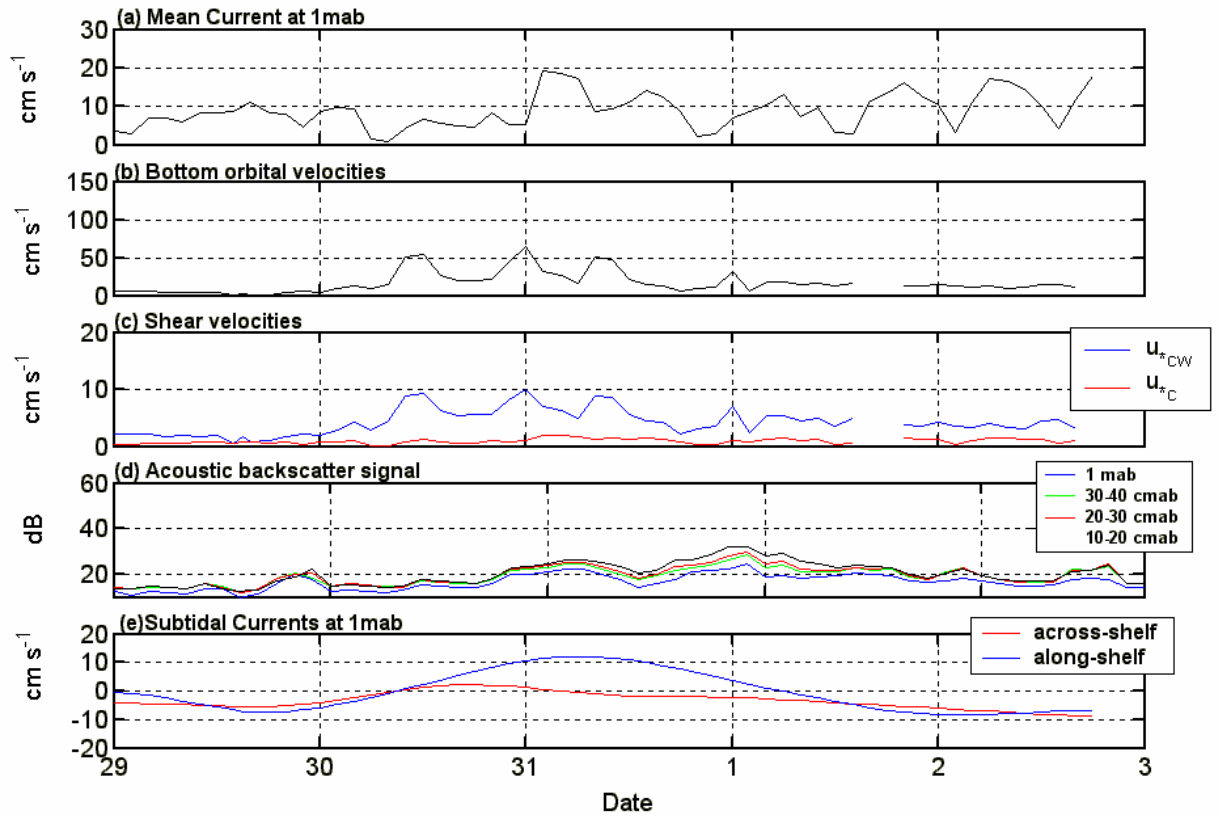


**Figure 20.** May northerly wind event (a) mean current speed at 1 mab (b) bottom orbital velocities (c) wave-current and current bed shear stresses (d) acoustic backscatter signal (e) along- and across-shelf subtidal currents.

heights increased to 1.5 – 2.5 m for 48 hours. Near-bottom orbital velocities generally ranged from 20-60 cm s<sup>-1</sup> throughout the duration of the event (Fig. 20). The mean current data from the PCADP shows that near bottom flows did not respond to the shift in wind direction until approximately 30 hours later on the 31<sup>st</sup>, shifting from northerly to south-southwesterly. Raw current data from the PC-ADP were run through a 60 second lowpass filter to remove surface waves and resulted in maximum flow magnitudes of 20 cm s<sup>-1</sup>. Currents measured by the ADCP at approximately 4 mab corresponded closely with the PC-ADP velocity time series after waves were removed. Subtidal flows of over 10 cm s<sup>-1</sup> towards the southwest developed in the bottom boundary layer after the water column responded to local winds and switched in direction on the 31<sup>st</sup> (Fig. 20e).

Combined wave-current shear velocities calculated by the bblm were approximately 6 - 10 cm s<sup>-1</sup>, corresponding to bed stresses of 37 - 100 dynes cm<sup>-2</sup> over the storm duration (Fig. 20c). The sediment transport associated with this magnitude wind event was evident in the acoustic signal and seabed elevation trace. The acoustic backscatter signal (Fig. 20d) exhibited an increase of 10-15 dB above background levels (15–20 dB) and remained high even after the wave activity waned. This pattern suggests sediment resuspension and possible transport at the site. The subtidal wind generated flows did not become developed until midway through the event, which limited the time in which sediment transport could occur, as well as the distance of transport. The ABS does, however, indicate that the suspended sediment concentration continued to increase after storm peak conditions, and measurements remained elevated for 48 hours after peak

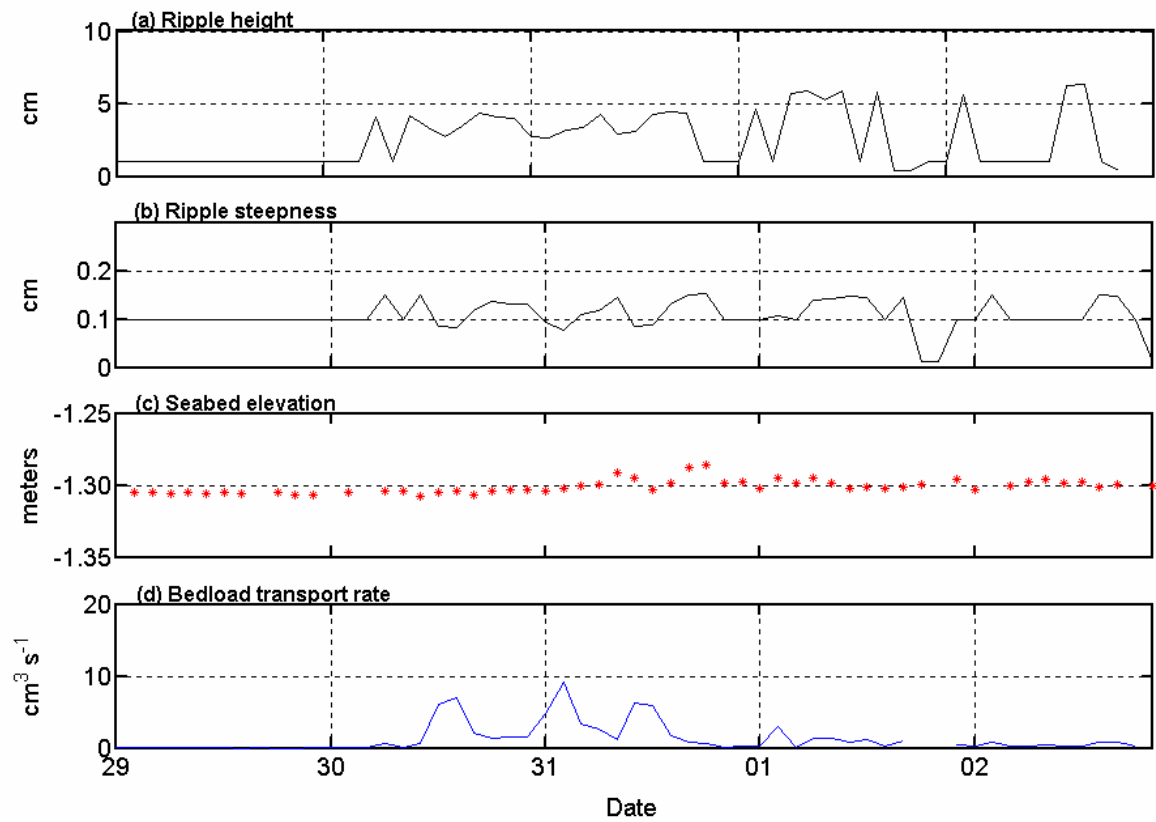


**Figure 21.** May northerly wind event: (a) model calculated ripple height and (b) ripple steepness (c) measured seafloor elevation (d) bedload transport rate.

storm conditions. This suggests that suspended sediment transport continued to take place for two days after the small northerly wind event. The suspended sediment transport that occurred during this event was predominantly in the positive along-shelf direction, or towards the southwest, in the direction of the subtidal currents.

The seabed altimetry data suggest that ripples were generated during the event. Small fluctuations of less than 1cm in relief are apparent in seabed altimetry time series over the course of the event, and there was little significant net change in elevation (Fig. 21c). According to model calculations, ripple heights were on the order of 3 – 4 cm during the event, with a steepness of approximately 0.1 (Fig. 21a,b). The model predicts that immediately after the event, ripple heights increased to 5 – 6 cm and steepness increased to 0.3. Larger fluctuations of 1 –2 cm are apparent in the seabed altimetry data at this time. Bedload transport calculations based on model calculated shear stresses and skin friction bed stress using the grain size of medium sand (0.04 cm) which would have been transported via bedload instead of suspension, indicated bedload transport occurred at a rate of  $2 - 9 \text{ cm}^2 \text{ s}^{-1}$  towards the south-southeast for 48 hours (Fig. 21d). The discrepancy between the model and the measured ripple heights is consistent in all the events and will be addressed later in this chapter.

#### *3.3.3.2 Event II - June 2-23, 2000*

Event II occurred during a period of fair weather and was associated with a Gulf Stream intrusion event. After the spring northerly wind event, the seabed altimetry data showed a gradual increase in elevation over the next 21 days (Fig 22), while the pressure sensor showed no evidence of frame settling. The water temperature near the bottom and at mid-depth increased from approximately 23.5 °C to 25.5 °C in a two day period from



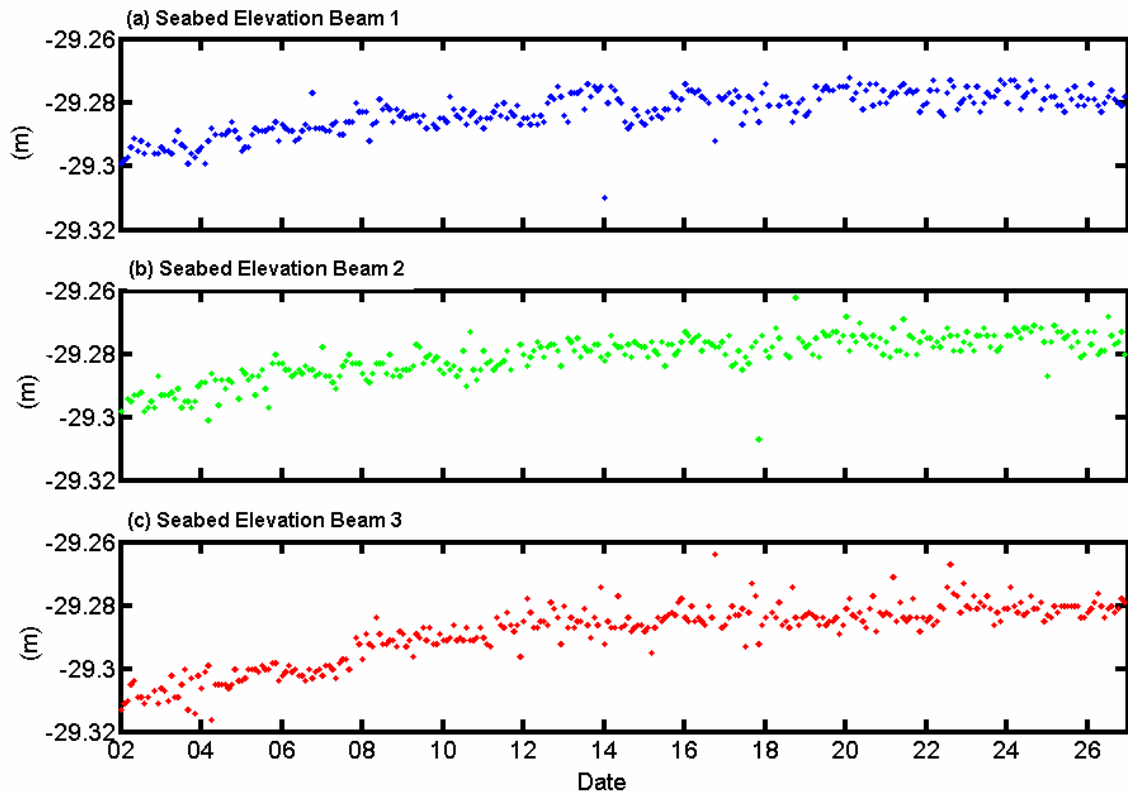


**Figure 22.** June 2 – 26, 2000 - the 3 individual beams of the PCADP all show a gradual increase in seabed elevation during the Gulf Stream intrusion event.

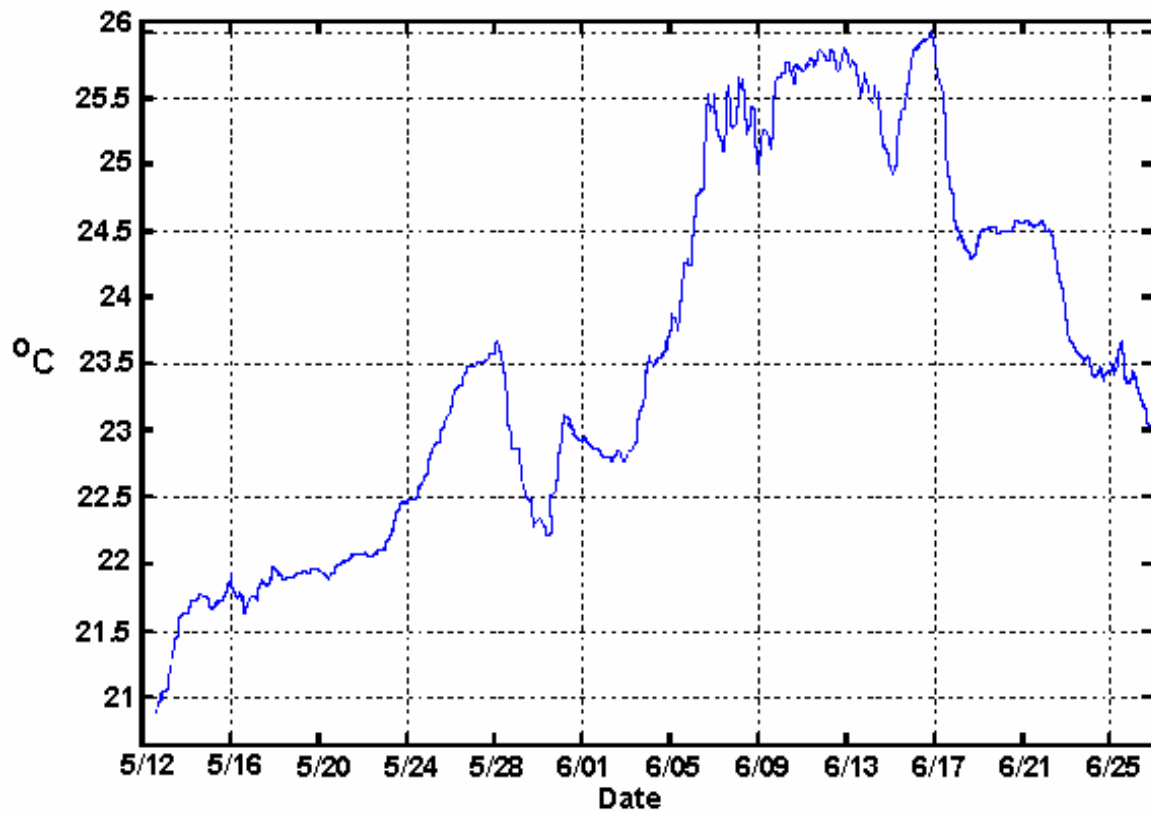


**Figure 23.** Pulse-Coherent Acoustic Doppler Profiler bottom temperature record from May 12- June 26, 2000. The Gulf Stream intrusion event occurred from approximately June 3 – June 23, 2000.

June 5<sup>th</sup> -7<sup>th</sup> (Fig. 23). Near-bottom and mid-depth salinities also increased concurrently with temperature during this time to greater than 36.5 ppt. This concurrent rise in temperature and salinity is indicative of a Gulf Stream intrusion on the shelf (Pietrafesa and Janowitz, 1980; Brooks and Bane 1981). Temperature and salinity data recorded in the upper water column during this 3-week period indicate that the water column was well mixed. At the end of the 3-week period, the water column became stratified again and near-bottom temperatures and salinities returned to values typical for June (23°C, 35.5ppt).

On June 1<sup>st</sup>, southwesterly winds of less than 10 m s<sup>-1</sup> began blowing and persisted over the next three weeks. These conditions were punctuated only by a 2 day period (7<sup>th</sup>-9<sup>th</sup>) of northerly 10 m s<sup>-1</sup> winds. Waves during this time were 1 m or less with dominant periods of approximately 9 seconds, except during the 2-day period of north winds when wave heights increased to 1.25 m with shorter dominant periods (Figs 24b,c). Near-bottom orbital velocities during this time were generally between 2 – 15 cm s<sup>-1</sup> over the three-week period (Fig. 25b). Near-bottom mean currents rotated between north and east and were between 0 and 20 cm s<sup>-1</sup> (Figs. 24d, 25a) due to the semi-diurnal tidal flows superimposed on the low frequency subtidal currents. Large subtidal flows at 4 mab were from 10-20 cm s<sup>-1</sup> toward the northeast, except during the two-day occurrence of northerly winds when flows reversed direction and decreased in magnitude. The near bottom flows were similar throughout the period with magnitudes of approximately 5 – 10 cm s<sup>-1</sup> towards the north, or negative along- and across-shelf directions. During this three-week period, shear velocities due to wave-current interactions were between 1 – 5 cm s<sup>-1</sup>, corresponding to bed shear stresses between right below critical shear to 25 dynes

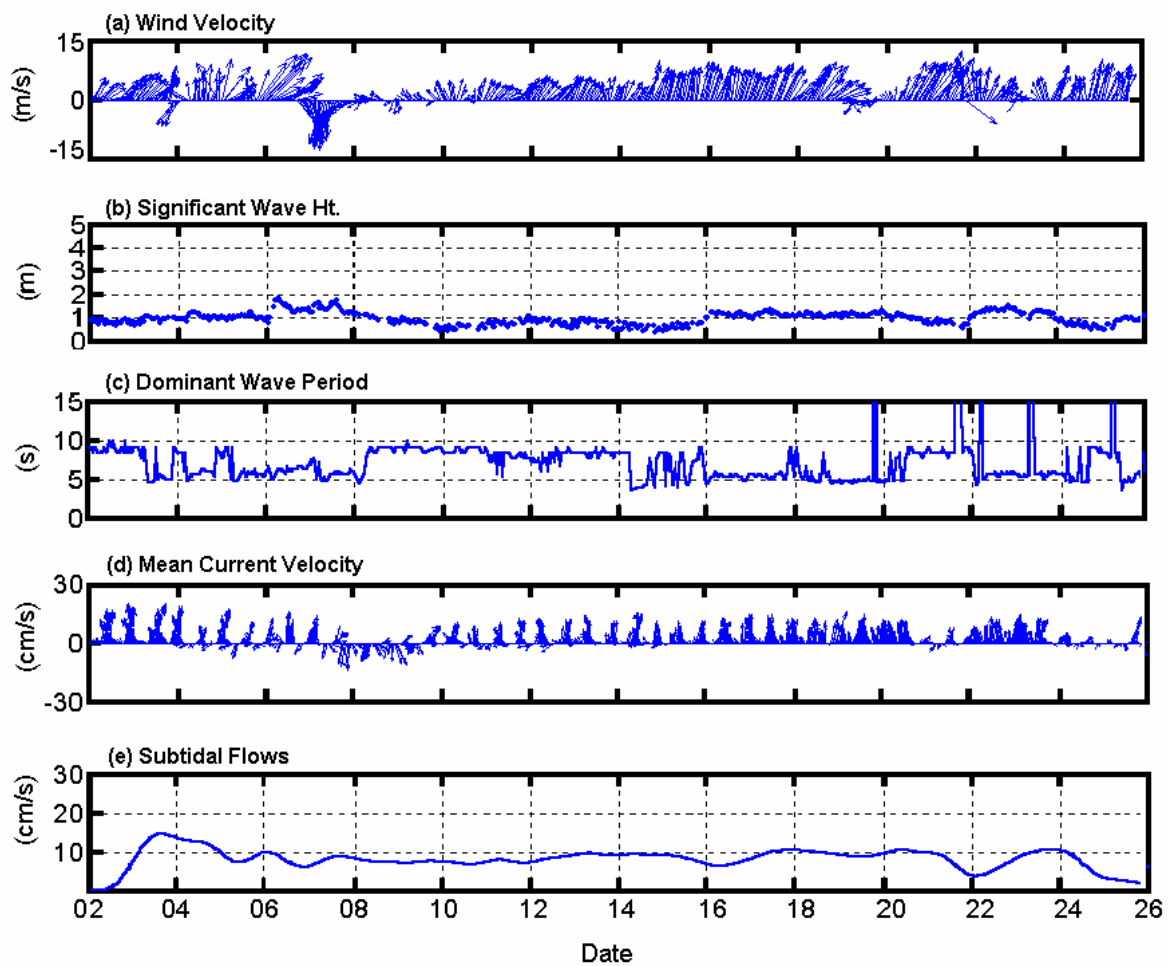


**Figure 24.** June 2 – 26, 2000 physical data: (a) wind velocity (b) significant wave height (c) dominant wave period (d) mean current velocity at 1 mab (e) subtidal flow speed.

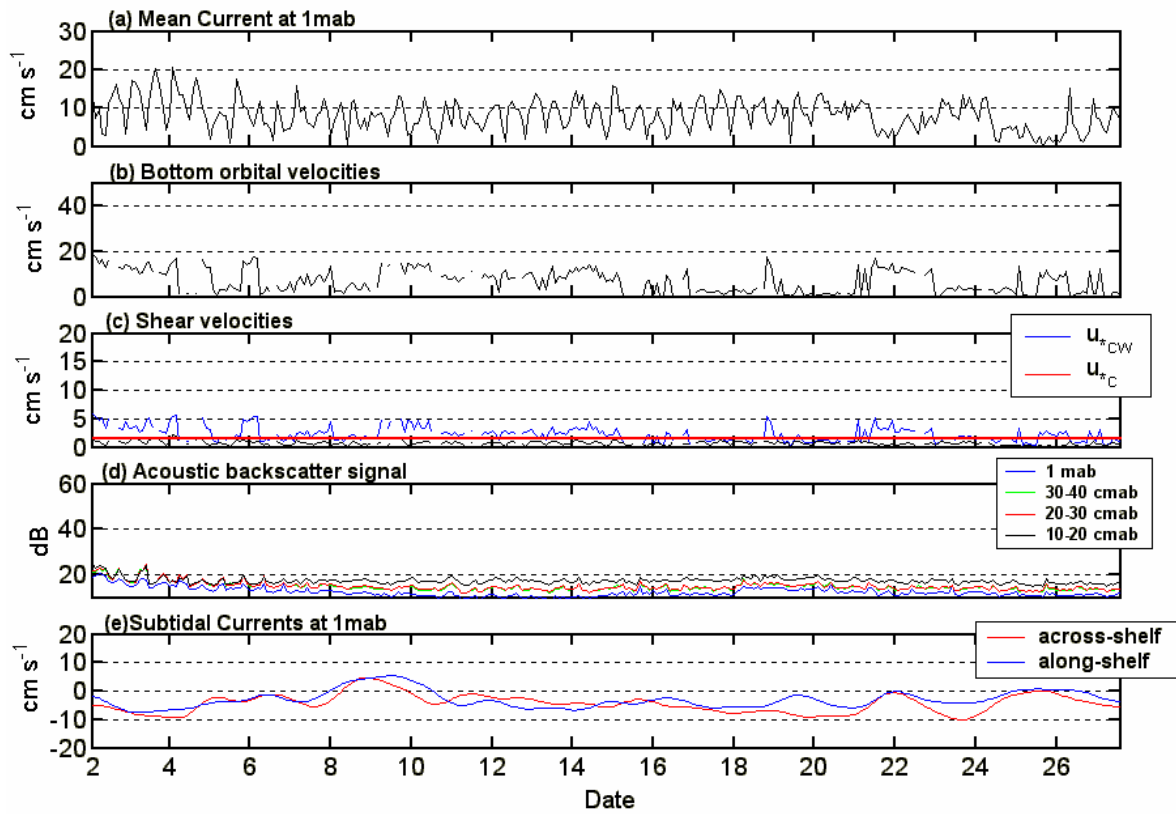


**Figure 25.** June 2 – June 26, 2000 (a) mean current speed at 1 mab (b) bottom orbital velocities (c) wave-current and current bed shear stresses (d) acoustic backscatter signal (e) along- and across-shelf subtidal currents. The red line in the third panel represents the threshold for sediment movement.

$\text{cm}^{-2}$  (Fig. 25c). The acoustic backscatter signal indicates that there was still a small amount of sediment suspended in the bottom boundary layer at the beginning of this three week-period (Fig. 25d). This is due to the spring northerly wind event (Event I) that immediately preceded this Gulf Stream intrusion event. Presuming sediments were suspended during this time, the change in direction of subtidal currents due to the Gulf Stream intrusion towards the northeast could have resulted in suspended sediment transport in opposition to that occurring during the previous wind event and returned some sediments to the site. These subtidal flows remained consistent towards the northeast over the next several days as ABS measurements returned to background levels.

The seabed elevation record from the PCADP measured a gradual and steady increase in seabed elevation ranging from 2.5 – 4.0 cm (Fig. 22). Further, the presence of small (1cm) ripples is evident in the time series, thus suggesting sediment mobility at the bed during this time. Bedload transport calculations corroborate this transport and indicate that bedload transport occurred intermittently at rates of approximately  $0.8 \text{ cm}^2 \text{ s}^{-1}$  throughout this time period (Figure 26d). The direction of bedload transport, based on the equation  $\tan\Phi_{bl} = \tan\Phi_{cw}$  (USACE, 2002), was directed towards between  $30^\circ$  northeast to  $30^\circ$  northwest. This direction results in bedload transport directed from between  $4.4^\circ$  to  $64.4^\circ$  from directly onshore. The observed accretion of sediment in the study area was likely caused by the longer period fair weather swells moving across the shelf that potentially interacted with the existing tidal and subtidal currents. Such an interaction could cause a slow creep of the fine sands found extensively to the south of the study site into the study area and, therefore, an increase in the seabed elevation indicated by the altimetry data.

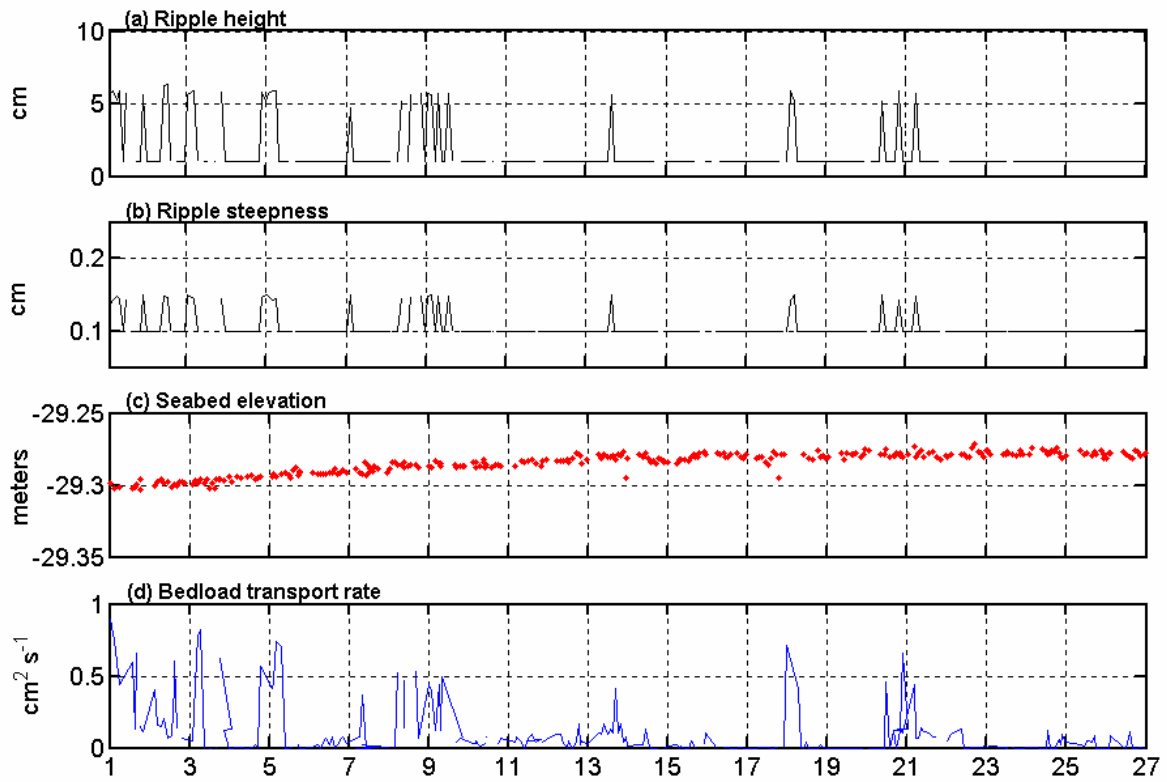


**Figure 26.** June 2 – June 26, 2000: (a) model calculated ripple height and (b) ripple steepness (c) measured seafloor elevation (d) bedload transport rate.

### 3.3.3.3 Event III – September 6-8, 2000

Event III was the second northerly wind event that occurred during early September at the site (Table 5). Preceding the event, wind and wave conditions were typical of fair weather conditions (winds  $<10 \text{ m s}^{-1}$  and waves  $<1 \text{ m}$ ). These conditions persisted for several days before winds suddenly intensified and switched to the northeast on September 6<sup>th</sup>. This type of activity is typical in September for Onslow Bay, when dominant winds begin to make the transition from the summer fair-weather conditions to the winter pattern due to pressure gradients from large-scale atmospheric systems (Pietrafesa *et. al.*, 1985). Therefore, Event III is classified as a late summer northerly wind event. After the shift in wind direction, significant wave heights increased to 2.0-3.0 m for 60 hours. Wave periods ranged from 5 to 8 seconds and were comparable to the wave periods measured during the spring northerly wind event. Near-bottom orbital velocities during this event ranged from 20-55  $\text{cm s}^{-1}$  (Fig. 27b). Maximum near bottom mean currents were 30  $\text{cm s}^{-1}$  in the along-shelf direction (southwest). The ADCP velocity time series and the 60-second low-passed PC-ADP velocities corresponded very closely and maximum mean currents were directed towards the southwest at 40  $\text{cm s}^{-1}$  at 4 mab during the event. Near bottom along-shelf subtidal flows were wind driven and dominated the velocity time series at 20  $\text{cm s}^{-1}$ .

During this wind event, the sediment response was rapid and substantial. Model derived wave-current shear velocities were of the order of 5-10  $\text{cm s}^{-1}$  during the event (Fig. 27c), corresponding to a range in bed shear stresses of approximately 25-100  $\text{dynes cm}^{-2}$  over the 60-hour duration. Current shear velocities were approximately 2  $\text{cm s}^{-1}$  during the event, creating bed shear stresses that exceeded the critical shear due to



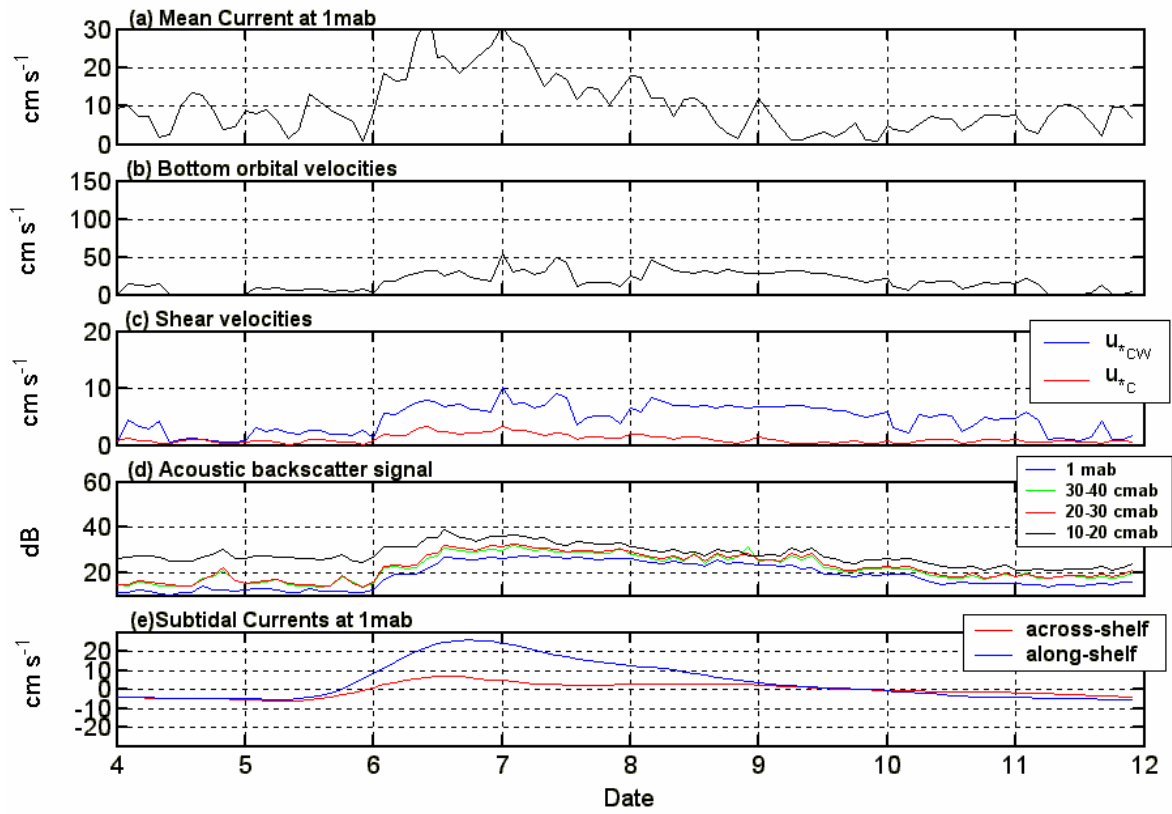


**Figure 27.** September northerly wind event (a) mean current speed at 1 mab (b) bottom orbital velocities (c) wave-current and current bed shear stresses (d) acoustic backscatter signal (e) along- and across-shelf subtidal currents.

currents alone. The ABS measurements were higher during this storm than during the May northerly wind event (Fig. 27d). The ABS increased immediately in response to surface winds and wave conditions, and the 40 hour low-passed filtered signal indicated that an increase to 35-40 dB was sustained throughout the event. Peak values during the peak storm conditions between 0000 UTC on the 6<sup>th</sup> and 0000 UTC on the 8<sup>th</sup> exhibited zero lag with surface conditions. The strong wind driven flow that occurred during the storm ranged from 10-30 cm s<sup>-1</sup> throughout the storm duration. As a result, the resuspended sediments were transported in the direction of the low-frequency flow, which was mainly along-shelf (southwest) with a slight component directed offshore (Fig. 27e).

The seabed elevation record for this event showed erosion of 3cm occurred during the first 24 hours of the event (Fig.28c). Fluctuations of 1cm in relief were observed in the time series over the subsequent two days suggesting continued ripple migration. The bblm predicted 4 cm ripples with a steepness of 0.1 during the event, except for late on the 7<sup>th</sup> when the bblm increases the steepness to 0.3 (Fig. 28 a,b). At the time the model increases the steepness, the fluctuations in the seabed elevation increase slightly. This is most likely due to the fact that steeper ripples can be detected more easily by the acoustic signal at the 15° angle from which is transmitted. The rates of calculated bedload were 2 - 9 cm<sup>2</sup> s<sup>-1</sup> throughout the storm event (Fig. 28d). Based on the critical shear for full suspension, all of the fine grained sediments would have been in suspension during this time, and bedload calculations were for the medium sands found at the site. Pre- and post storm boxcores collected approximately 1 meter from the frame(not under the frame where scouring could be a factor), showed approximately 3-4 cm of fine sediment erosion

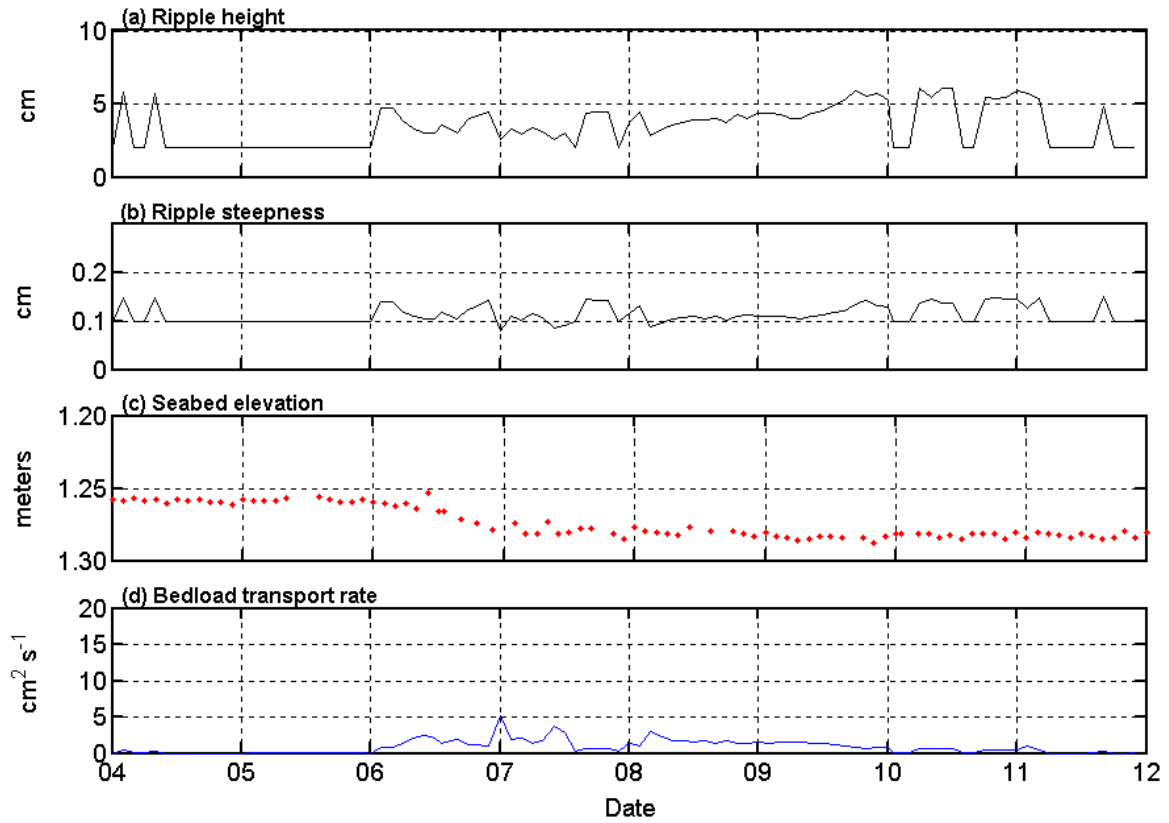


**Figure 28.** September northerly wind event: (a) model calculated ripple height and (b) ripple steepness (c) measured seafloor elevation (d) bedload transport rate.

from the surface. There was also less evidence of bioturbation in the post-storm cores, especially closer to the surface, again suggesting the removal of the upper more heavily bioturbated sediments. The observed erosion is most likely a consequence of a limited source of fine sediment on the hardbottom area located north and north east of the site, unable to replace that which was transported from the site.

#### *3.3.3.4 Event IV – November 25-26, 2000*

Event IV took place in late November and differed from the previous two events because winds were from a southerly direction (Table 5). Preceding this event, winds were typical of late autumn producing moderate sized northerly waves. On November 25<sup>th</sup>, winds shifted to southeasterly and then southwesterly and ranged in speed from 16 to 21 m s<sup>-1</sup>. Due to the large southeast and southwest fetch, waves immediately increased to over 4 m and remained between 4-5 m for 12 hours with dominant wave periods of 9-10 seconds. Near bottom wave orbital velocities were 65 – 70 cm s<sup>-1</sup> for approximately 12 hours, which then decreased to 40 cm s<sup>-1</sup> for the next 4 hours (Fig. 29 b). The near bottom current response to these intense southerly winds was minimal. Near bottom currents were dominated by the semi-diurnal tidal signal, although the tidal signal was dampened during the event. Mean current speeds at 4 m and 1 m above the bed were on the order of 10 cm s<sup>-1</sup>. Subtidal flows were less than 5 cm s<sup>-1</sup> in both the ADCP and PC-ADP time series (Fig. 29 e). During this event, shear velocities and bed stresses were the highest of any of the events on record. Shear velocities due to wave-current interactions increased from less than 2 cm s<sup>-1</sup> to slightly over 11 cm s<sup>-1</sup> within a few hours (Fig. 29c). This was primarily due to the high wave energy that created bed shear stresses in excess of 120 dynes cm<sup>2</sup> (Fig. 12c). The acoustic backscatter signal increased rapidly to

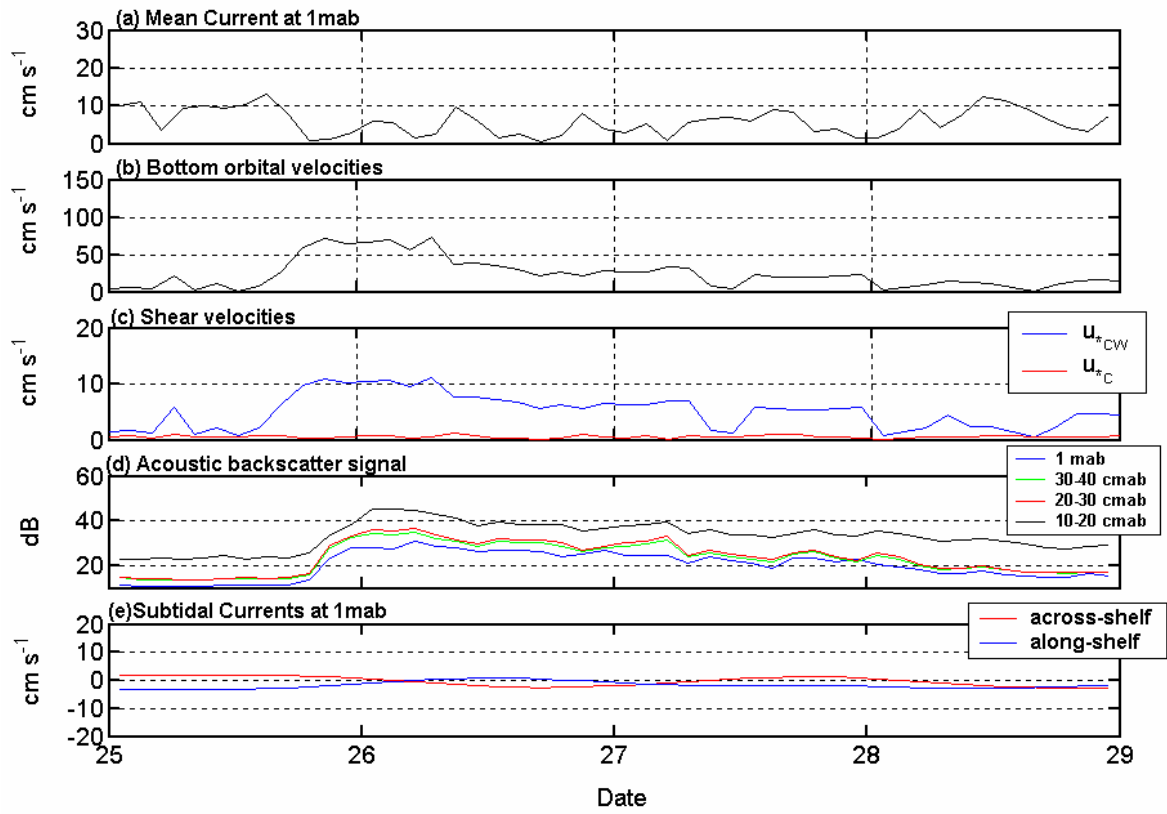


**Figure 29.** November southerly wind event (a) mean current speed at 1 mab (b) bottom orbital velocities (c) wave-current and current bed shear stresses (d) acoustic backscatter signal (e) along- and across-shelf subtidal currents.

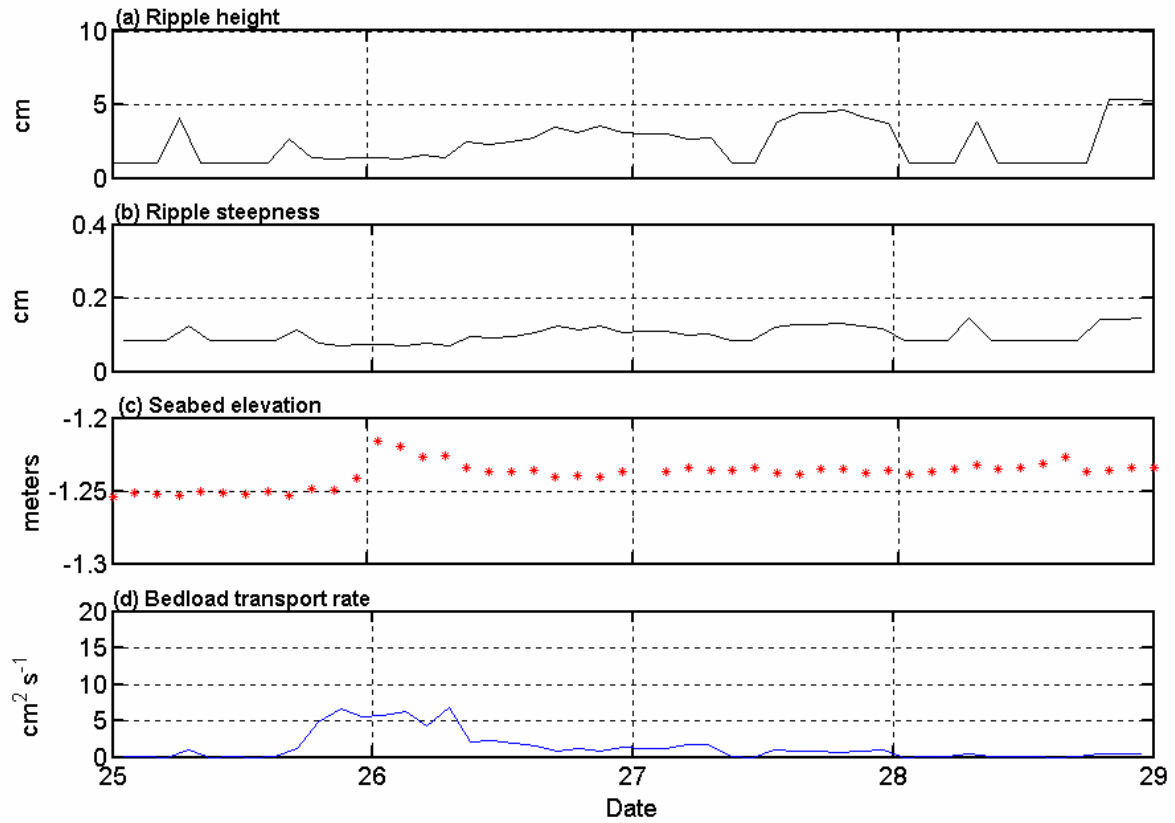


**Figure 30.** November southerly wind: (a) model calculated ripple height and (b) ripple steepness (c) measured seafloor elevation (d) bedload transport rate.

30-40 dB and remained elevated for 48 hours, and even longer in the lowest bin (Fig. 29d). Although the bed stresses computed for this event were the highest of all events recorded, wind driven subtidal flows were not generated because of the short duration of the event (12 hours). As a result, the suspended sediment transport during this event was very limited.

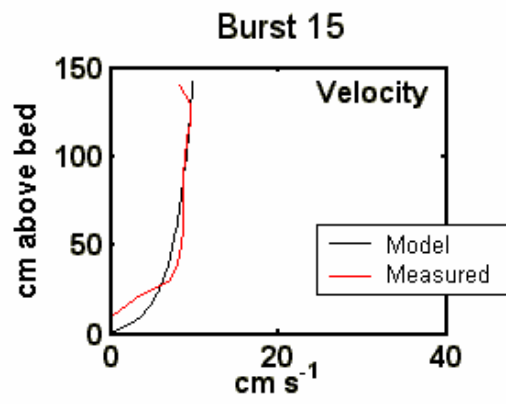
Model calculated ripple heights indicate that during the peak of this event, the ripples were washed out and “sheet-flow” conditions prevailed (Fig. 30a,b). After the waves resided, however, ripples formed with heights of 2-4 cm and wavelengths of 20 – 25 cm over the next 24 hours (Fig. 30 a,b). This activity is reflected in the seabed elevation data that show fluctuations of 1-2 cm in elevation after the intense wave conditions and net accretion of approximately 1-2 cm (Fig. 30 c) for the entire event. Due to the expanse of fine sands to the south of the study site, the small amount of sediment transport still resulted in a small amount of accretion at the site.

#### *3.3.4 Field measurements vs. model profiles*

The September northeasterly wind event and the November southerly wind events were selected to compare field measurements from the PC-ADP in the bottom boundary layer with the bblm generated current profiles. In addition, the suspended sediment concentration profiles from the model were compared with the ABS profile measurements to verify shape and magnitude as the storms increased and waned. In general, there was good agreement between the measured and model derived current profiles, and between ABS measurements and the model concentration profiles.

For the comparison, five bursts were selected from both Event III and Event IV. Bursts 15 (Event III) and 6 (Event IV) occurred before the storm during fair-weather

(a).



(b).

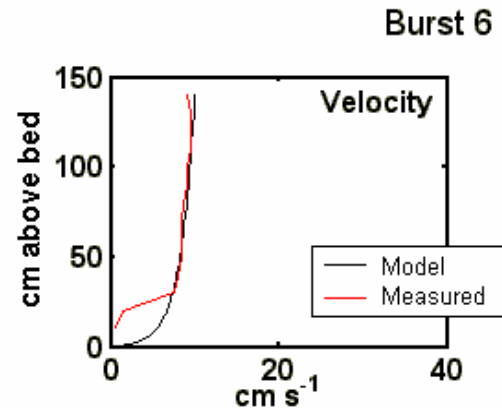


**Figure 31.** (a). Burst 15 – Pre-storm conditions before September event (b). Burst 6 – Pre-storm conditions before November event.



conditions (Fig. 31a,b). Current profiles generated from the model for these bursts were consistent with the measured profiles in both shape and magnitude. These conditions, representative of fair-weather conditions in the bottom boundary layer, were insufficient to actively resuspend sediments. Consequently neither the model output nor the ABS measurements indicated significant levels of suspended sediment at these times. Further, as no sediments were in suspension, the model output indicated no sediment transport.

The second burst for each event (bursts 30 and 8) coincides with the onset of storm conditions (Figs. 32, 33). For these bursts, bed shear stresses on the bottom approximate the critical threshold for sediment movement at this time. The model current profile during Event III (Fig. 32) shows that the flow speed has doubled from the previous burst, whereas the current profile for Event IV (Fig. 33) does not show an increase in current speed from the previous fair-weather conditions. The measured current profile for Event IV differs in shape from the model output, and resembles a wave-dominated profile with more of a linear profile shape in the lower 30 cmab. This resembles a wave-dominated profile shape more than a purely logarithmic current profile shape. Also, the model slightly overestimates the speed of the current for both events at this time. The ABS profile for Event III (Fig. 32) shows an increase in the suspended material in the boundary layer from the previous burst, and this is reflected in the model predicted concentration profile also. The model indicates that for the sediment grain sizes at the site, sediment suspension would be confined primarily to the lower 50 cm, although small concentrations were shown throughout the bottom boundary layer. The ABS profile is in agreement, showing higher measurements below 50 cm with slightly more of an increase than the model at all heights above the bed. This increase at all

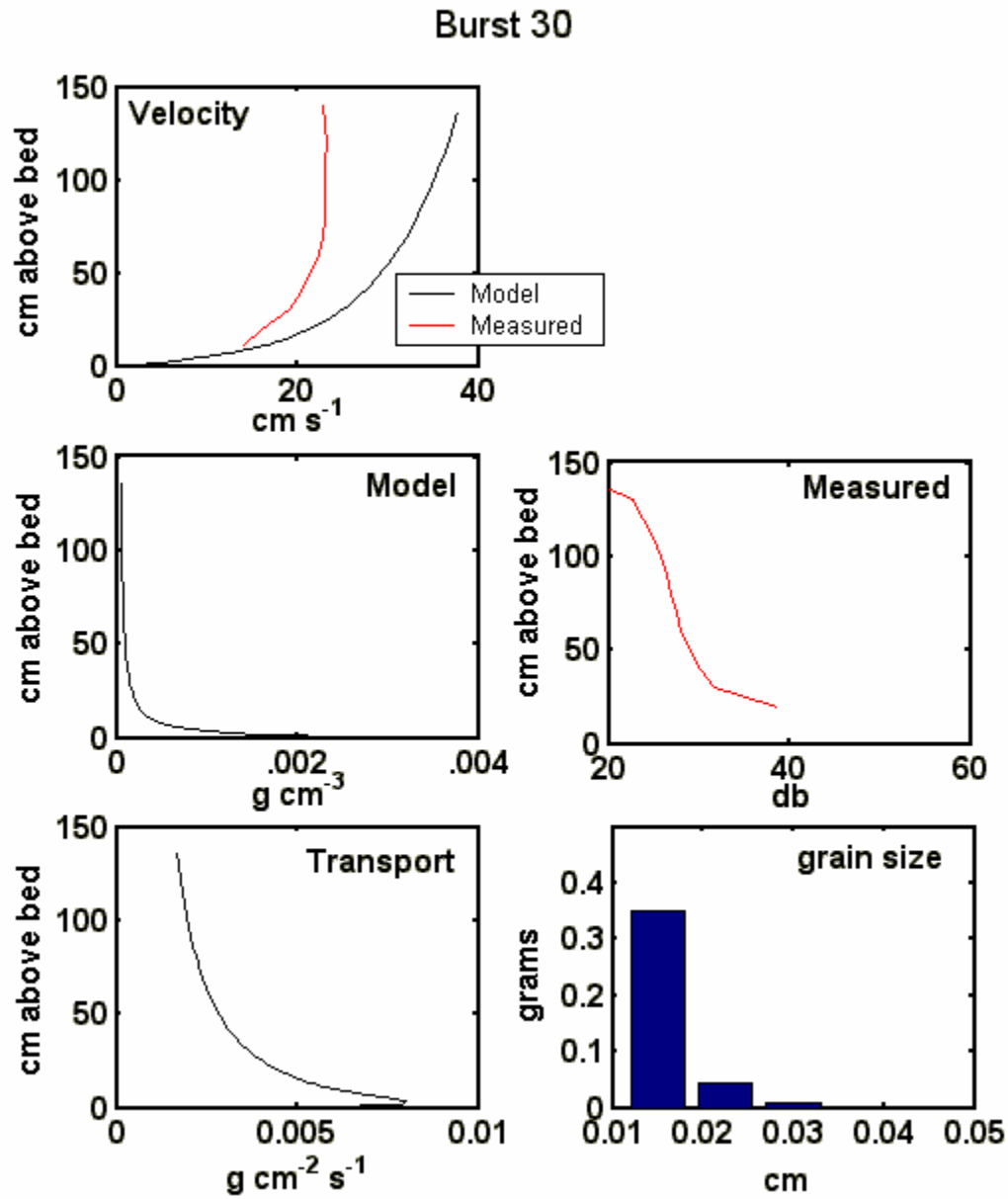


**Figure 32.** Burst 30 – Critical conditions are reached at the onset of September event. The measured and modeled current velocity profiles and a comparison between the sediment concentration profiles the ABS measurements are shown in the top three graphs. The bblm calculated sediment transport profile and suspended sediment grain sizes of are shown in the bottom two graphs.

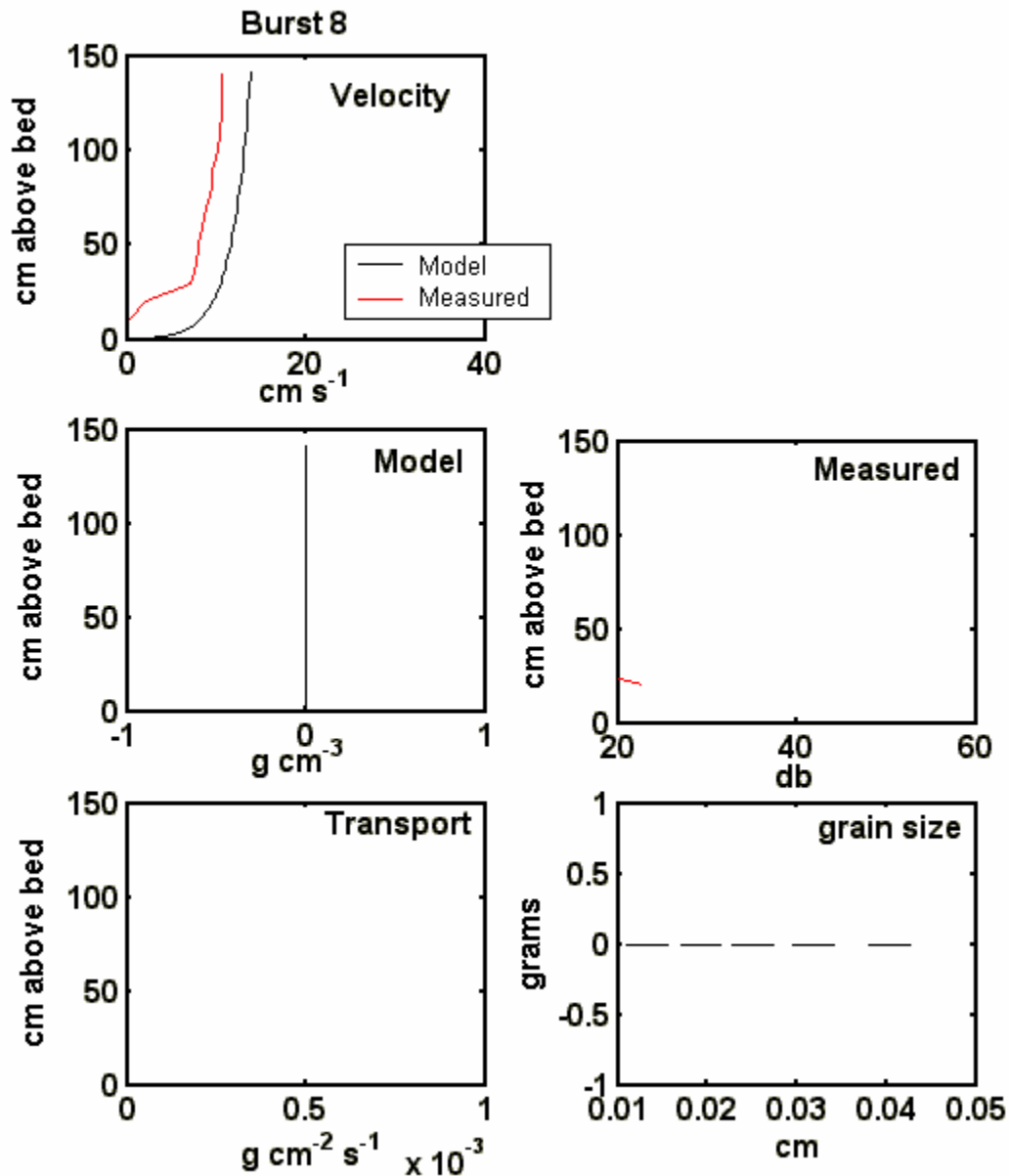


**Figure 33.** Burst 8 –Critical conditions are reached at the onset of November event. The measured and modeled current velocity profiles and a comparison between the sediment concentration profiles the ABS measurements are shown in the top three graphs. The bblm calculated sediment transport profile and suspended sediment grain sizes of are shown in the bottom two graphs.

heights in the lower water column is most likely due the very fine particulate in the water column. The model concentration profile and the ABS measurements for Event IV (Fig. 33), however, show no suspended sediments in the boundary layer at this time. Therefore, the model predicts that no sediment transport was occurring in Event IV at this time. The sediment transport profile for Event III shows that sediments were being suspended throughout the bottom boundary layer and the shape of the profile is similar to the ABS profile. This was due to higher current velocities that were able to interact with the waves and help facilitate vertical mixing in the boundary layer.

Bursts 37 and 15 occurred at peak storm conditions during both Events III and IV. For both events, the modeled and measured current profiles show good agreement (Figs. 34, 35). During this burst for Event III (Fig. 34), there was a large increase in flow speed from the previous burst, although the model slightly overestimates the velocity in the upper portion of the boundary layer. The current profile for Event IV (Fig. 34) shows that there was very little current in the bottom boundary layer during peak storm conditions. As will be seen, this had a major impact on the amount of sediment transport that occurred during this event. Also, during these peak storm conditions, both the modeled and the measured concentration profiles show an increase from previous bursts in the amount of material suspended in the bottom boundary layer. The suspended sediment concentrations given by the model showed that Event IV had the same amount of suspended sediment in the boundary layer than Event III at this time, which was a large increase in suspended sediment concentration for Event IV from the previous burst. The observed ABS profiles were consistent with the model output, and showed similar

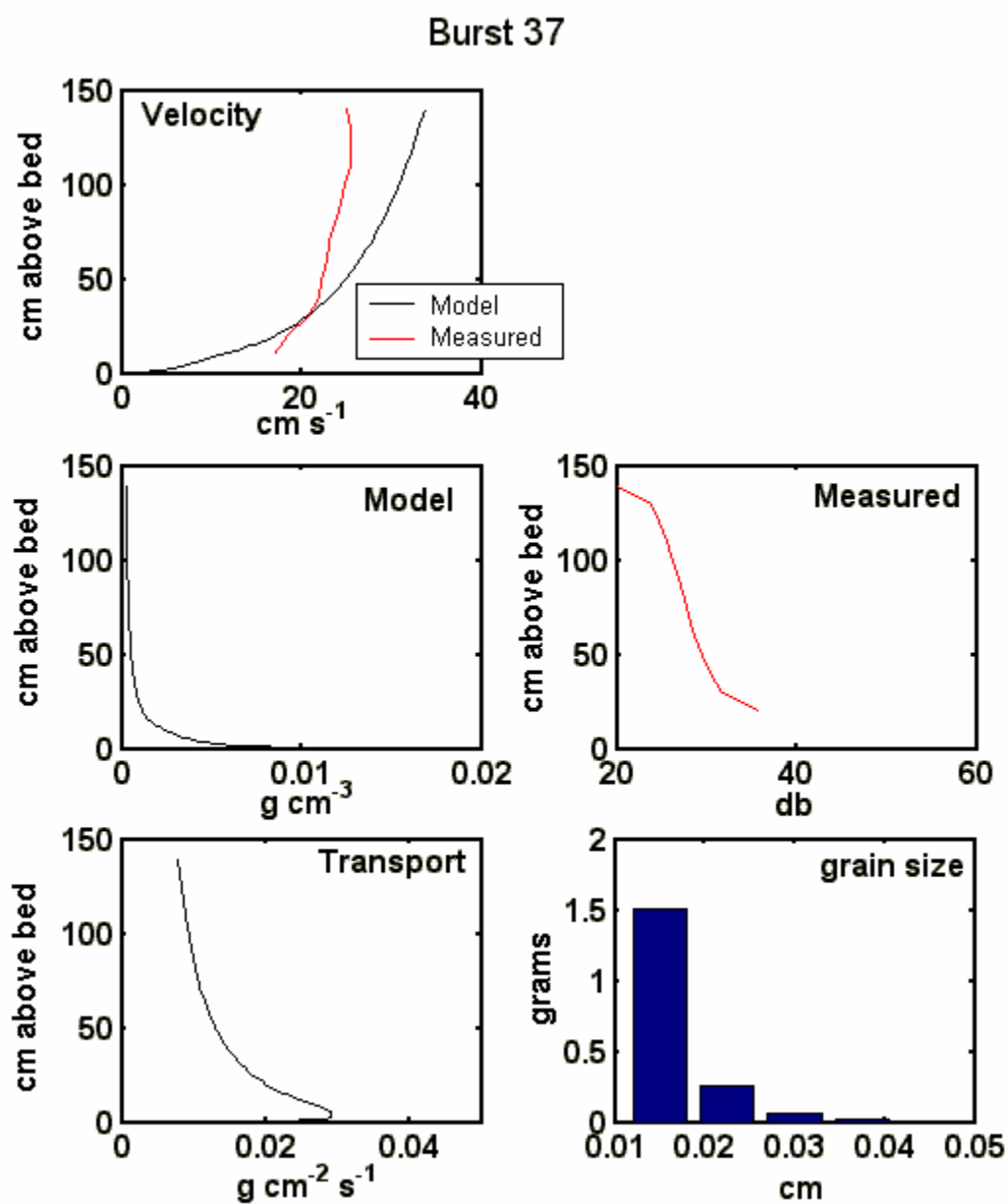


**Figure 34.** Burst 37 – Peak of September northerly wind event. The measured and modeled current velocity profiles and a comparison between the sediment concentration profiles the ABS measurements are shown in the top three graphs. The bblm calculated sediment transport profile and suspended sediment grain sizes of are shown in the bottom two graphs.

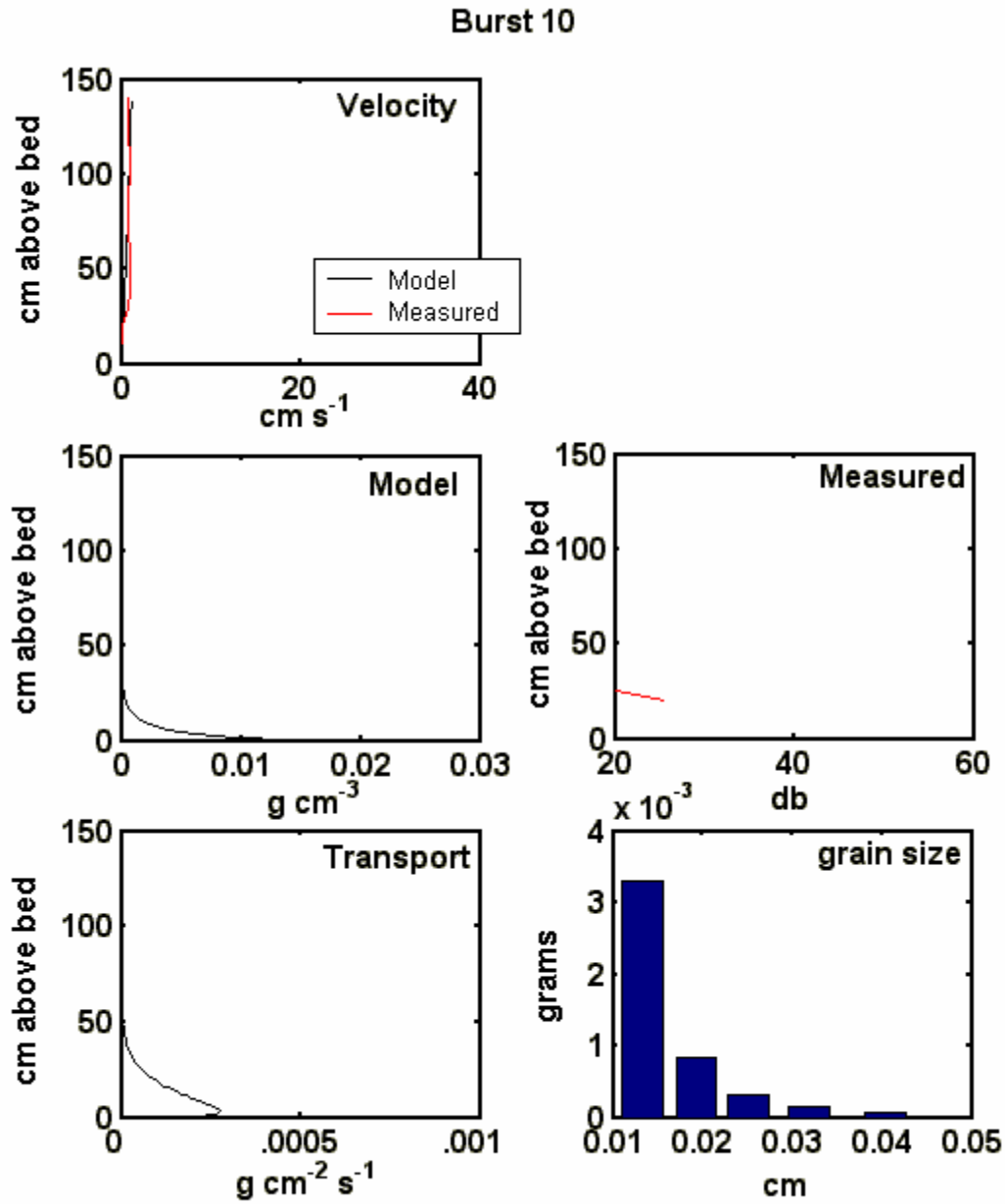


**Figure 35.** Burst 10 – Peak of November southerly wind event. The measured and modeled current velocity profiles and a comparison between the sediment concentration profiles the ABS measurements are shown in the top three graphs. The bblm calculated sediment transport profile and suspended sediment grain sizes of are shown in the bottom two graphs.

measurements at this time for both events. However, there was a discrepancy for Event IV because the model concentration profile showed sediments only being suspended in the lower 30 cm, and ABS measurements indicated an increase at all heights above the bed. The sediment transport profiles show that almost an order of magnitude less sediment transport occurred during Event IV than Event III at peak storm conditions, due to the lack of sufficient current to transport the high concentration of sediments suspended in the boundary layer. As the storm began to wane, waves and currents were still suspending sediment.

Bursts 55 and 18 are shown for Events III and IV (Figs. 36, 37). These bursts occurred at a time when the larger particles that were in suspension would have settled leaving only the finer fraction in suspension. The current profiles showed agreement between the model output and measured currents for both events, slightly overestimating the current speed above the weak measured current in both of the events at this time. The suspended sediment concentration profiles agree with the ABS measurements for both events, in that they both show a proportional decrease in the concentration and ABS signal from the previous burst. There is, however, a disagreement between the model concentration and the measured ABS data. The model shows that sediments were suspended only to 20 cmab in Event IV and 50 cmab in Event III, where the ABS signal shows the opposite. The ABS profile shows slightly higher values for Event IV than Event III at 30 – 40 cmab, as well as continued elevated values at all heights above the bed. The model output suggests that little material should have been actively resuspended at this time for both events given the existing conditions included in the

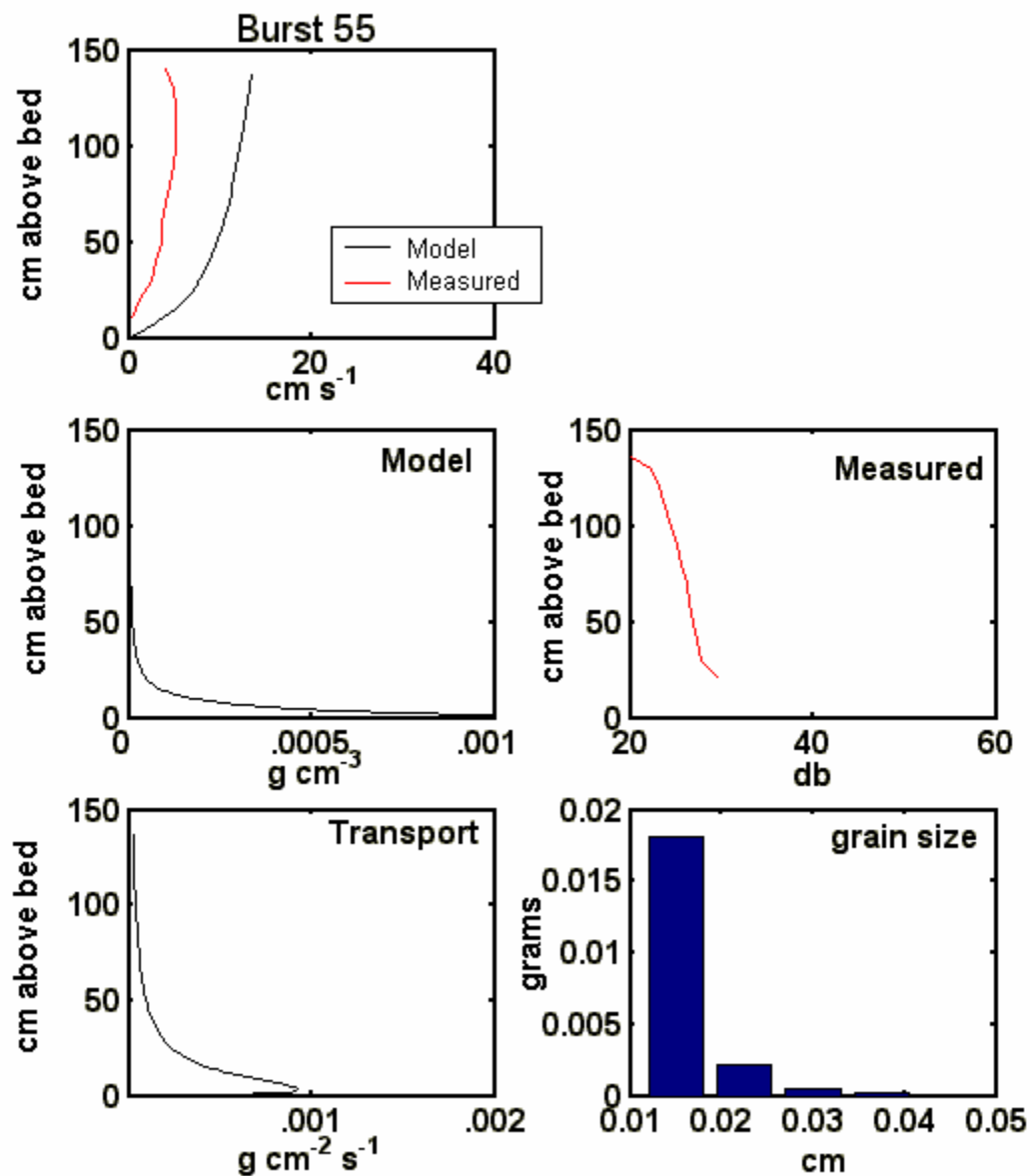


**Figure 36.** Burst 55 – Waning down of September event. The measured and modeled current velocity profiles and a comparison between the sediment concentration profiles the ABS measurements are shown in the top three graphs. The bblm calculated sediment transport profile and suspended sediment grain sizes of are shown in the bottom two graphs.



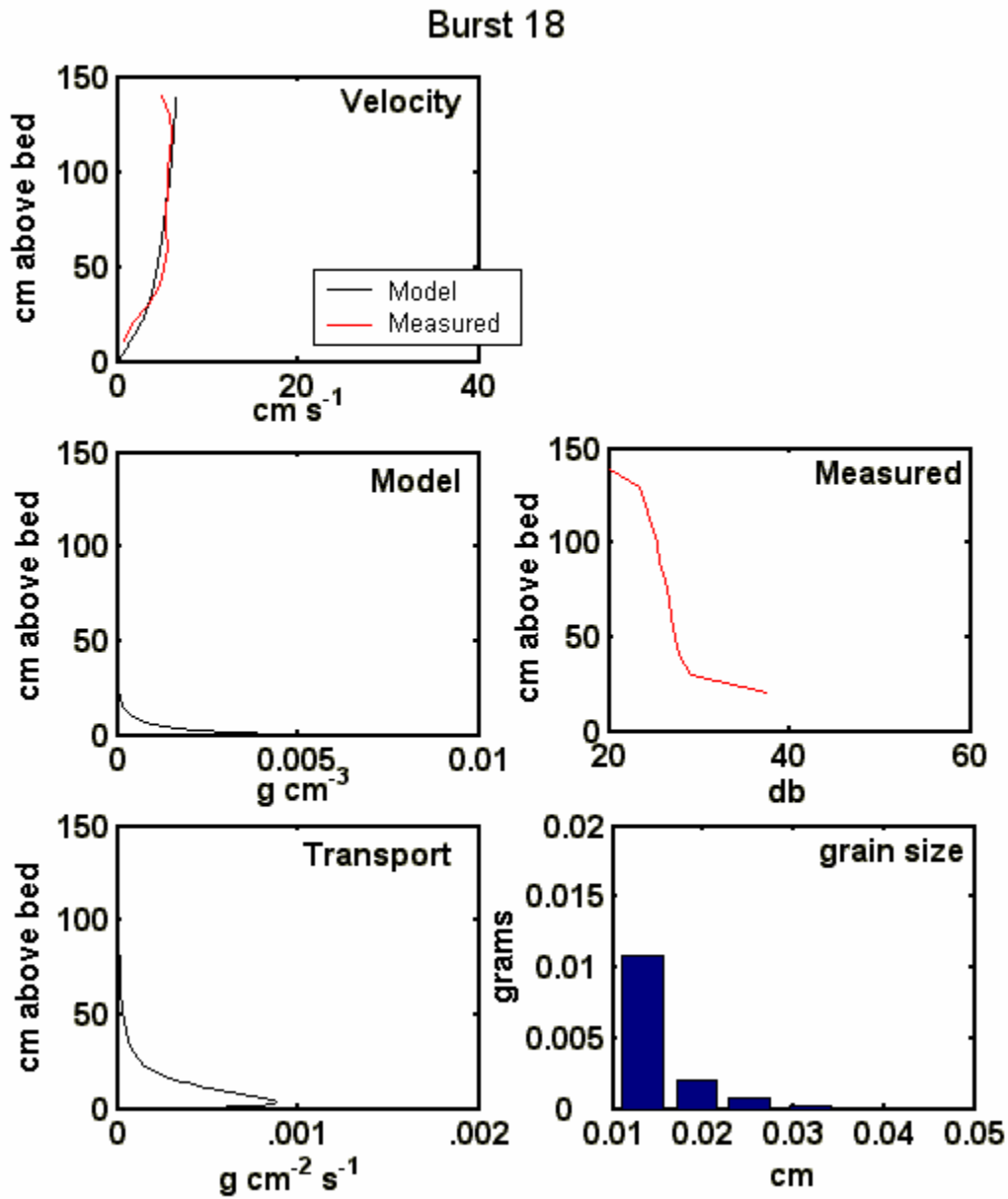
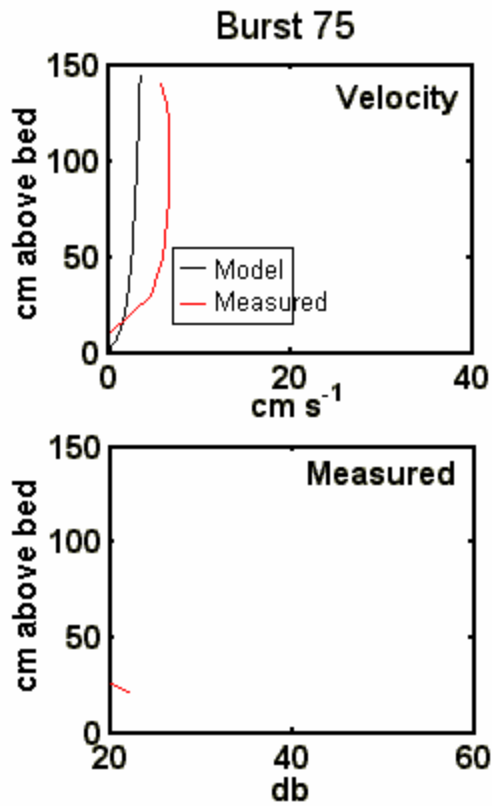


**Figure 37.** Burst 18 - Waning down of November event. The measured and modeled current velocity profiles and a comparison between the sediment concentration profiles the ABS measurements are shown in the top three graphs. The bblm calculated sediment transport profile and suspended sediment grain sizes of are shown in the bottom two graphs.

a.)



b.)

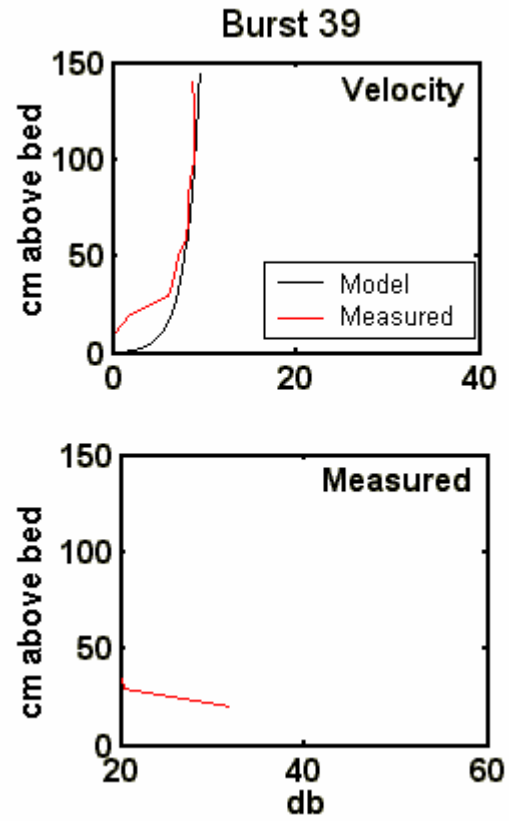


**Figure 38. (a).** Burst 75 – Post-storm conditions after September event. The top graph shows the current profiles and the bottom graph indicates that there are still suspended sediments being measured in the lower water column. **(b).** Burst 39 - Post-storm conditions after November event. The top graph shows the current profiles and the bottom graph indicates that there are less suspended sediments being measured in the lower water column than after the September event due to the low subtidal currents.

model input (e.g. ambient grain size, orbital velocities, etc.), but does not account for the fine material that was already in suspension. The disparity between the model and the observed ABS suggests the presence of suspended sediments that had not yet settled, even though storm conditions were beginning to wane. The 1-D model could not account for the advection of fine suspended sediments that were already in suspension at this time during both events.

In the last burst of the two events (Figs. 38 a,b) the velocity profiles are similar in shape and magnitude, but the measured ABS data indicate that there is still some sediment in suspension in the lower part of the boundary layer while the model output suggests that the sediment transport event is over by this time. Again, the model could not account for the advection of fine sediments in the water column at this time.

Overall, the model derived velocity profiles showed a good agreement during both events III and IV. Suspended sediment concentration profiles were less consistent with ABS measurements for Event IV than they were for Event III. The model was better at estimating the sediment transport during Event III, which was characterized by waves and wind-driven currents, than during Event IV, which was a wave event with little current. Although the model slightly underestimated sediment transport during the waning of the storm, there was, overall, good agreement between the shape and magnitude of the current, ABS measurements, and concentration in the boundary layer for both events. The model appears to reasonably quantify the amount of sediment transport associated with storms of this magnitude on the continental shelf at this location.

### 3.4 Discussion

Data collected during this study suggest that subtidal flows are a main contributor to fair weather sediment mobilization in Onslow Bay and potentially in other regions of the South Atlantic Bight. The role of subtidal currents has been demonstrated for west coast shelves as part of the 1990-1991 STRESS experiment where sediments were resuspended by waves in the presence of (statistically) unrelated currents during periods of fair weather on the northern California coast (Sherwood *et al.*, 1994). In another study on the northern California coast, Washburn *et al.*, 1993 observed that large eddies spinning off the eastern boundary current offshore created “quasi-steady” currents on the shelf, in which large amounts of suspended sediments can be transported. In the present study, low frequency, subtidal currents were a key factor in sediment transport.

Significant sediment transport occurred only during the storms when strong subtidal flows existed, and during fair weather only when strong subtidal flows were present. In storm events these flows were wind driven and acted as the transport mechanism for the suspended sediments, as well as enhancing bedform formation and helping to facilitate bedload transport. These types of low frequency flows determine the direction of the suspended sediment transport, and also influence the direction of the migrating ripples during bedload transport. The data from the three wind events on record show that the storms that generated the largest and most persistent subtidal flows were associated with greater amounts of sediment transport. For example, the late summer northerly wind event, Event III, exhibited the highest rates of sediment transport, although the shear stresses were higher during the southerly wind event. During the late summer northerly wind event the subtidal currents were quite large (greater than  $25 \text{ cm s}^{-1}$ ) and dominated

the near-bottom flow. During the southerly wind event, which was of short duration, subtidal flows were too weak to result in significant sediment transport. As a result, the sediment transport that could have potentially occurred under the prevailing wave conditions was greatly reduced. During the spring northerly wind event, Event I, peak sediment transport did not occur until there was sufficient time for the larger scale circulation in the bay to be established and subtidal flows were generated. It has been shown in previous studies that northerly winds cause a geostrophic along-shore current to the southwest due to the coastal setup and a barotropic flow directed offshore, veering southwestward via Ekman steering. This setup of the larger scale circulation in the bay produces a lag between surface winds and lower water column velocities which has been shown to be approximately 8 hours (Pietrafesa *et. al.*, 1985). In this event, the lag time appeared to be longer, most likely due to the relatively low wind speed. The transport of suspended sediments on the mid-shelf would thus be in the direction of the along-shelf current to the southwest. These results are consistent with work done by Ogston and Sternberg (1999) who suggest that low frequency and mean currents appear to determine the direction and magnitude of sediment flux on the northern California shelf.

Subtidal flows were also associated with the intrusion of Gulf Stream water on the shelf during the study. In the absence of significant wind activity (i.e., winds  $< 10 \text{ m s}^{-1}$ ), longer period fair-weather swells ( $> 8 \text{ sec}$ ) and tidal currents, neither by themselves nor in combination, were effective in transporting sediments at the mid-shelf site. During the remainder of the summer months, fair weather winds and waves were present and interacting with the tidal flows, but there was no evidence in the data that significant sediment transport occurred. In order for significant sediment mobilization to occur,

these mechanisms must be coupled with another type of quasi-steady flow, which the Gulf Stream intrusion provided.

Gulf Stream intrusions on the mid-continental shelf during this time of year are common (Pietrafesa *et al.*, 1985), and Gulf Stream intrusions and upwelling events have been observed to occur at the site during the study period (Quattrini, 2002). Gulf Stream waters were present on the shelf in the vicinity of the instrument frame as seen in satellite imagery in June 2000 (Quattrini, 2002). Following the spring wind event, May 29<sup>th</sup> – June 1<sup>st</sup>, longer period swells moved across the shelf, accompanied by some of the highest tidal ranges of the monitoring period. Subtidal flows in excess of  $10 \text{ cm s}^{-1}$  towards the NNE also were present at this time and were able to completely offset the tidal currents when in opposition. An increase in northerly directed currents has been shown to occur during times of rapid temperature increase in the water column during previous studies in the SAB (Lee *et al.*, 1985). Mean currents of  $0\text{-}20 \text{ cm s}^{-1}$  towards the north existed over these two days. The mean current at 4 mab reached magnitudes of  $40 \text{ cm s}^{-1}$  during this time. Strong tidal currents associated with the higher astronomical tide and subtidal flows towards the north interacting with longer period swells had greater potential for sediment transport. Further, the fact that this GS event occurred immediately after a wind event helped to facilitate suspended sediment transport, as ABS measurements show that sediments were still in suspension at the beginning of the GS event.

The only mechanism that remained constant over this time were the subtidal flows toward the north. Bed shear stresses show that the critical shear stresses for the fine to medium sands were exceeded and that bedload transport was most likely occurring. The

longer period swells moving across the shelf interacted with low frequency currents to cause a slow creep of the fine sands, extensive to the south of the study site, towards the reef area. This pattern is consistent with observations off the Long Island coast on the inner shelf of the Mid-Atlantic Bight (Swift *et al.*, 1984). This study demonstrates that fair-weather wave-current interactions tend to cause a landward creep of sediment on the mid-shelf in Onslow Bay due to symmetrical wave orbital currents interacting with slowly varying subtidal currents.

#### *3.4.1 Seabed altimetry and model predicted ripples*

When using the bblm to predict ripple heights and comparing this to the measured seabed altimetry data, a consistent discrepancy was noted. The seabed altimetry data that were collected during this study indicated ripple heights were approximately 1 – 2 cm during all three of the wind events, where the bblm indicated ripples were typically 4-6 cm during these events. Anecdotal diver observations at the study site during moderate wave conditions agree with the 4 – 6 cm bblm ripple heights. The bblm's estimation of ripple geometry has been compared with ripple measurements from the LEO-15 site (Traykovski *et. al*, 1999) where the model showed good agreement with the field measurements. The seabed altimetry data from PC-ADP does not have a small enough temporal or spatial resolution to accurately determine a time series of ripple heights during an event. The PC-ADP only makes one measurement of seabed elevation once every burst interval (2 hours). Consequently, this limitation of the temporal resolution suggests that the seabed altimetry data should only reliably be used to determine the location of the seabed over an event time scale. Nonetheless, the seabed altimetry data can be used to verify the presence of ripples on the seabed. Further, the acoustic signal is

emitted at a 15° angle from the transducer head and the transmitted acoustic signal from the beam is reflected off the seabed detecting the vertical change where it is reflected off of the seabed. Therefore, a steeper ripple would be more detectable from an angle because of the larger slope, and therefore would reflect more of a vertical change as ripples were migrating under the frame. The seabed altimetry data were, however, an essential part of the study because they indicated when, and how much, sediment erosion or deposition occurred during the events.

### **3.5 Conclusions**

On the shelf of the South Atlantic Bight (SAB), small to moderate storms and fair weather processes all contribute to sediment transport. In the SAB storms are less frequent and intense than on the U.S. west coast. Therefore, smaller storms and fair weather processes play a more important role in sediment transport on the mid-continental shelf in the SAB. Two different types of winds events that occur frequently in the area were shown to result in a significant amount of sediment resuspension and transport. In addition, the Gulf Stream effects were also shown to facilitate sediment transport during the summer months.

Subtidal flows are one of the important processes in sediment transport at the mid-shelf site. Low frequency, subtidal flows were a key forcing mechanism for sediment transport during the Gulf Stream event and were the driving force for sediment transport during the wind events.

The bottom boundary layer model used in this study appears to reasonably quantify the amount of sediment transport associated with storms of this magnitude on



the continental shelf at this location and is a useful tool for quantifying and predicting sediment transport that occurs during these types of events.

## **Chapter IV**

### **Sediment transport during Hurricane Isabel on the mid-continental shelf in Onslow Bay, North Carolina**

#### **4.1 Introduction**

It is well documented that storm driven processes dominate sediment transport on many continental shelves (Madsen *et al.*, 1993; Traykovski *et al.*, 1999; Li and Amos, 1999; Williams and Rose, 2001). The importance of the role of storms in sediment transport on shelves and the effect of these events on coastal change has become more apparent in recent years. With improvements in instrumentation and technology, more field studies have been initiated and conducted to measure sediment transport processes on continental shelves during storms. However, due to the unpredictability of storms and the difficulties and expense in obtaining measurements during these conditions, a paucity of field data exist. Empirical information on near-bottom currents, suspended sediment concentrations, and seabed changes that occur during storm events are needed to verify and further refine the existing process-oriented models that pertain to sediment transport on shelves.

Along the southeastern U.S. east coast, tropical cyclones are a common occurrence during the hurricane season, which traditionally extends from June 1 – November 30. When these storms cross the continental shelf, sediment transport processes that typically occur during the usual small to moderate wind events are extremely magnified. The consequences of these storms can be devastating in some

cases, not only to humans along the highly developed coastline, but to offshore benthic communities that are vital to sustaining productive fisheries habitats.

As part of the Coastal Ocean Research and Monitoring Program (CORMP) at the University of North Carolina at Wilmington, an instrumented quadrapod frame has been maintained on the mid-continental shelf in Onslow Bay since April 2000. This instrumentation was present on the shelf when Hurricane Isabel passed approximately 160 km from Onslow Bay and made landfall along the lower Outer Banks of North Carolina near Cape Lookout, NC on September 18<sup>th</sup>, 2003 (Fig. 39). The instrumented frame is moored 27 miles off the coast of Wilmington, NC at a depth of approximately 30 m. The attached instrumentation includes a downward looking Pulse-Coherent Acoustic Doppler Profiler (PC-ADP) and an upward looking Acoustic Doppler Current Profiler (ADCP). Simultaneous measurements of flow velocities from the surface to the seabed along with acoustic backscatter measurements and seabed elevation were obtained during this storm event and are reported here. A bottom boundary layer (bbl) model (Styles and Glenn, 2000; 2002) was used to calculate bed shear stresses due to wave-current interactions during the event. The bbl model also generated near-bottom current, suspended sediment concentration and transport profiles and current profiles were compared to the high-resolution current profiles measured in the lower boundary layer. Bedload transport was calculated using the Meyer-Peter-Muller equation (1948). The bottom boundary layer model was also used to predict ripple heights and wavelengths

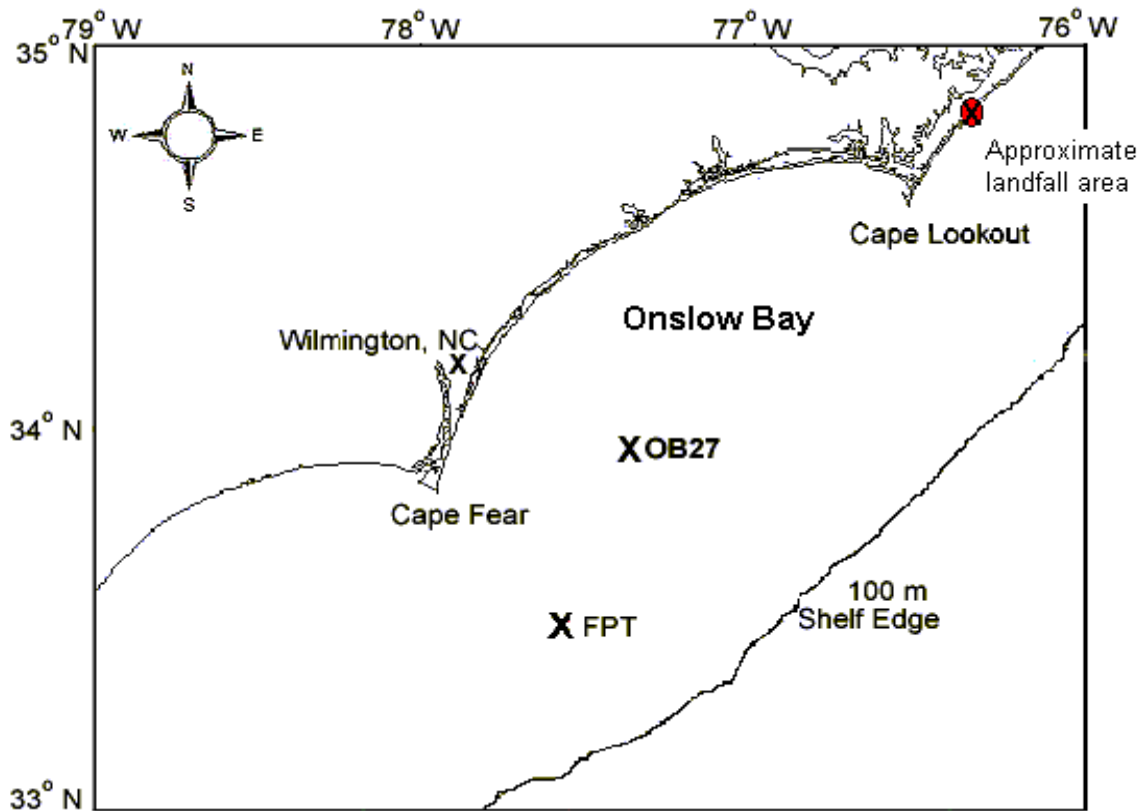


**Figure 39 (a).** Onslow Bay is located between Cape Lookout and Cape Fear, NC. OB27 marks the study site, 27 miles off the coast of directly east of Wilmington, NC. FPT is the location of the NOAA C-man station where wind and wave data were collected. Hurricane Isabel made landfall northeast of the study site.

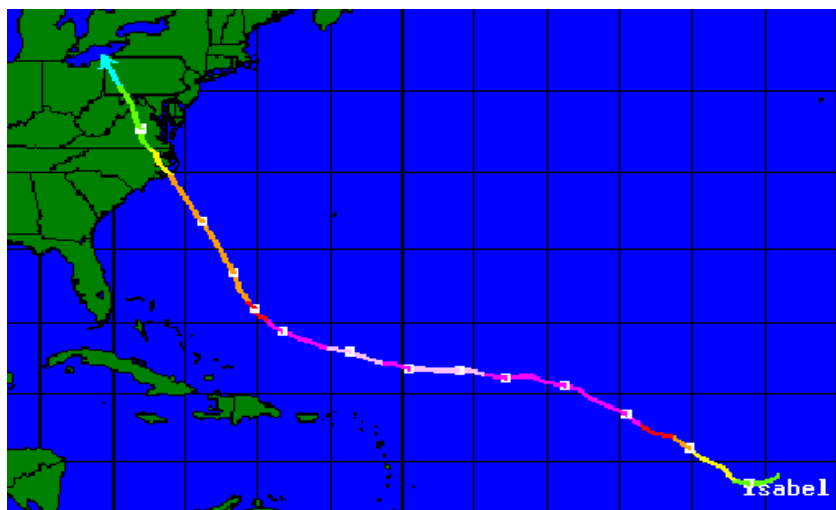


**Figure 39 (b).** Hurricane Isabel's track from formation on September 6<sup>th</sup> in the central tropical Atlantic Ocean, to making landfall near Cape Lookout, NC on September 18<sup>th</sup>. The square tick marks indicate positions at 0000 UTC.

generated during the storm, and these have been compared to the seabed altimetry data. This study is unique given that diver observations, boxcores and sediment samples were able to be collected at the mid-shelf site as the hurricane began to impact the area, as well as immediately after hurricane passage. These types of data and observations were critically important in correctly interpreting the instrumentation measurements and the bbl model output.

## **4.2 Field Experiment**

Onslow Bay is located off the southeastern coast of North Carolina in the northern region of the South Atlantic Bight (SAB). It is bounded to the northeast by Cape Lookout and to the southwest by Cape Fear, and by the shelf edge and Gulf Stream to the east (Fig. 1). The mean tidal range in Onslow Bay is approximately 1.0 m and is dominated by the M2 component (Pietrafesa *et al.*, 1985). Average significant wave heights are 1.5 m with a dominant period of 8.0 seconds as measured at the NOAA C-Man station (FPT) (Fig. 1). The “sediment-starved” continental shelf is characterized by a complex sequence of rocky outcrops with relief up to 10 m (Renaud *et al.*, 1997) and a thin and discontinuous veneer of Holocene sediment which is generally not accumulating on the shelf. These hardbottom sites in Onslow Bay form the framework for the highly productive “livebottom communities” that are important to commercial and recreational fisheries and thus are of major economic importance (Riggs *et al.*, 1998).

### *4.2.1 Methods and instrumentation*

In late April of 2000, a downward looking Sontek Pulse-Coherent Acoustic Doppler Profiler (PC-ADP) and an upward looking Acoustic Doppler Current Profiler (ADCP) were deployed on the mid-continental shelf (33° 59'N, 77° 21'W). The



**Figure 40.** NOAA satellite imagery of Hurricane Isabel as the storm approached the NC coast on September 18<sup>th</sup>. The red dot indicates the approximate location of the study site (for visual purposes only).

instruments were mounted on a 2 m tall frame situated at approximately 30m depth. The PC-ADP samples in “burst mode” at 2 Hz for 10 minutes every 2 hours. Secured 150 cm above the seabed, the downward looking 1.5 MHz PC-ADP measures velocity profiles of the bottom boundary layer in 10 cm bins. The ADCP is an upward-looking 600 kHz RDI Workhorse Sentinel that profiles the overlying water column in 1m bins at 1 Hz. The ADCP data are averaged over a 60 second averaging interval and create a velocity profile of the upper water column every 5 minutes. When examining bottom conditions and calculating bed shear stresses, the burst-averaged velocity time series from the PC-ADP at 1 mab was used. The along-shelf axis is taken at 55.6° east of north following Pietrafesa *et al.* (1994) and is positive towards the southwest in this paper; the across-shelf direction is positive in the offshore direction.

The PC-ADP also measures temperature and pressure, and serves as a bottom altimeter to monitor changes in seabed elevation. The 3 acoustic beams in the downward-looking transducer detect where the seabed is located under the frame once during each 10 minute burst and these data are used to determine changes in seabed elevation throughout the event. To measure relative changes in turbidity, the 1.5 MHz PCADP acoustic backscatter signal (ABS) was used. This approach was useful for approximating relative changes in suspended particulate in the water column, and is similar to the Acoustic Backscatter Sensor which has been shown to be especially successful with sands in sediment transport studies in the U.S. and the U.K. (Traykovski *et. al.*, 1999; Battisto, 2000; Williams and Rose, 2001).

Seabed altimetry and diver collected boxcores, pre- and post-storm, were used to examine the depth of sediment reworking following storm disturbance. A sediment tube

attached to the frame approximately 30 cm above the bottom collected sediments that were suspended in the water column during the storm. Following collection, the boxcores were sub-sampled at 5 cm intervals. The grain size distributions of these sub-samples and the material collected in the sediment tube were determined using a Beckmann-Coulter LS 200 particle sizer. These data were subsequently input into the bbl model. Pre- and post event stratigraphy was examined to identify distinct storm deposits and the depth of reworking due to physical processes and post-event bioturbation.

In order to examine atmospheric forcing over the duration of the study, available wind, wave, and atmospheric data from a National Oceanic and Atmospheric Administration (NOAA) C-Man station were used (<http://www.ndbc.noaa.gov/FPSN7>). The Frying Pan Tower (FPT) station is located at the southern boundary of Onslow Bay approximately 61 km southwest of the study site (Fig. 1). Characteristics of hurricane swell data reported at the FPT station from 15 through 17 September were consistent with wave data collected north of the study area at the Army Corps of Engineers Field Research Facility in Duck, North Carolina.

## **4.3 Results**

### *4.3.1 The hurricane*

Hurricane Isabel made landfall along the lower Outer Banks of North Carolina near Cape Lookout on September 18<sup>th</sup>, 2003. The eye of the hurricane passed close enough to the instrumentation in Onslow Bay that quality hurricane data were recorded. Fortunately, the strength of the storm combined with the distance of the eye from the site allowed for the instruments to be retrieved without any loss of data (Figure 40). Isabel became a tropical storm on September 6<sup>th</sup>, 2003 in the central Atlantic Ocean. Within



less than 48 hours, Tropical Storm Isabel was a major category 3 hurricane on the Saffir-Simpson scale. Isabel was soon upgraded to a category 4 hurricane on September 9<sup>th</sup>. Isabel reached Category 5 strength on September 11<sup>th</sup> with maximum winds above 155 mph. Although Isabel's intensity fluctuated over the next 4 days, Isabel maintained winds of 150 mph or greater, with maximum sustained winds reaching 160 mph and gusts to 195 mph. By September 15<sup>th</sup> Isabel was north of the Dominican Republic at approximately 25.0° N and 70.0° W and began a turn to the northwest heading for the southeast U.S. coast. Isabel began to weaken in intensity as it traveled north. Isabel was a category 2 hurricane as it approached the North Carolina coast and made landfall at approximately 1600 UTC on September 18<sup>th</sup>.

Large swells preceded the hurricane and are evident in the wave data collected in Onslow Bay on September 15 through mid-day on the 18<sup>th</sup> (Figure 41). As the hurricane traveled closer to the site, significant wave heights steadily increased. On September 15<sup>th</sup>, three days prior to landfall, winds were from the north and less than 10 m s<sup>-1</sup> at the study site. Significant wave heights were approximately 2 m with wave periods ranging from 13 -17 seconds. Early on the 16<sup>th</sup>, the first storm-related winds were observed in the study area. Local winds switched around to the NNE early on the 16<sup>th</sup>, wave heights began to build to 4 meters and wave periods decreased. Over the next 24 hours, wave conditions consisted of a combination of hurricane swells and locally generated seas. Northerly winds increased to 15 m s<sup>-1</sup> late on the 16<sup>th</sup> and significant wave heights at this time were 3 – 4 meters. Approximately 24 hours prior to the hurricane passage, wave heights increased to 4 – 5m and winds were from the north and sustained at approximately 15 – 20 m s<sup>-1</sup>. Dominant wave periods ranged from 14 – 17 seconds.

# Hurricane Isabel FPT hourly observations September 15 – 20, 2003

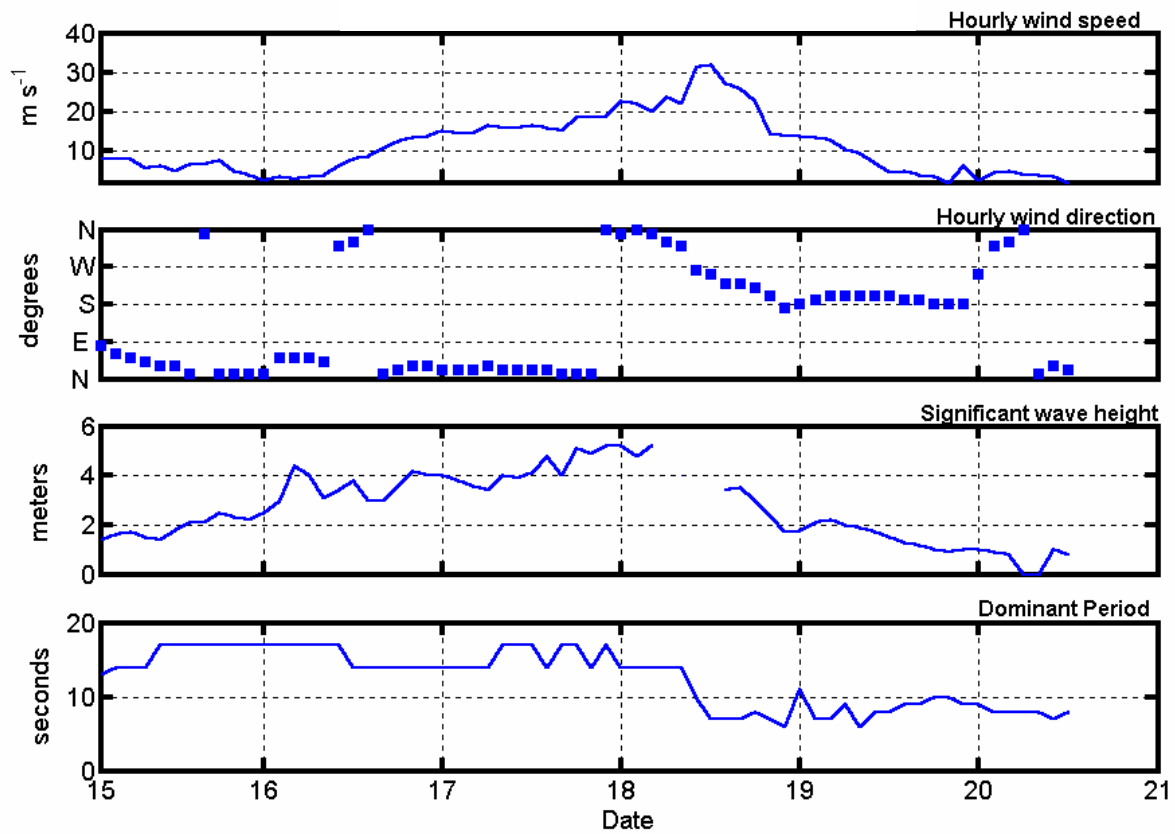


**Figure 41.** Hourly wind and wave data were obtained from the NOAA Frying Pan Tower C-Man station (<http://www.ndbc.noaa.gov/FSN7>) during Hurricane Isabel. The wave buoy failed during the peak storm conditions on September 18<sup>th</sup>.

Winds remained from the north at slightly greater than  $20 \text{ m s}^{-1}$  until early on the 18<sup>th</sup> when they began to gradually shift from northerly to westerly and increased to over  $30 \text{ m s}^{-1}$ . By 1000 UTC on the 18<sup>th</sup>, winds were from the west at  $30 \text{ m s}^{-1}$ . These conditions were sustained for 2 hours and were the maximum wind velocities measured in the study area during the hurricane. Wave periods suddenly dropped to 7 seconds and the NOAA accelerometer malfunctioned at this time, therefore wave height data was not available during peak storm conditions. Winds continued to veer around to a southwesterly and then southerly direction over the next 8 hours and decreased to  $15 \text{ m s}^{-1}$ . Significant wave heights also decreased to 2 m late on the 18<sup>th</sup> as the hurricane passed to the north and northeast of Onslow Bay and made landfall. Southerly winds persisted for the next 24 hours and significant wave heights decreased to less than 1 m with wave periods between

#### *4.3.2 Bottom boundary layer dynamics*

##### *September 15<sup>th</sup>*

The initial influence of Hurricane Isabel at the site was associated with the swells that propagated out from the storm and began impacting the area on 15 September, three days prior to landfall. These longer period (13-17 second) swells caused the bottom wave orbital velocities to increase from  $25$  to  $80 \text{ cm s}^{-1}$  in a 24-hour period beginning on 15 September (Figure 43). Mean currents at this time were tidally dominated and less than  $10 \text{ cm s}^{-1}$  at 1 mab and  $15 \text{ cm s}^{-1}$  at 4 mab (Figure 42). Shear velocities calculated from the bbl model increased from approximately  $7 \text{ cm s}^{-1}$  to  $12 \text{ cm s}^{-1}$  over the course of the day (Figure 43). Measured and modeled vertical velocity profiles generated at 1000 UTC on the 15<sup>th</sup> (Figure 44) were in very good agreement and showed flow speeds less than  $5 \text{ cm s}^{-1}$  in the bottom boundary layer. The ABS profile indicates the presence of

suspended sediments in the bottom boundary layer at this time, especially in the lower 30 cm of the bottom boundary layer. This observation generally agrees with the model output, which predicted that most of the suspended sediment should occur in the lower 30 cm (Figure 44). Using calculated shear velocities and grain size characteristics of bottom sediments at the site, only particles with grain diameters of less than 0.0175 cm were in full suspension at this time. The sediment transport profile produced by the bbl model suggests that only a small amount of sediment transport occurred at this time due to a combination of fairly weak currents (Figure 44), and relatively low concentrations of suspended sediments in the bottom boundary layer. 8 – 10 seconds. The impacts of Hurricane Isabel on wave and current conditions were felt at the site for approximately 4-1/2 days.

Model calculated ripple heights at this time were predicted to be approximately 5 cm, with a steepness of 0.09. These results are consistent with the empirical formulations of Wiberg and Harris (1994). When using the wave height and period for this time of the storm with the median grain size and depth, Wiberg and Harris (1994) indicate that ripples would be anorbital. Anorbital ripples are the most common ripples that occur in shelf environments, and have a steepness of 0.12 or less and decrease with increasing wave energy. These results are also consistent with the seabed elevation trace (Fig. 45c) that shows slight fluctuations of 1 – 2 cm during this time. Model calculated shear stresses and median grain diameters were used to determine the bedload transport rate (Meyer-Peter and Muller, 1948). During this phase of the storm, bedload transport rate

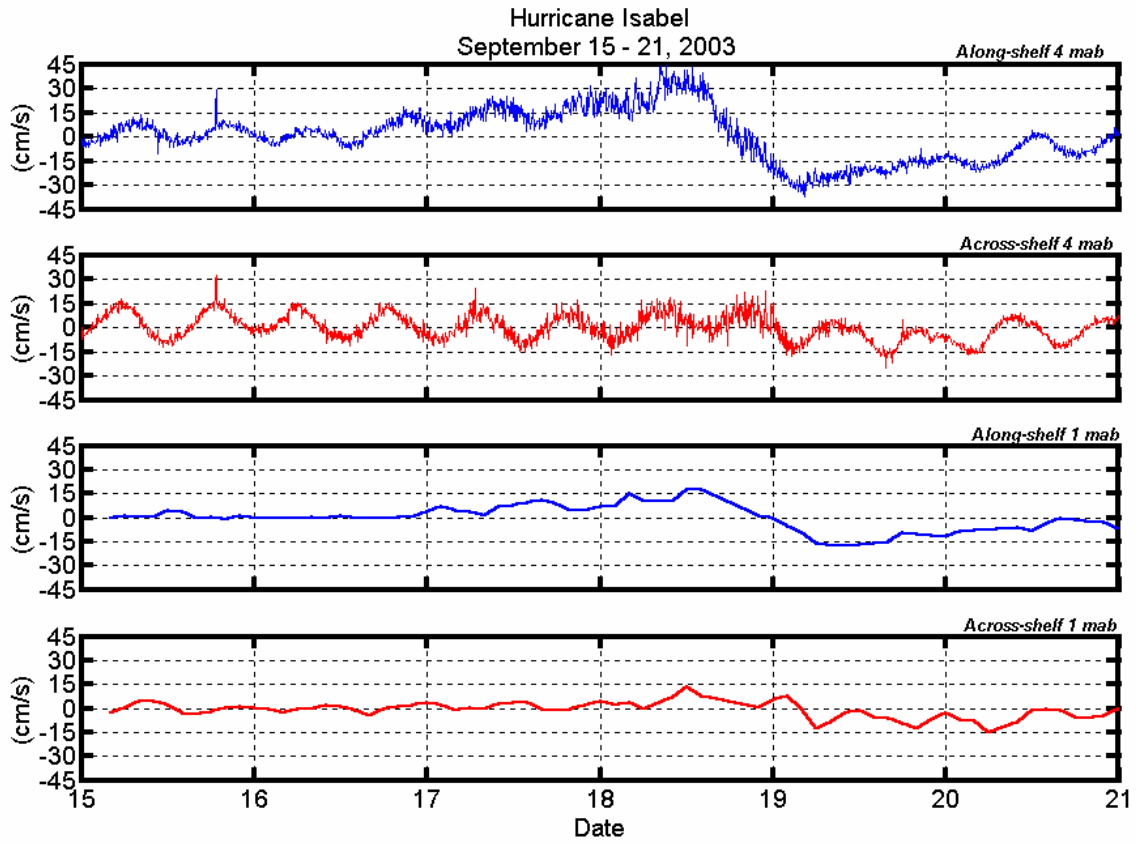


**Figure 42.** The top two panels show the Acoustic Doppler Current Profiler velocity data. The bottom two panels show the burst-averaged currents from the Pulse-Coherent Acoustic Doppler Profiler.

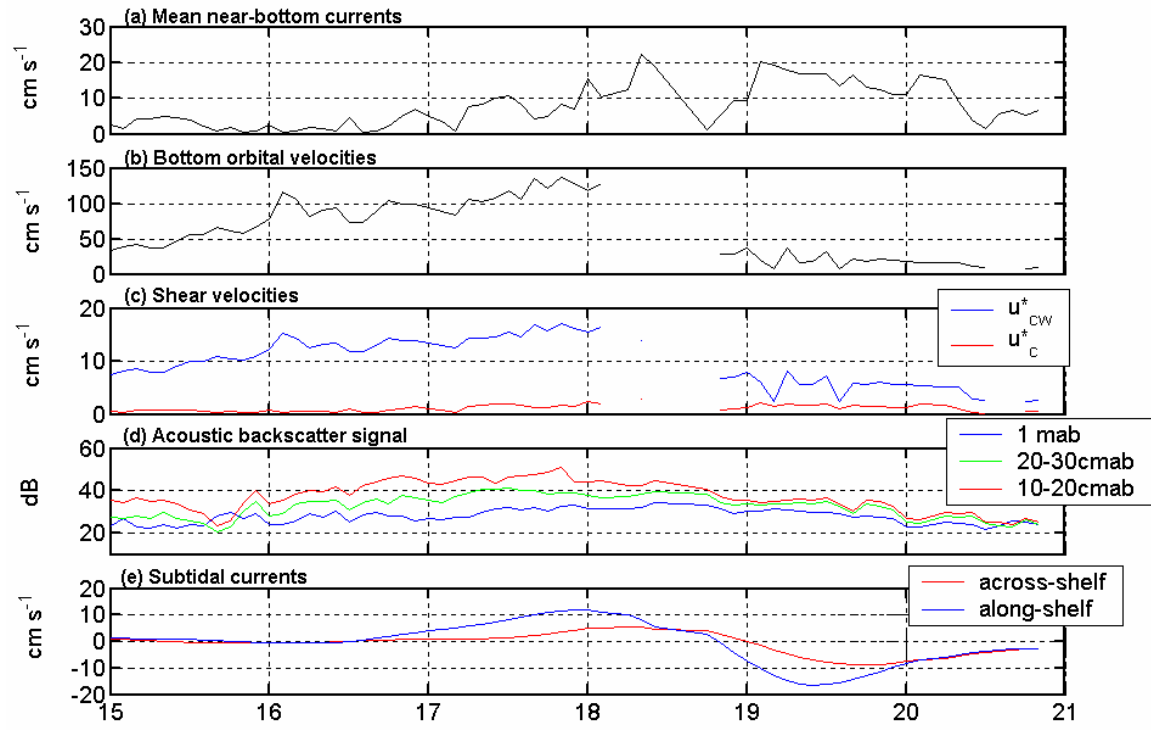


**Figure 43.** Hurricane Isabel (a) mean current speed at 1 mab (b) bottom orbital velocities (c) wave-current and current bed shear stresses (d) acoustic backscatter signal (e) along and across-shelf subtidal currents.

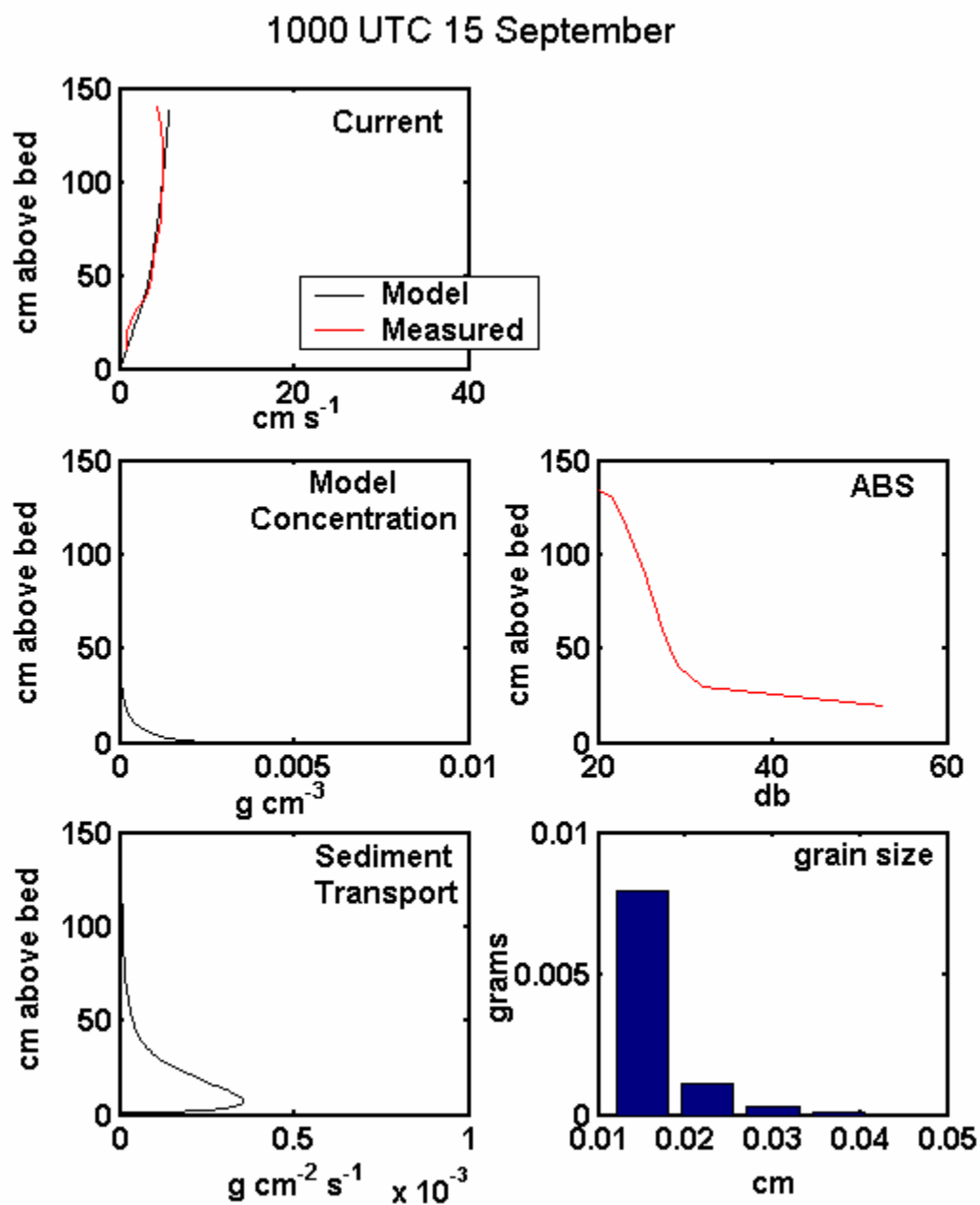


**Figure 44.** Comparison of the model calculated current profile with the PCADP measured current profile in the bottom boundary layer. Burst 5 represents pre-storm conditions at 1000 UTC on September 15<sup>th</sup>.

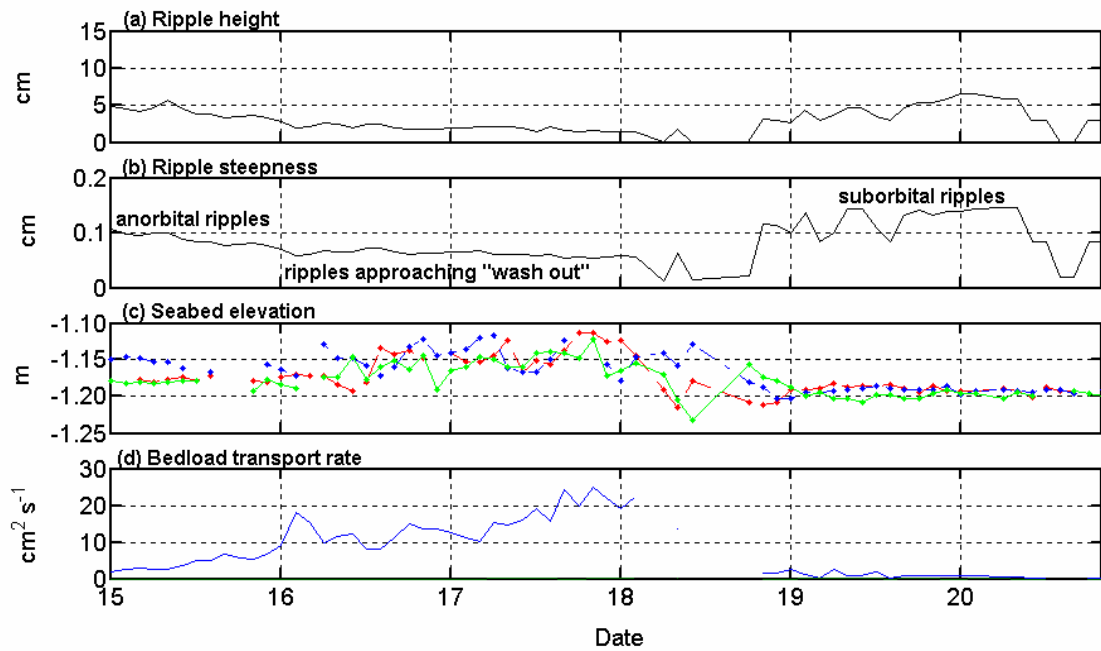


**Figure 45.** Hurricane Isabel: model calculated (a) ripple heights and (b) ripple steepness (c) measured seabed altimetry data from each of the three beams (d) calculated bedload transport rates. The missing portion of the bedload transport rate time series is due to the lack of available wave data when the hurricane was at its closest approach to the study site.



was approximately  $2.5 \text{ cm}^2 \text{ s}^{-1}$  (Fig. 45d) and was in the direction of the swells, which was  $16^\circ$  north of directly onshore.

By 1800 UTC on 15 September, bottom orbital velocities had increased to  $60 \text{ cm s}^{-1}$  and currents were still weak ( $< 10 \text{ cm s}^{-1}$ ). Wave-current shear velocities, however, had increased to more than  $10 \text{ cm s}^{-1}$ . The shape of the bblm current profile continues to agree with the measured current profile, and both profiles indicate that currents were still very weak in the bottom boundary layer. The burst averaged ABS profile shows slightly elevated levels in the lower part of the boundary layer during this part of the storm. The bblm is in agreement as the concentration profile indicates higher concentrations in the boundary layer, but shows that sediments were being mixed slightly higher into the boundary layer as well. The ABS time series data measured at 1 mab increased to slightly greater 30 dB (Figure 46) by 1800 UTC. The sediment transport profile indicates that the amount of suspended sediment available for transport was restricted to the lower 25 cm of the water column. Further, based on the sediment size fractions that were used to calculate sediment transport, only fine sands of less than 0.0225 cm in diameter were in suspension. The seabed altimetry data were unavailable at this time due to the presence of divers at the site. Anecdotal reports from the divers, however, indicate that ripples of approximately 4 cm were present on the seabed. These observations are consistent with the model calculated ripple height at this time, which was 4 cm. Calculated bedload transport was occurring at a rate of  $6 \text{ cm}^2 \text{ s}^{-1}$  during this period of storm approach, and continued to be in the onshore direction.

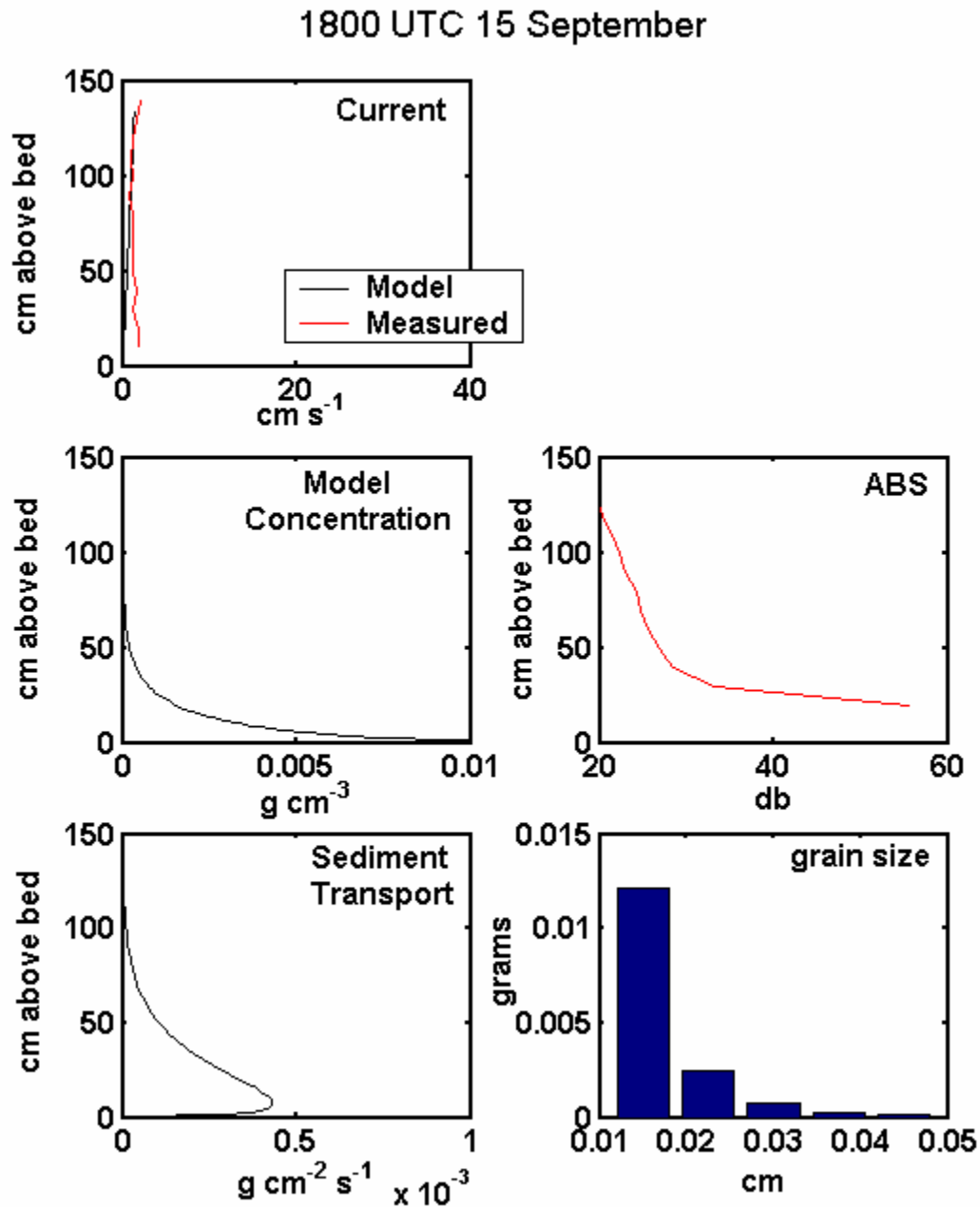


**Figure 46.** Comparison of the model calculated current profile with the PCADP measured current profile in the bottom boundary layer. The ABS and sediment concentrations are also shown, along with the model calculated sediment transport profile. The bar graph shows what sediments comprise the total amount of the suspended sediments. Burst 9 is at 1800 UTC on the 15<sup>th</sup> and is the first burst that model calculated sediment transport occurred.

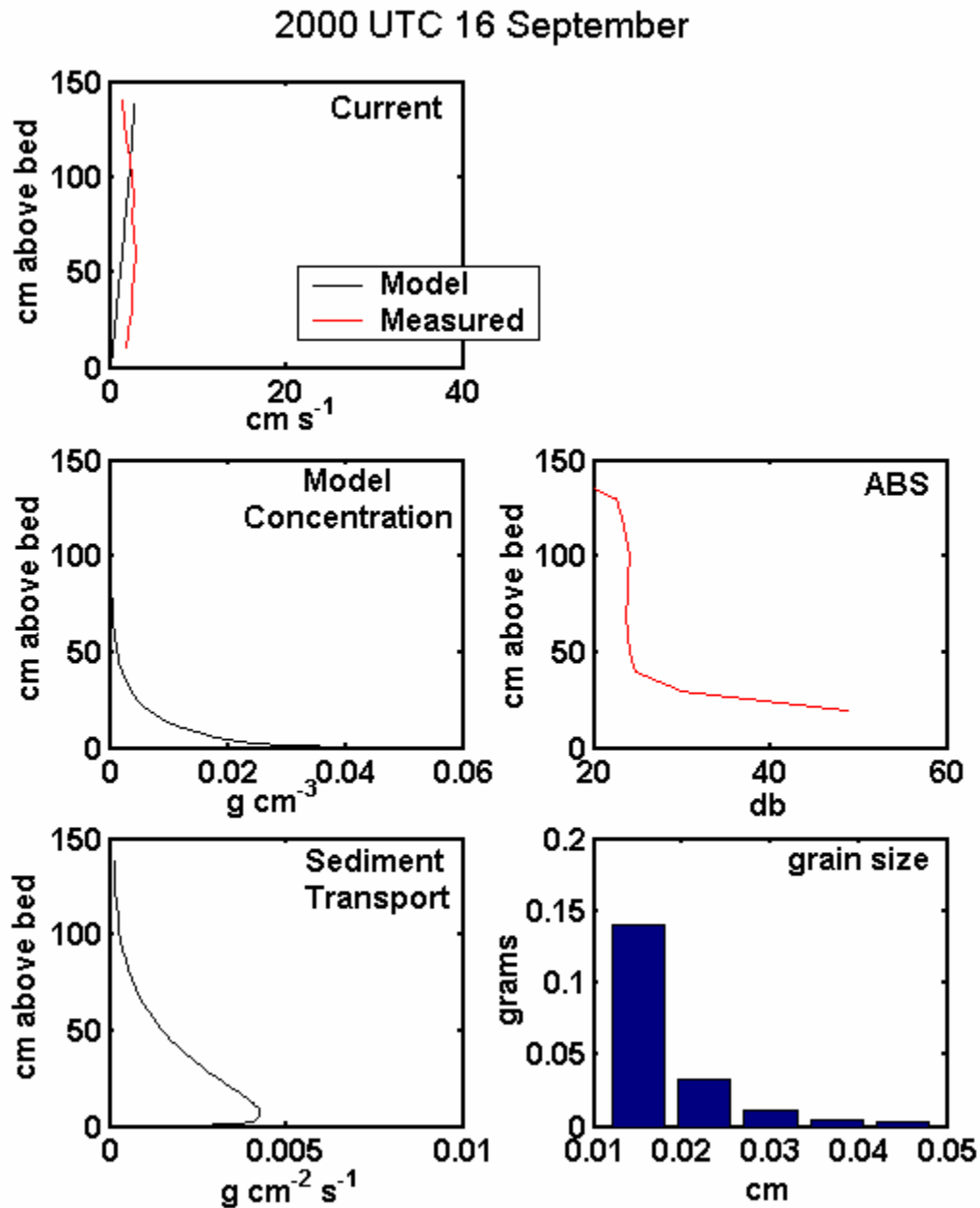


**Figure 47.** Comparison of the model calculated current profile with the PCADP measured current profile in the bottom boundary layer. The ABS and sediment concentrations are also shown along with the model calculated sediment transport profile. The bar graph shows sediments are mostly fine sands, with a small amount of medium sand being suspended. There is an order of magnitude more total suspended sediment in the bottom boundary layer at 2000 UTC on the 16<sup>th</sup> than 1800 UTC on the September 15<sup>th</sup>.

*September 16<sup>th</sup>*

Sediment transport processes continued to intensify over the next 60 hours. On the beginning of 16 September, long period swells (17second) were propagating over the shelf with significant wave heights of 3 – 4 meters. At approximately 1000 UTC, dominant wave periods dropped to 14 seconds, as northerly winds began to increase and wave conditions changed from swell dominant to a combination of locally generated waves and hurricane swell. The bottom orbital velocities associated with these waves ranged from 120 cm s<sup>-1</sup> to 75 cm s<sup>-1</sup>, although by 1800 UTC bottom orbital velocities were 100 cm s<sup>-1</sup> (Figure 44). Mean currents continued to be tidally dominated and weak (<5 cm s<sup>-1</sup> at 1 mab) in the bottom boundary layer. However, by 2000 UTC, a weak subtidal current had been generated in the along-shore direction due to the increase in sustained northerly winds, which had increased to 15 m s<sup>-1</sup>. Combined wave-current shear velocities increased to approximately 12 – 14 cm s<sup>-1</sup> by this time, creating bed shear stresses of approximately 200 dynes cm<sup>2</sup> (Figure 44). Bed shear stresses of this magnitude occur infrequently in the study area and, for example, these shear stresses were comparable to the highest maximum bed shear stresses observed at the site in year 2000 (Wren and Leonard, 2002).

The ABS increased slightly at all heights above the bed from those measured the previous day. The measured suspended sediment profiles also show increased suspended sediments in the bottom boundary layer, especially between 75 and 125 cm above the bed (Figure 47). In situ and model calculated current profiles at 2000 UTC on 16 September (Figure 47) generally agree and indicate that mean currents continued to be weak in the bottom boundary layer during this time. Although suspended sediment concentrations

had increased, little suspended sediment transport was occurring in the bottom boundary layer due to the weak current that was present (Figure 47). A weak subtidal current existed in the along-shelf direction at this time (Figure 43) and it is this current that steered the direction of suspended sediment transport. In addition to this, across-shelf bedload transport was still occurring at the site in association with low amplitude anorbital ripples consisting of sands with grain size diameters of greater than 0.0315 cm. Sediments with grain diameters smaller than 0.0315 cm would have been in full suspension based on the condition for full suspension where  $w_s/ku_{*m} \approx 1$  (Wiberg and Harris, 1994). The seabed elevation measured by the 3 PCADP beams all show fluctuations of 2-5 cm with an increase over the course of the day on 16 September (Figure 45c). However, there is a discrepancy here between the model and the measured data. The model clearly shows that the ripples are beginning to be washed out, exhibiting heights of approximately 2 cm with low steepness of only 0.08 (Figure 44). Calculated bedload transport rates were  $10 - 18 \text{ cm}^2 \text{ s}^{-1}$  throughout the day on 16 September based on a grain size of 0.0315cm.

#### *September 17th*

As the storm continued to approach the site, bottom orbital velocities and current velocities continued to increase. Maximum sediment transport conditions occurred at approximately 2200 UTC on 17 September. Northerly winds increased in magnitude from  $16 \text{ m s}^{-1}$  to  $22 \text{ m s}^{-1}$  (Figure 41) and significant waves heights reached 5 m with periods between 14 and 17 seconds (Figure 41). Bottom orbital velocities continued to increase reaching  $130 \text{ cm s}^{-1}$  late in the day. The along-shelf wind-driven current at 1 mab reached a maximum of  $12 \text{ cm s}^{-1}$  late in the day and was significantly stronger than the

across-shelf current that began to develop midday on 17 September (Figure 43). Wave-current shear velocities were as high as  $17 \text{ cm s}^{-1}$  (Figure 43) and bed shear stresses approached  $300 \text{ dynes cm}^{-2}$ . The acoustic backscatter signal increased to maximum levels of 40 dB, 20 to 30 cm above the bed and was even greater in the lower 20 cms of the water column (Figure 43). This increased concentration of suspended sediment throughout the bottom boundary layer is especially evident in the ABS profile data (Figure 48). The burst-averaged measured velocity profile at 2200 UTC, the time of peak storm conditions, shows stronger currents than the model generated current profile (Figure 48). Both of these profiles, however, show an increase in current speed at all heights within the bottom boundary layer compared to the previous day. The suspended sediment transport profiles provided by the model indicate that transport was occurring at rates of  $0.005 - 0.02 \text{ g cm}^{-2} \text{ s}^{-1}$  (Figure 48) and that most of this material consisted of fine sands less than 0.02 cm in diameter. The seabed altimetry trace at this time shows fluctuations of 2 – 5 cm throughout the day as well as an increase in elevation. These results, however, are inconsistent with the model output that predicted ripples with heights of less than 2 cm with a steepness of 0.05. Based on the condition for full suspension, all grain sizes less than or equal to 0.05 cm would have all been in full suspension during these conditions.

#### *September 18<sup>th</sup> and 19<sup>th</sup>*

The hurricane made closest approach to the site on 18 September. As the storm passed by the site on 18 September, the direction of the wind shifted from north to west between 400 UTC and 1000 UTC (Fig. 41). The along-shelf mean currents at 4 mab and 1 mab were dominated by the wind driven response and the semi-diurnal tidal signal was

2200 UTC 17 September

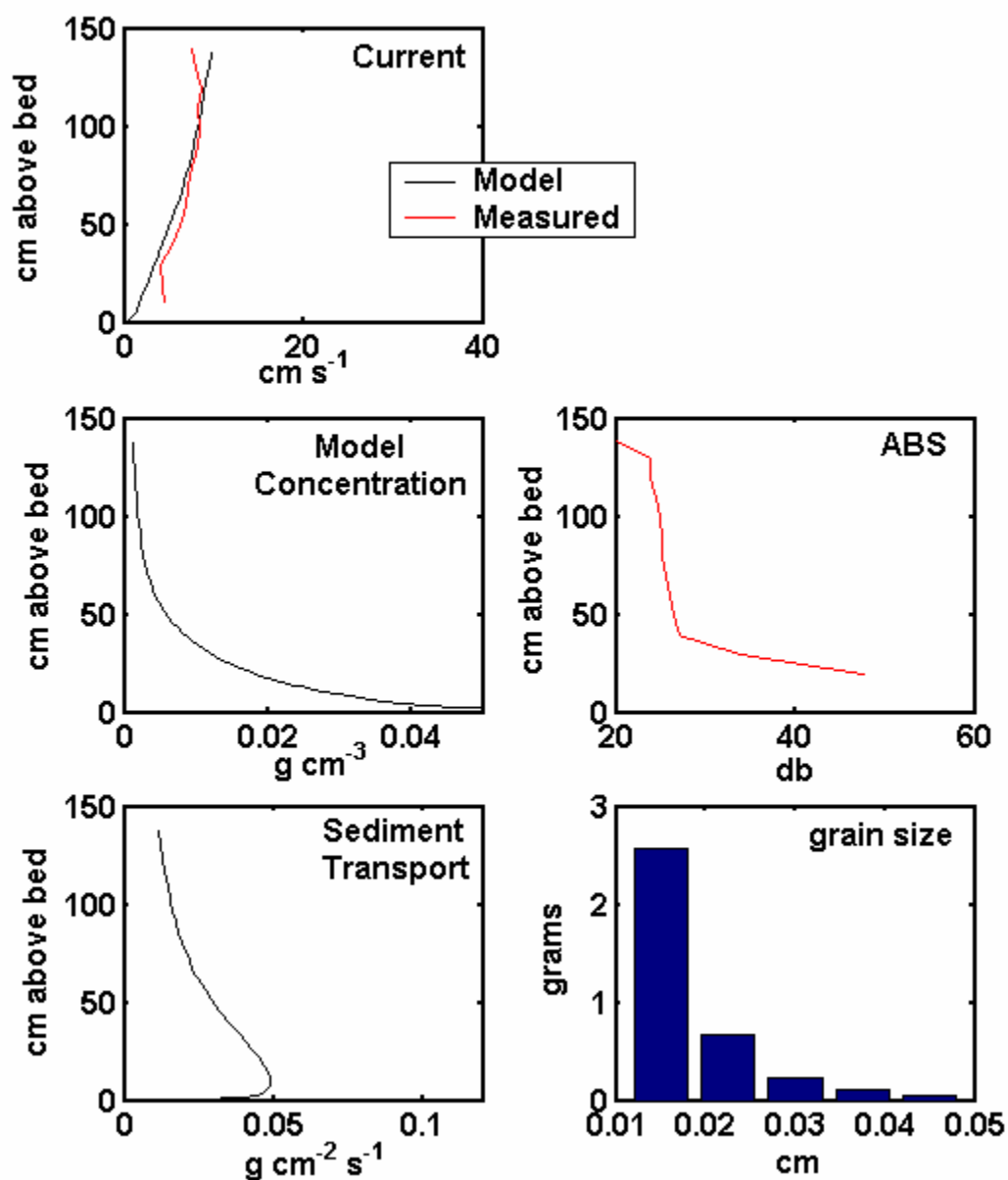


**Figure 48.** Peak sediment transport conditions during burst 35 at 2200 UTC on September 17<sup>th</sup>. Comparison of the model calculated current profile with the PCADP measured current profile in the bottom boundary layer. The ABS and sediment concentrations are also shown along with the model calculated sediment transport profile. The bar graph shows sediments being suspended are mostly fine sand to medium sands.

only apparent in the across-shelf flows (Fig. 42). Along-shelf currents reached over 30  $\text{cm s}^{-1}$  at 4 mab and 15  $\text{cm s}^{-1}$  at 1 mab when winds were from the north. As the winds switched around to the west, wind-driven flows of 5  $\text{cm s}^{-1}$  were also generated in the positive across-shelf direction (offshore) (Figure 43). Maximum wind velocities for this event occurred at 1200 UTC and were from the west-southwest sustained at 30  $\text{m s}^{-1}$ . During maximum wind conditions, wind-driven currents were equal in both the positive along and across-shelf directions (southwest and offshore) with a magnitude of 5  $\text{cm s}^{-1}$ . These conditions lasted for only a few hours, as the wind continued to shift around to a southerly direction and subtidal currents responded very rapidly (Figure 43). The along-shelf subtidal currents then reached 30  $\text{cm s}^{-1}$  in the negative along-shelf direction at 4 mab and 15  $\text{cm s}^{-1}$  at 1 mab at this time (Fig. 42).

As the storm reached the point of closest approach, waves became locally generated and had smaller dominant periods ranging from 6 – 10 seconds. At this point in the hurricane passage, there was a malfunction at the NOAA C-Man station and wave data was lost. This can be seen in the wave and bottom boundary layer data (Fig. 43) on the 18<sup>th</sup>. Although, the data is missing, the observed wave height and bottom orbital velocity data show a substantial decrease from 125  $\text{cm s}^{-1}$  early on 18 September to 30  $\text{cm s}^{-1}$  late in the day. Combined wave-current shear velocities also decreased rapidly on 18 September from 16  $\text{cm s}^{-1}$  at 0000 UTC to 7  $\text{cm s}^{-1}$  by 2200 UTC (Figure 43). Thus, reducing the resuspension of bottom sediments that occurred during the previous three days.

By 0000 UTC on 19 September, winds were from the south at less than 15  $\text{m s}^{-1}$ . Significant wave heights were approximately 2 m with periods of 10 seconds. Mean



currents at 1 mab were 0 and 5 cm s<sup>-1</sup> for the along-shelf and across-shelf components, respectively (Figure 43). At 0000 UTC, subtidal currents in the across-shelf direction were close to zero. These currents increased in strength over the next ten hours and reached 15 cm s<sup>-1</sup> by 1000 UTC in the negative along-shelf direction (northeast), while a weak across-shelf component of 5 – 10 cm s<sup>-1</sup> was directed inshore.

The vertical current profiles generated by the bbl model for this time agreed very well with the measured burst-averaged current profile (Figure 49). Currents in both profiles increased in intensity compared to earlier profiles and reached magnitudes of 18 cm s<sup>-1</sup> 1 mab. Both profiles had a perfectly logarithmic shape (Figure 49). The suspended sediment concentration profile generated by the model is vastly different from the concentration profile measured using the ABS signal. The model output suggests that little material should have been actively resuspended given the existing conditions included in the model input (e.g. ambient grain size, orbital velocities, and current), but does not account for the fine material that was already in suspension. The disparity between the model output and the observed ABS signal suggests the presence of suspended sediments that had not yet settled even though storm conditions were beginning to wane.

The ABS measurements collected on 19 September (Figure 43) gradually decreased over the day, but were still elevated, especially in the lower 30 cm of the boundary layer. These data most likely reflect the settling of the coarser fraction and the retention of the finer materials in suspension. It is for this reason that the sediment transport profile generated by the model likely underestimates the actual suspended

0400 UTC 19 September

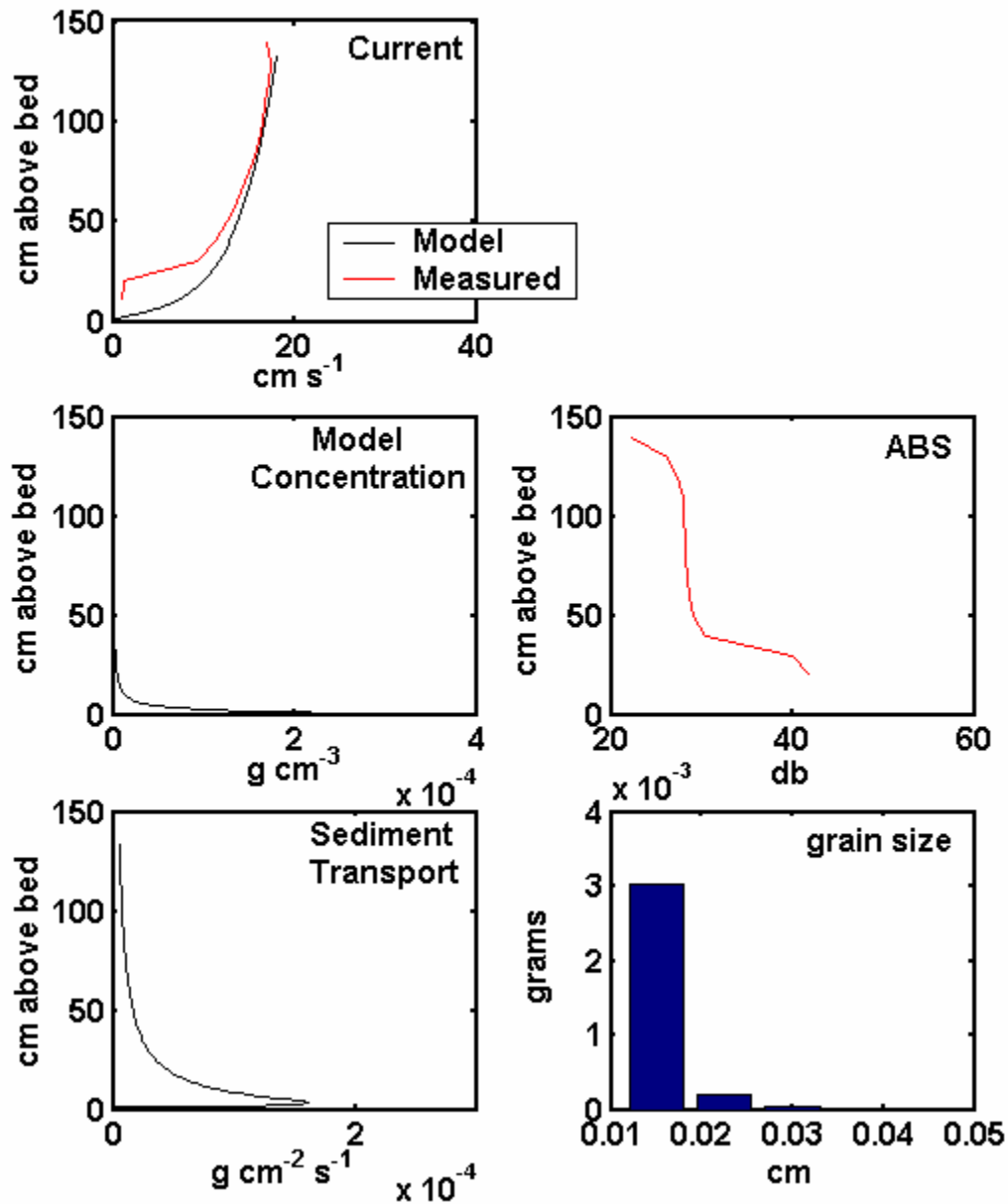


**Figure 49.** Burst 50 occurred at 0400 UTC on September 19<sup>th</sup>. The bblm indicates that only a small amount of sediment transport is occurring at this time, although the ABS measurements still show elevated levels suggesting there are still suspended sediment in the bottom boundary layer.

sediment transport that occurred during this time. The low concentrations predicted by the model, and subsequently used to calculate suspended sediment transport, resulted in a very low rate of only  $1.5 \times 10^{-4} \text{ g cm}^{-2} \text{ s}^{-1}$  that occurred only in the lowest 10 cm. The model did not take into account the finer fraction of sediments that were still retained in suspension even after wave heights had subsided to 2 m and transport of these sediments occurred due to the presence of subtidal currents. These subtidal currents also helped facilitate the bedload transport (Figure 43) through interaction with the waves that were present.

Due to the advection of the fine sediments retained in suspension, sediment transport continued over the next 24 hours. As the storm effects waned on 19 September, wave orbital velocities decreased to between  $10 - 30 \text{ cm s}^{-1}$  and wave periods were 8 – 10 seconds. Seabed altimetry data collected at this time show fluctuations of approximately 1 cm. Under the given wave and current conditions, the bbl model predicted that ripples of 4 – 6 cm developed on the seabed and ripples increased in steepness from between 0.12 – 0.17, which would be classified as suborbital ripples according to Wiberg and Harris (1994). Surface sediments at the site most likely consisted of the coarser fraction, as all of the fine sediment was still in suspension at this time.

#### *September 20<sup>th</sup>*

On 20 September the sediment transport associated with Hurricane Isabel began to come to an end. Shear velocities decreased throughout the day from  $5 \text{ to } 2 \text{ cm s}^{-1}$  (Figure 43). The ABS time series indicates that suspended sediment levels decreased at all measured heights above the bed rapidly. By 0000 UTC on 20 September, which was 120

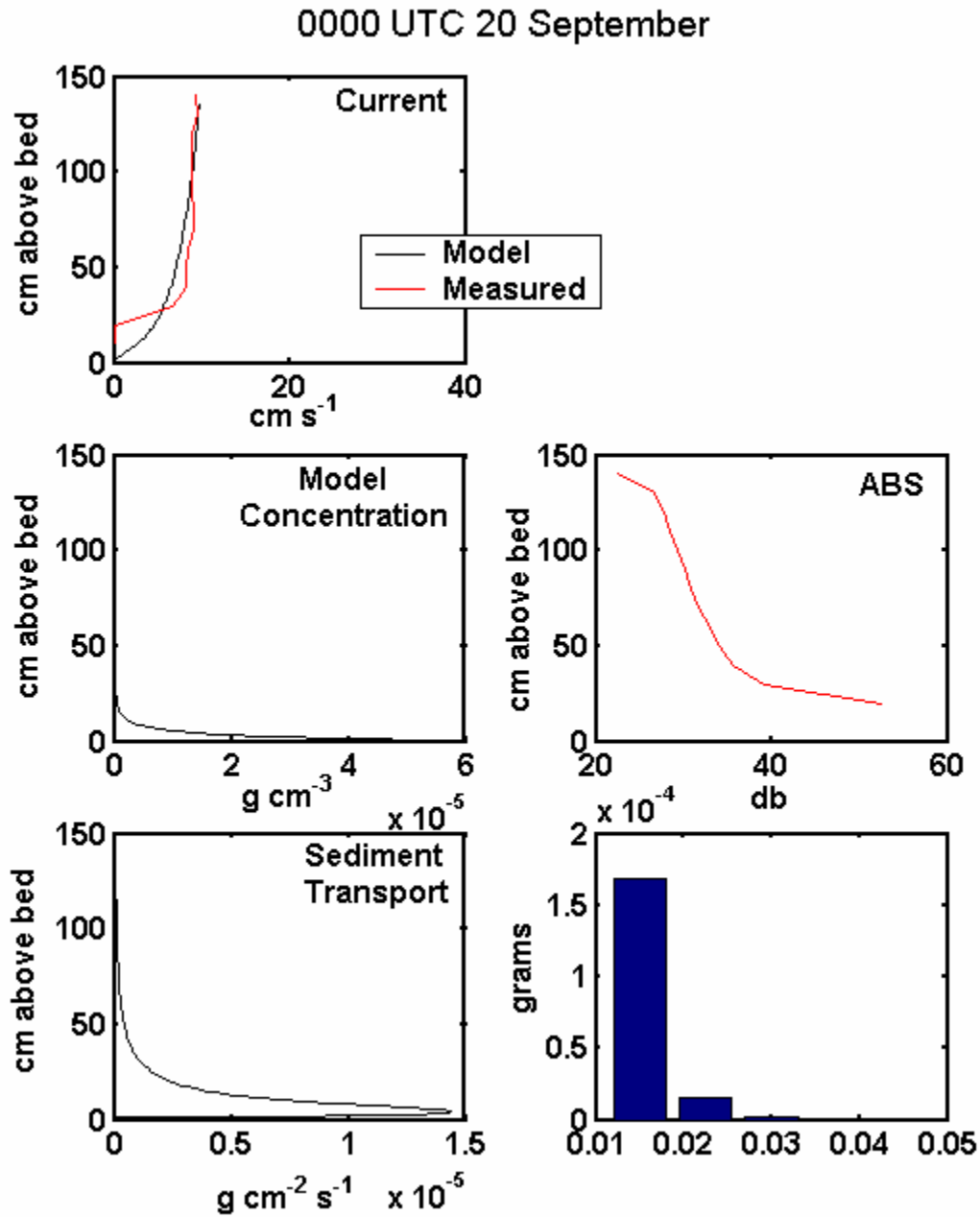


**Figure 50.** Burst 60 was at 0000 UTC on September 20<sup>th</sup>. Both the model and measurements indicate that the sediment transport event is over at this time. Current profiles show good agreement, both indicating very weak currents at this time.

hours after the hurricane began to impact the site, only a small amount of fine sediment was still in suspension in the boundary layer (Figure 50). For the remainder of the day, the ABS measurements suggest that suspended sediment concentrations decreased until they finally reached below pre-storm levels (Figure 43). The ripple heights predicted by the bbl model returned to model default input by the end of the day, even though fluctuations of 1 cm were still recorded in the seabed altimetry data. Wind-driven, subtidal flows in the bottom boundary layer diminished on 20 September, as well (Figure 43).

#### *4.3.3 Spectral analysis*

A spectral analysis of the raw PC-ADP current data at 1 mab was undertaken to examine the frequencies with the most energy in the bottom boundary layer (Figure 51). Energy spectra from data collected approximately 72 hours prior to hurricane passage indicate that most of the energy was between 0.03 – 0.7 Hz, (14 - 33.3 seconds) in the across-shelf direction, corresponding to the individual swell wave frequency (14 – 17s) and wave group (infragravity) frequencies. A comparison between the pre-storm along-shelf and across-shelf spectra show that an order of magnitude less energy occurred in the along-shelf direction than in the across-shelf direction. This was due to dominant wave direction. A peak in the along-shelf spectra occurred at the same frequencies as the across-shelf direction due to the long period swells having a small directional component in the along-shelf direction. The angle of maximum variance for each burst indicates that wave direction varied by less than 20° north from directly on-shore, until hurricane winds began to directly affect the area early on 18 September.

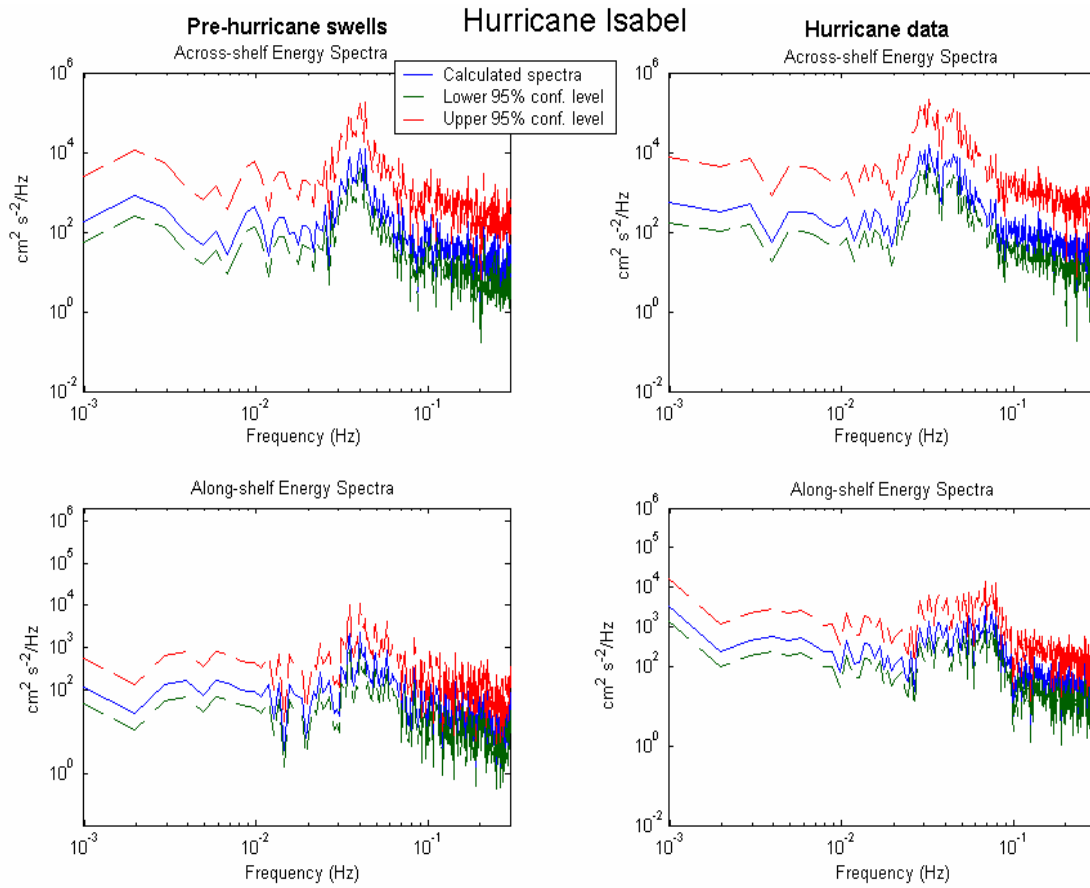


**Figure 51.** Spectral analysis of raw PCADP data at 1 mab show high energy levels in the swell frequency bands before the storm and more energy in the local wind wave bands during the storm. Along-shelf subtidal flows, generated when winds from hurricane directly impacted the site, show up well in the along-shelf spectra during the storm.

Both pre-storm and storm spectra show a shift in the energy as the storm approached the site. The storm spectra were generated from the PC-ADP velocity data at 1 mab early on 18 September as the hurricane was starting to directly impact the area. During the storm, a wide range of energy occurred in the across-self direction between frequencies of 0.02 – 0.9 Hz (11.11 – 50 seconds). The spectra exhibited a double peaked shape, with peak energy corresponding to periods of 20 – 25 seconds and 33 seconds. This double peak shape of the spectra commonly occurs during storms. These data suggest an increase in energy at frequencies corresponding to shorter period, locally generated wind waves and an increase in the infragravity motion (between 30 – 50 seconds) during the time that tropical storm force winds were present in the study area. This increase in infragravity energy is consistent with observations by Wright *et al.* (1994) during the “Halloween storm” of 1991, a large nor’easter storm off the Mid-Atlantic coast.

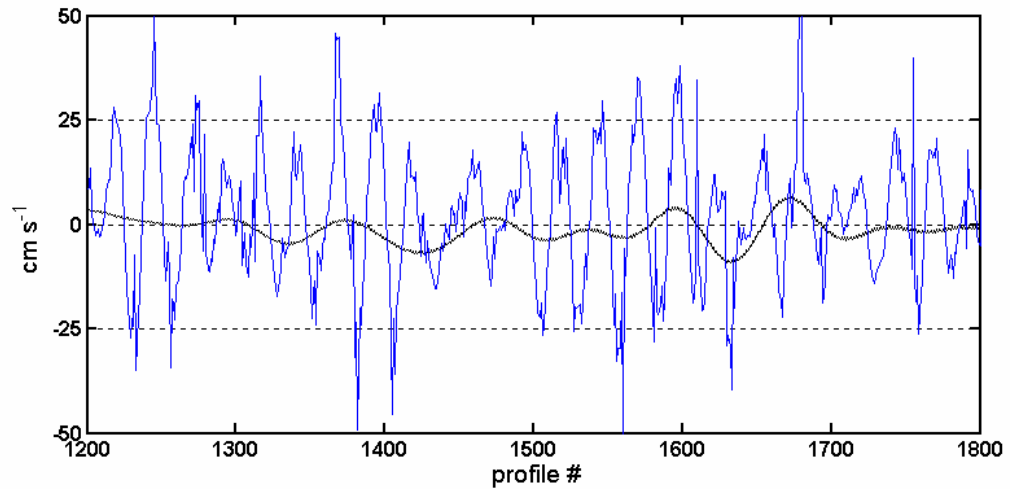
In the along-shelf direction, the spectra generated from data collected during storm conditions show close to an order of magnitude increase, relative to the pre-storm spectra, at lower frequencies of 0.001 – 0.002, as well as at higher frequencies of 0.06 – 0.09 Hz (Fig. 51). These frequencies correspond to periods of approximately 10 minutes and 11.11 – 16.6 seconds, respectively. These data suggest that as the hurricane approached and passed the site, the importance of winds as a forcing mechanism increased in the along-shelf direction. Waves were locally generated during this time, 0000 - 0200 UTC on 18 September, by winds in the along-shelf direction, and this, in turn, increased energy in the higher wave frequencies. Larger waves were also propagating from the center of the storm that was now located northeast of the site, and

these waves were oriented in the along-shelf direction as well. This switch in wave direction due to the storm track increased the energy at the wave frequencies by an order of magnitude. The along-shelf spectra also indicate a large increase in energy in the lower frequency band between 0.001 – 0.002 Hz. These frequencies are mostly likely associated with set up of a wind-driven current in the along-shore direction. The across-shelf spectra show a slight increase (Fig. 51), as there was a small onshore component in the wind driven flows. An increase in energy in the lower frequencies between 0.001 and .000138 Hz has been shown previously to be a typical shallow water response to hurricanes (Bingham *et al.*, 2003). Because our burst interval was only 10 minutes, however, it was only possible to resolve the increase in energy at 0.001 Hz from the raw data spectra.

In the pre-storm and storm spectra, most of the energy was contained in the infragravity frequencies and indicated that wave groups contained more energy than individual waves. This result is expected considering the distant source of the waves and the fact that swells organize themselves into wave groups, which travel faster than the individual waves. A spectral analysis of both the near bottom flows and ABS measurements suggest that infragravity waves were an important contributor to the across-shelf suspended sediment transport throughout the 4-day event. In the across-shelf raw velocity data, fluctuations of  $(-)10 - (+)10 \text{ cm s}^{-1}$  can be seen at infragravity frequencies both before and during the storm (Fig. 52a, 53 a). These same fluctuations are apparent in the raw ABS signal before and during the storm (Figure 52b, Figure 53b). Therefore, it appears that the infragravity waves also played a role in the transport of suspended sediments in the across-shelf direction. These results are consistent with the



a.



b.

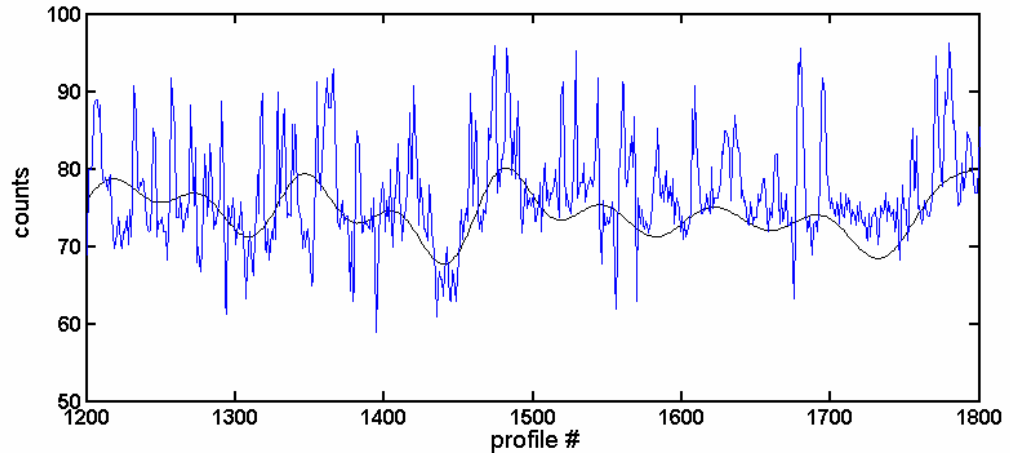
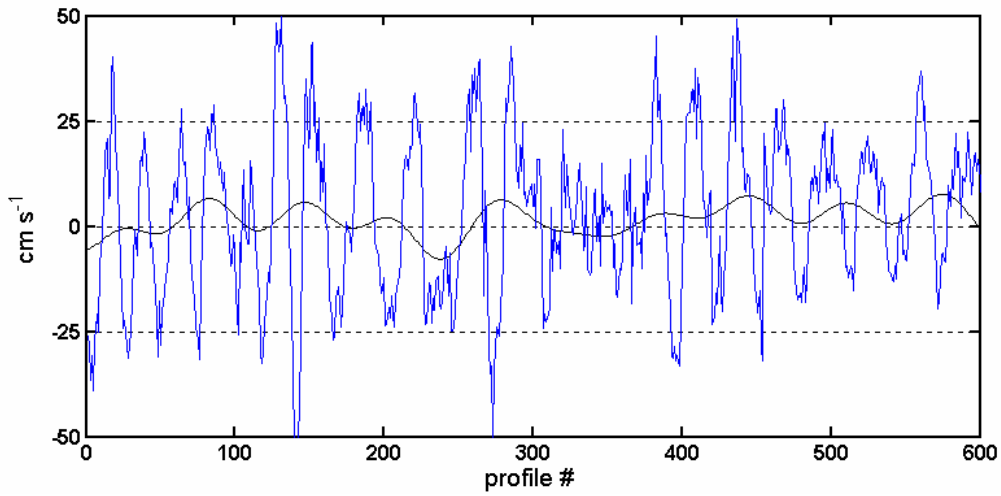


**Figure 52 (a.)** The raw PC-ADP across-shelf velocity data at 1 mab from a pre-storm burst of data on 15 September. Infragravity oscillations are shown in black. **b.)** The raw acoustic backscatter signal (in counts) during the same burst of data with infragravity waves shown in black.

a.



b.

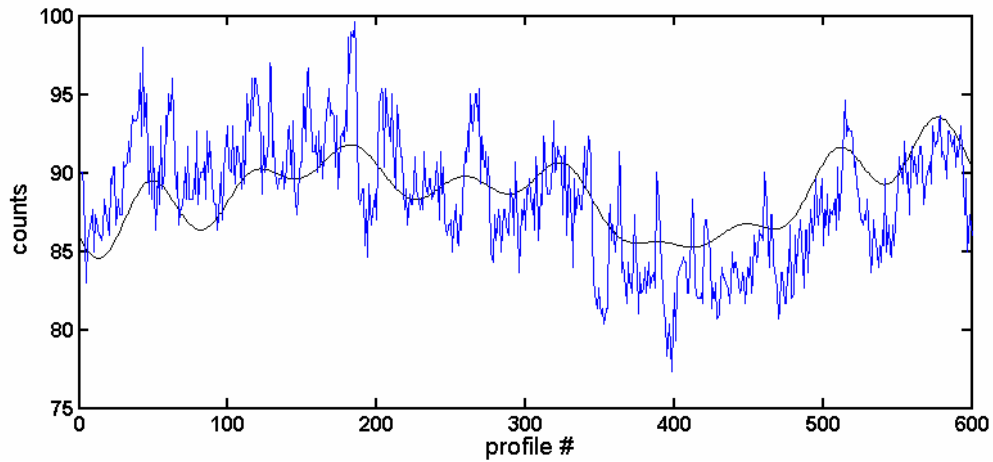


**Figure 53 (a).** The raw PC-ADP across-shelf velocity data at 1 mab for from a burst of data collected during the storm at 0200 UTC on 18 September. Infragravity oscillations are shown in black. **(b.)** The raw acoustic backscatter signal (in counts) during the same burst of data with infragravity waves shown in black. A longer period oscillation due to wave group interactions is also apparent during the storm.

inference that infragravity motions can contribute to the suspension of sediment to heights well above the boundary layer (Wright et. al, 1994). The suspension of sediments to heights outside of the boundary layer was observed during most of this event.

## **4.4 Discussion**

### *4.4.1 Sediment transport*

The two most contributing factors to the sediment transport that occurred during the hurricane were long-period swells and subtidal flows. As the hurricane swells propagated across the shelf from the distant hurricane that was located to the southeast of the site, large bed shear stresses were generated on the mid-shelf that caused suspended and bedload transport to occur as early as 3 days prior to the actual storm. These effects can be seen in the ABS time series data and the various suspended sediment and sediment transport profiles on 15 September. One important aspect of the hurricane swells was that they propagated across the shelf from the southeast and caused significant bedload transport to occur via migrating ripples in the (negative) across-shelf direction, towards the coast. The wave direction continued to be from the southeast throughout the event varying by less than 20° north of directly on-shore, until 18 September when winds from the storm began to directly impact the site. At this point, wave periods decreased and wave direction shifted to the northeast.

Bedload sediment transport was the main mechanism for across-shelf sediment transport throughout the storm, although at peak conditions almost all sediment grain sizes at the site ( $d < 0.05$  cm) went into suspension. Long two-dimensional, narrow crested ripples with broad troughs were observed by divers at three locations across the shelf, including the study site, on 15 September. Evidence of these ripples is present in

the seabed altimetry data and also predicted to be present by the bbl model for the conditions that existed on 15 September. Ripples that formed under these conditions were wave-dominated ripples that formed under the influence of relatively weak current speeds and high wave bottom orbital velocities. According to Traykovski *et al.* (1999), the temporal evolution of ripple direction generally follows the dominant wave direction. Thus, the long period swells approaching the site from the southeast caused bedload transport in the across-shelf direction, towards the coast, from 15 September – 17 September until these bedforms approached “wash out” at peak storm conditions. Bedload transport calculations indicate that the rate of bedload transport varied from 3 – 20 cm<sup>2</sup> s<sup>-1</sup> mid-day on the 15<sup>th</sup> to mid-day on the 17<sup>th</sup>. This onshore transport of sand has significant implications for coastal managers and residents in southeastern North Carolina where shorelines are highly developed and actively eroding and where both private and federal monies are used to undertake beach re-nourishment projects (where and when sand is available).

The other important sediment transport mechanism identified during this study was the strong subtidal currents that developed in the lower boundary layer during the hurricane. Subtidal currents have been shown to determine the direction of sediment flux during storms off the northern California coast (Ogston and Strenberg, 1999). The along-shelf subtidal currents formed during the hurricane were positively correlated with along-shelf wind velocity ( $R = 0.68$ ). The across-shelf subtidal current magnitudes also were well correlated with across-shelf wind speeds ( $R = 0.70$ ). Both the subtidal flows and burst-averaged currents responded rapidly to local wind forcing (Figs. 43e), changing in

magnitude and direction when winds shifted from northerly to southerly on 18 September.

The positive along-shelf subtidal currents coincided with the time of maximum bottom orbital velocities at approximately 2200 UTC on 17 September (Figure 43). This provided the mechanism for the largest quantities of suspended sediment transport to occur in the positive along-shelf direction. Transport was predominantly towards the southwest when subtidal currents of  $12 \text{ cm s}^{-1}$  occurred in the positive along-shelf direction, in association with winds that were from the north. The sediments suspended during this phase of the storm were potentially transported 1 km in the along-shelf direction, towards the southwest, during a 2-hour interval by the subtidal flows that had developed. As the hurricane continued on its track to the north of the site, the wind driven currents responded rapidly to local winds and shifted first to eastward (offshore), and then eventually to northeasterly; directly opposite to the direction during peak conditions. Much less sediment was transported after the winds switched to southwesterly due to the rapid and concurrent decrease in bed stresses and wave energy on 18 September (Figure 43). By 1000 UTC 19 September, when winds had shifted to southerly and subtidal currents of  $16 \text{ cm s}^{-1}$  existed in the negative along-shelf direction, wave orbital velocities and shear velocities had decreased substantially, and therefore less sediment was suspended and transported during this time towards the northeast (negative along-shelf direction). The bbl model output corroborates the data and indicates that a significantly larger amount of suspended sediment transport occurred at 2200 UTC on 17 September, than any other time before, during, or after the storm. A compass plot of the total suspended sediment transport that occurred during each burst throughout the

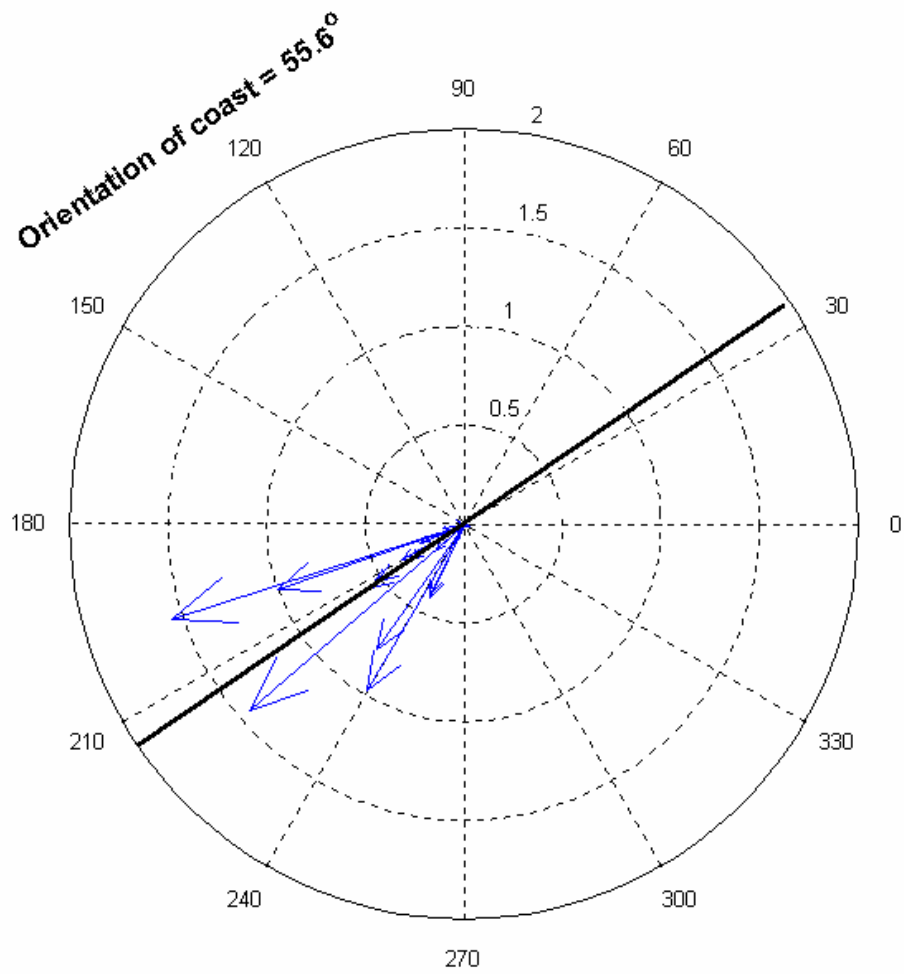


**Figure 54.** Compass plot showing the direction of suspended sediment flux that occurred at the site throughout sediment transport event.

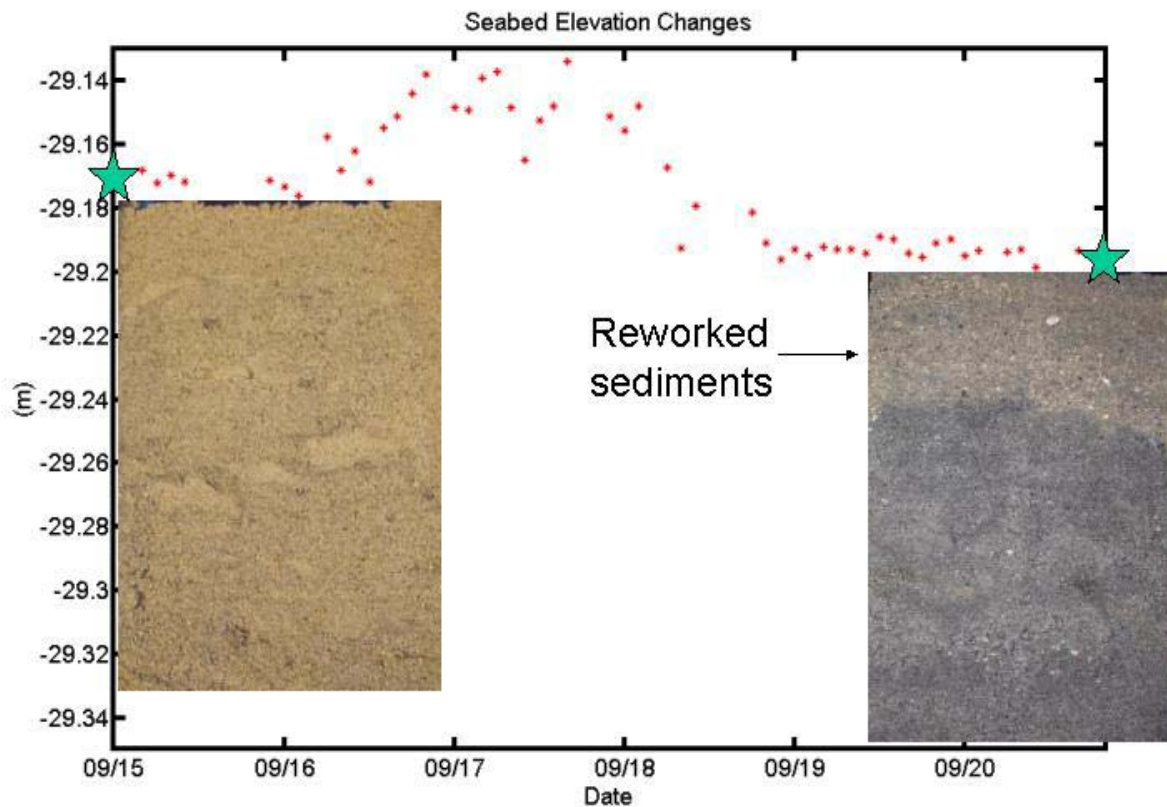


**Figure 55.** Pre- and post boxcores are aligned with the seabed elevation data. The storm layer is visible in the post-storm core as oxidized sediment. There was approximately 2 cm of net erosion of the seabed following storm passage although at least 7 cm of reworking is indicated given the deposition of a 5-6 cm thick storm deposit.

duration of the event shows that suspended sediment transport was predominantly towards the southwest (Fig. 54). When the subtidal currents on 19 September had the potential to return the suspended sediments that had been carried away from the site on 17 and 18 September, less material was in suspension by this time having settled under the less energetic bottom conditions that existed. As a result, the seabed in the vicinity of the instrumented frame underwent net erosion due to the storm. The post- storm seabed elevation was approximately 1 cm lower than the pre-storm elevation.

#### *4.4.2 Seabed altimetry*

A 5 - 6 cm thick storm deposit was present in the post-hurricane boxcores taken on 23 September, approximately 5 days after the hurricane passed the site (Fig. 55). This storm deposit indicates the depth of re-working at the site by the physical processes previously described. When both the thickness of the storm deposit and the pre- and post-storm bed elevations are accounted for, there was approximately 7 cm of storm reworking at the site (Fig. 55). This finding, however, conflicts with the seabed altimetry data collected during peak storm conditions. These data show an approximate 5 cm increase in the seabed elevation with large variations (up to 6 cm) in the signal during the highest energy conditions of the storm. The seabed elevation data suggest that during the storm from midday on 16 through 17 September, sediments were accreting and that large ripples were present at the site. On 18 September the seabed altimeter data shows that 5 cm was eroded from the site within a few hours. This was the time when shear velocities actually started to significantly decrease, due to the significant decrease in wave orbital velocities caused by locally generated, shorter period waves.



A more reasonable explanation is that the seabed altimeter was detecting a very highly concentrated layer of suspended sediments that had been suspended by the hurricane swells. During this period of elevated seabed elevation, the wave boundary layer thickness ranged from 20 – 37 cm and there were weak currents available during this time to transport the high amount of suspended sediments in the wave boundary layer. The seabed altimetry data seems to be coupled with the shear velocities and although there are missing data on the 18<sup>th</sup>, it is apparent that there was a significant decrease in the shear velocities throughout the day on the 18<sup>th</sup>. This is when the seabed altimetry data showed the recently elevated seabed decreased by approximately 7 cm in each of the three beams (Fig. 55). The presence of a highly concentrated layer of suspended sediment is further corroborated by the ABS time series measurements which yielded very high returns between 10 and 30 cmab (Figure 43) and the output from the bbl model which showed high amounts of suspended sediments in the bottom 30 cm centimeters during this time (Figs. 45, 46 & 47). This is also apparent in the ABS contour plots of the time series (not shown – Sontek visualization software) of the two lower bins from the PC-ADP. Where there is usually a sharp contrast between the bottom two bins that defines where the seabed boundary is, during this part of the storm the signal from these two bins became mixed and there was no sharp return in the signal that defined the seabed boundary. The presence of a highly concentrated layer of suspended sediment is one scenario that seems feasible particularly if anecdotal diver reports are considered. The existence of an oscillating suspended sediment layer (of lesser magnitude) immediately above the seabed has been observed by divers at the site during periods of long period swell during distant hurricane passages to the east of the site. The sediment

tube, which contained approximately  $400\text{cm}^3$  of fine to medium sands that were suspended during the event, also confirms that sands at the site were in suspension to a height of at least 30 cm during the storm.

It can also be shown, by simple calculations, that what the seabed altimeter measured during the storm was a highly concentrated layer of suspended sediments rather than the true bottom. By the end of the day on 15 September, the critical shear velocity threshold for full suspension had been exceeded for all grain sizes less than or equal to 0.03 cm, which is over 50 % of the volume of surface sediment found at the site, based on grain size analysis from previously collected samples. Based on the condition for full suspension and the shear velocities that existed during peak storm conditions, all grain sizes of 0.05 cm (approximately 90% of sediments at the site) would have been in full suspension, while the remaining small amount of coarse sediment would have formed low amplitude ripples on the bed. This result more closely agrees with the bbl model output that predicted ripples less than 2 cm with a low steepness approaching “wash out” conditions during this part of the storm than the measured seabed elevation at the time.

Thus, multiple lines of evidence exist that suggest the presence of a layer of highly concentrated sediments that were suspended in the lower boundary layer. The existence of such a layer easily accounts for the large discrepancy between the bbl model output and the seabed altimetry data and indicates that the seabed altimeter was not detecting the bottom during the height of the storm.

While the discrepancy between the seabed elevation data and the bblm can be explained, there is the matter of the disagreement between the boxcores collected pre- and post storm, which clearly show a storm *deposit* layer of 5cm, and the seabed

elevation data, which indicates there was a net decrease in seabed elevation of 1 cm. This can be explained by the large amount of sediment that was suspended in the vicinity of the study area during the storm (as discussed above), which was subsequently re-deposited as the storm waned, and the effect that the hardbottom has on the study site. Due to the location of the hardbottom to the north and northeast of the site, suspended sediment transport towards the southwest results in erosion, because of the limited source of sediment “upstream” on the hardbottom surface that is available to be transported towards the site. During peak conditions the suspended sediments were transported towards the southwest, away from the site, and as currents reversed not as much was brought back to the site and deposited as the storm waned. Therefore, when the seabed altimetry data showed the artificially elevated seabed due to the high suspension of sediments and transport towards the southwest, erosion most likely occurred at this time to the depth of the storm deposit layer (~7cm). Then, when bottom conditions became less energetic and transport occurred towards the northeast on 18 and 19 September, only approximately 5 cm of sediment settled out of suspension and was deposited at the site producing the storm layer.

#### **4.5 Conclusions**

Sediment transport occurred at the mid-shelf site due to the close passage of Hurricane Isabel over a four-day period. The extended impact duration was due to hurricane swells that preceded the passage of the storm by 72 hours. Ripples were observed on the bed as early as 72 hours prior to storm passage. Because swell direction remained from the southeast over a three-day period, ripple migration resulted in extensive bedload transport in the shoreward direction. Maximum subtidal flows in the

along-shelf direction coincided with maximum orbital velocities due to local wind forcing. The synergy between these two processes resulted in increased suspended sediment transport in the positive along-shelf direction, towards the southwest, with a slight across-shore component. The presence of high levels of suspended sediments within the wave boundary layer caused the 1.5 MHz seabed altimeter to not detect the bottom during periods of large swell-dominated bottom conditions. Overall, the net sediment flux associated with the hurricane was to the southwest and shoreward. Shear velocities measured during this event were larger than any on record during year 2000 (Wren and Leonard, 2002).

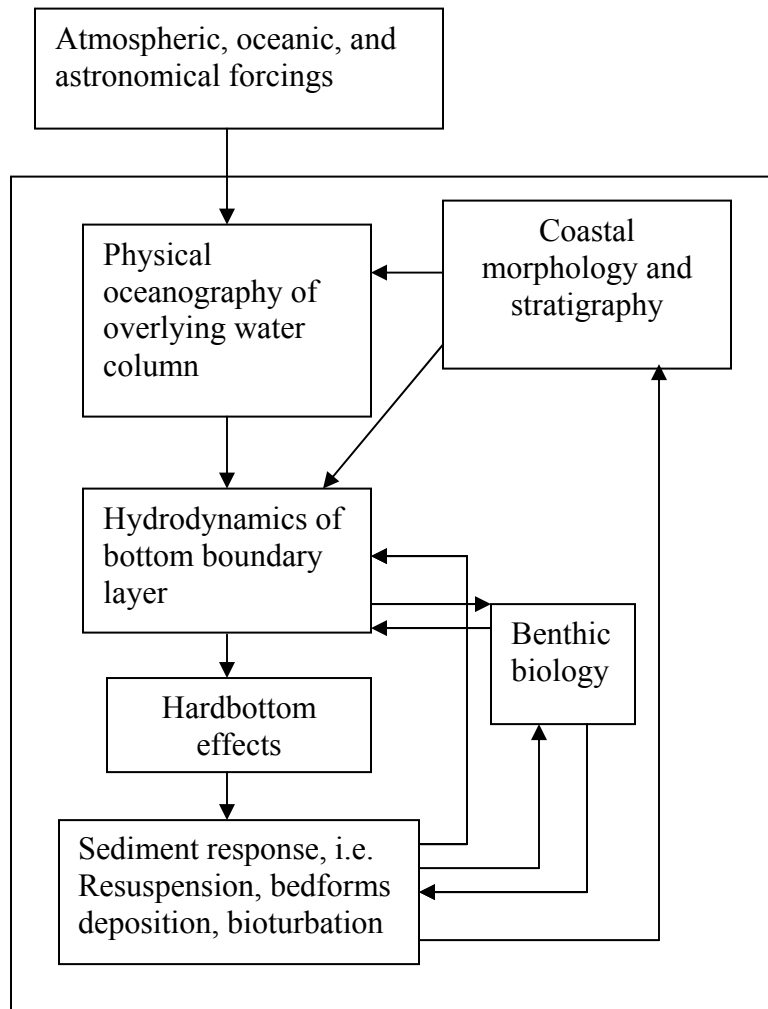
## Chapter V

### Summary

#### 5.1 Conclusions

The mid-continental shelf in this region of the South Atlantic Bight appears to be an active area of sediment transport, based on the work presented here. The forcing mechanisms for sediment transport on the mid-shelf in Onslow Bay appear to be a complex combination of: waves, tidal currents, and low-frequency and mean shelf currents (Fig. 56). Shear velocities due to wave-current interactions exceeded the critical threshold for sediment motion 75% of the time during a year of sediment transport measurements. This year of study was a “typical” climatologic year based on the past ten years of wind directions. The total net sediment flux at 1 mab was in the positive along-shelf direction (southwest) and in the negative across-shelf direction (onshore). During the year of record, there was several times more net transport of sediment in the onshore direction than the along-shelf direction. This indicates that sand would be transported on to the hardbottom reef area located landward of the site. It is also evidence that cross-shelf sediment flux is not limited to the inner-shelf or shoreface, and that sediments on the mid-shelf (at least the fine sands) are a part of a larger system encompassing the inner-shelf and shoreface. These data show that if the prevailing winds during the year are consistent with local climatology, that sediments can be transported from the mid-shelf towards the coast. The data collected in this study was only from one point on the shelf, and at this location sediment transport was onshore. The spatial variation of

**Figure 56.** A flow diagram showing the potential complex interactions that can occur on the mid-shelf in Onslow Bay, NC.



sediment flux on the shelf, however, was not known at the time of this research and was beyond the scope of this study. However, the mean velocities from 4mab and 1 mab in both the along-shelf and across-shelf directions were very similar over the course of a year. This result suggests that current data collected in large-scale circulation studies, if collected within the bottom several meters of the water column, can be used to characterize sediment transport patterns on the shelf when Ekman steering in the bottom boundary layer is taken into account.

On the shelf of the South Atlantic Bight (SAB), small to moderate storms and fair weather processes are important in ascertaining when sediment transport occurs. Unlike the West Coast or the Mid-Atlantic Bight, the SAB has a lower frequency and intensity of large storms and, therefore, these types of events play an important role in the sediment transport that occurs on the mid-continental shelf. However, the shear velocities measured during Hurricane Isabel were larger than any on record during year 2000 (Wren and Leonard, 2002). The net suspended sediment flux associated with Hurricane Isabel was an order of magnitude larger than that associated with a moderate sized nor'easter storm, and was towards the southwest and onshore. Bedload transport in the onshore direction occurred three days prior to the storm passage due to hurricane swells traversing the shelf. This onshore sediment flux during a close passage of a hurricane is consistent with seabed elevation measurements on the inner-shelf region (13m) offshore of Duck, NC in the Mid-Atlantic Bight (Beavers, 1999).

**More specific conclusions from this research are:**

- The mid-shelf in Onslow Bay is an active region for sediment transport. Shear velocities exceeded the critical shear threshold for sediment movement for fine sands at the site for 75% of the time during a year, and 50% of this time sediments were being suspended from the bed.
- Current data collected in large-scale circulation studies, if collected within the bottom several meters of the water column, can be used to characterize sediment transport patterns on the shelf when Ekman steering in the bottom boundary layer is taken into account. However, the hydrodynamics and sediment transport patterns adjacent to reef ledges on the shelf may vary.
- Subtidal flows were one of the key forcing mechanisms for sediment transport at the site. Low frequency, subtidal flows were a key forcing mechanism of sediment transport during the Gulf Stream event. Wind driven, subtidal currents were the driving force for sediment transport during the wind events. A wind event with large wind-driven, subtidal currents resulted in almost an order of magnitude more suspended sediment transport than a similar wind event with equal shear velocities and smaller wind driven currents.
- The Styles and Glenn (2000) bottom boundary layer model used in this study appears to reasonably quantify the amount of sediment transport associated with



storms of large magnitude and small to moderate wind events on the mid-continental shelf at this location. However, the model cannot account for the advection of suspended sediments at the waning of a storm event. The bbl model calculates current and sediment transport profiles at a given time, and if there are sediments that are already suspended in the bbl it cannot account for this; i.e., the model has “no memory” in a sense.

- Sediment transport occurred at the mid-shelf site over a four-day period due to the close passage of Hurricane Isabel. Swell direction as the storm approached remained from the southeast over a three-day period, resulting in extensive bedload transport in the onshore direction. The amount of suspended sediment transport that occurred during the hurricane was an order of magnitude larger than a moderate northerly wind event, and was predominantly in the along-shelf direction.

## 5.2 Future efforts

I believe that the future efforts in collecting sediment transport data should be focused on the spatial variability of sediment transport on the shelf. The data presented here has shown that the mid-shelf in Onslow Bay ( $d = 30\text{m}$ ) is an active environment where sediment transport is occurring 75 % of the time during a climatologically “typical” year. This is somewhat inconsistent with the existing paradigm that on the U.S. east coast, sediment transport at these depths is insignificant throughout most of the year and may only occur during large magnitude storm events. Now that we are aware that sediment transport is occurring regularly on the mid-shelf, the next step would be to spatially examine the large-scale behavior and try to determine areas of sediment flux divergence and convergence. Sediment transport measurements should be collected across the shelf, from inner shelf to depths to the outer shelf at a depth where sediment transport occurs only approximately 10% of the time, and cross-shelf sediment flux examined. These measurements could also be combined with knowledge of the large-scale circulation patterns known to occur in the bay, which have been shown to be consistent with recent bottom boundary layer measurements. These types of measurements made over several years on the shelf could enlighten the present knowledge of the large-scale behavior of sediment transport on continental shelves on the U.S. east coast and would be beneficial to coastal engineers and commercial fisheries management.

## References

- Atkinson, L.P., Singer, J.J., Dunstan, W.M., and Pietrafesa, L.J., 1976. Hydrography of Onslow Bay, NC: September 1976 (OBIS II). 76-2, Georgia Marine Science Center, Skidaway Island, Georgia.
- Battisto, G.M., 2000. Field measurement of mixed grain size suspension in the nearshore under waves. M.S. Thesis, Virginia Institute of Marine Science, Gloucester Point, VA, unpublished.
- Beavers, Rebacca L., 1999. Storm sedimentation on the surf zone and inner continental shelf, Duck, North Carolina. Ph.D. dissertation, Duke University, Durham, NC.
- Bingham, F.M., L.B. Cahoon, P.A. Wren, L.A. Leonard, B.L. Speckhart, 2003. Ocean response to Hurricane Isabel in Onslow Bay, NC. Abstract submitted to American Geophysical Union, *Ocean Sciences*, Portland, Oregon, 2004.
- Blackwelder, B.W., Macintyre, I.G., Pilkey, O.H., 1982. Geology of the continental shelf, Onslow Bay, North Carolina, as revealed by submarine outcrops. *American Association of Petroleum Geologists Bulletin*, 66, 44-56.
- Blanton, J. O., Pietrafesa, L.J., 1978. Flushing of the Continental Shelf south of Cape Hatteras by the Gulf Stream. *Geophysical Research Letters*, 5/6, 495-498.
- Bane, J.M., Jr., Brooks, D. A., 1979. Gulf Stream Meanders along the Continental margin from the Florida Straits to Cape Hatteras. *Geophysical Research Letters* 6(4), 280-282.
- Brooks, D.A. and J.M. Bane, 1981. Gulf Stream fluctuations and meanders over the Onslow Bay upper continental slope. *Journal of Physical Oceanography*, 11, 247-256.
- Cacchione D.A., Wiberg, P.L., Lynch, J., Irish, J., and Traykovshi, P., 1999. Estimates of suspended-sediment flux and bedform activity on the inner portion of the Eel continental shelf, *Marine Geology*, 154, 83-97.
- Cione, J.J., S. Raman, and L.J. Pietrafesa, 1993. The Effect of Gulf Stream-Induced Baroclinicity on U.S. East Coast Winter Cyclones. *Monthly Weather Review*, February.
- Cleary, W. J., Pilkey, O. H., 1968. Sedimentation in Onslow Bay: guidebook for field excursions. *Southeastern Geologists Special Publications* 1, 1-17.
- Glenn, S.M. and W.D. Grant, 1987. A suspended sediment stratification correction for combined wave and current flows. *Journal of Geophysical Research*, 92, 8244 – 8264.

- Glenn, S.M., 1983. A continental shelf bottom boundary layer model: The effects of waves, currents, and a moveable bed, Sc.D. thesis, Mass. Inst. of Technol., Cambridge.
- Grant, W.D. and O.S. Madsen, 1986. The continental shelf bottom boundary layer, *Annual Review of Fluid Mechanics*, 18, 365-305.
- Grant, W.D. and O.S. Madsen, 1979. Combined wave and current interaction with a rough bottom. *Journal of Geophysical Research*, 84, 1797 – 1808.
- Gutierrez, B T, G. Voulgaris, and E. Thielier, 2002. Wind-driven flow and the maintenance of a rippled scour depression: Wrightsville Beach, NC. *Eos Trans. AGU*, 83(47), Fall Meet. Suppl., Abstract OS52F-11, 2002.
- Harris, C.K. and R.P. Signell, 1999. Circulation and sediment transport in the vicinity of the Hudson Shelf Valley. *Proceedings of the American Society of Civil Engineers*, November 1999, New Orleans, LA, 380 – 394.
- Harris, C.K., B. Butman, and P. Traykovski, 2003. Winter-time circulation and sediment transport in the Hudson Shelf Valley. *Continental Shelf Research*, 23, 801-820.
- Hoffman, E.E., Pietrafesa, L.J., and Atkinson, L.P., 1981. A Bottom Water Intrusion in Onslow Bay, NC. *Deep-Sea Research* 28(4), 329-345.
- Janowitz, G.S. and L.J. Pietrafesa, 1980. A model and observations of time-dependent upwelling over the mid-shelf and slope. *Journal of Physical Oceanography*, 10, 1574 – 1583.
- Lee T.N., V. Kourafalou, and J.D. Wang, 1985. Shelf Circulation from Cape Canaveral to Cape Fear during the winter, In: *Oceanography of the Southeastern U.S. Continental Shelf*, 33-62.
- Li, M.Z. and C.L. Amos, 1999. Field observations of bedforms and sediment transport thresholds of fine sand under combined waves and currents. *Marine Geology*, 158, 147-160.
- Lynch, J.F., J.D. Irish, T.F. Gross, P.L. Wiberg, A.E. Newhall, P.A. Traykovski, and J.D. Warren, 1997. Acoustic measurements of the spatial and temporal structure of the near-bottom boundary layer in the 1990-1991 STRESS experiment, *Continental Shelf Research*, 17, 1271-1295.
- Madsen, O., 1994. Spectral wave-current bottom boundary layer flows. In: *Coastal Engineering 1994, Proceedings (24<sup>th</sup> international conference)* Kobe, Japan, 384 – 397.

- Madsen, O.S., Wright, L.D., Boon, J.D., Chisholm, T.A., 1993. Wind stress, bed roughness and sediment suspension on the inner shelf during an extreme storm event. *Continental Shelf Research* 13, 1303-1324.
- Meyer-Peter, E. and Muller, R., 1948. Formulas for Bed-Load Transport. Report on the Second Meeting of International Association for Hydraulic Research, 39-64.
- Milliman, J.D., 1972. Atlantic continental shelf and slope of the United States; petrology of the sand fraction of sediments, northern New Jersey to southern Florida. Geological Survey professional paper 529-J.
- Niedoroda, A.W., D.J.P. Swift, and TS Hopkins, 1984. Shoreface morphodynamics on wave-dominated coasts. *Marine Geology*, 60, (1-4), 331-354.
- Ogston, A.S., Sternberg, R.W., 1999. Sediment-transport events on the northern California continental shelf. *Marine Geology* 154, 69-82.
- Pearson, D.K., and S.R. Riggs 1981. Relationship of surface sediments on the lower forebeach and nearshore shelf to beach nourishment at Wrightsville Beach, North Carolina. *Shore and Beach*, 49: 26-31.
- Pietrafesa, L.J., Morrison, J.M., McCann, M.P., Churchill, J., Boehm, E., and Houghton, R.W., 1994. Water mass linkages between the Middle and South Atlantic Bights. *Deep-Sea Research II* 41, 365-389.
- Pietrafesa, L.J., 1989. The Gulf Stream and Wind Events on the Carolina Capes Shelf. In: R.Y. George and A. W. Hulbert (Eds.), *North Carolina Coastal Oceanography Symposium*. National Undersea Research Program, NOAA, Rockville, MD, 89-129.
- Pietrafesa, L.J., G.S. Janowitz, and P.A. Wittman, 1985. Physical oceanographic processes in the Carolina Capes, In: *Oceanography of the Southeastern U.S. Continental Shelf*, 23-32.
- Pietrafesa, L.J., 1983. Survey of a Gulf Stream frontal filament, *Geophysical Research Letters*, 10, 203-206.
- Pietrafesa, L.J. and G.S. Janowitz, 1980. On the dynamics of the Gulf Stream front in the Carolina Capes. *Stratified Flows: The Second International Symposium on Stratified Flows*, Tapen Publishing Co., 184-197.
- Pietrafesa, L.J. and G.S. Janowitz, 1979. A note on the identification of a Gulf Stream spin-off eddy from Eulerian data, *Geophysical Research Letters*, 6, 549-552.
- Quattrini, A., 2002. Distribution of Larval Fishes in Shelf and Gulf Stream Waters in Onslow Bay, North Carolina. M.S. Thesis, University of North Carolina at Wilmington, Wilmington, NC, unpublished.

- Renaud, P.E., Ambrose Jr., W.G., Riggs, S.R., Syter, D.A., 1996. Multi-level effects of severe storms on an offshore temperate reef system: benthic sediments, macroalgae and implications for fisheries. *Marine Ecology* 17, 383-389.
- Renaud, P.E., Riggs, S.R., Ambrose Jr., W.G., Schmid, K., Snyder, S.W., 1997. Biological-geological interactions: storm effects on macroalgal communities mediated by sediment characteristics and distribution. *Continental Shelf Research* 17 (1), 37-56.
- Riggs, S.R., Ambrose, W.G., Jr., Cook, J.W., and Snyder, S.W., 1998. Sediment Production on Sediment-starved Continental Margins: The Interrelationship between Hard Bottoms, Sedimentological and Benthic Community Processes, and Storm Dynamics. *Journal of Sedimentary Research Section A: Sedimentary Petrology and Processes* 68(1), 135-148.
- Sherwood, C.R., Butman, B., Cacchione, D.A., Drake, D.E., Gross, T.F., Sternberg, R.W., Wiberg, P.L., Williams III, A.J., 1994. Sediment-transport events on the northern California continental shelf during the 1990–1991 STRESS experiment. *Continental Shelf Research* 14, 1063–1099.
- Singer, J.J., Atkinson, L.P., and Pietrafesa, L.J., 1980. Summertime Advection of Low Salinity Surface Waters into Onslow Bay. *Estuarine and Coastal Marine Science* 11, 73-82.
- Smith, J.D., 1977. Modelling of sediment transport on continental shelves: in *The Sea*, Vol. 6, E.D. Goldberg, I.N. McCave, J.J. O'Brien, and J.H. Steele, editors. Wiley-Interscience, New York, pp.539-577.
- Smith, J.D. and T.S. Hopkins, 1972. Sediment transport on the continental shelf off of Washington and Oregon in light of recent current measurements. In: *Shelf Sediment Transport: processes and pattern*, D.J.P. Swift, D.B. Duane and O.H. Pilkey, editors, Dowden, Hutchinson, and Ross, Stroudsburg, PA, pp. 143-180.
- Sontek/YSI Inc., 2003. "ADP Versatility in San Felipe, Mexico Deployment", <http://www.sontek.com/apps/profiler/adp-sf/adp-sf.htm>.
- Sternberg, R. W., 1986. Transport and accumulation of river-derived sediment on the Washington continental shelf, USA. *Journal of the Geological Society, London*, 143, 945-956.
- Storlazzi, C.D., Jaffe, B.E., 2002. Flow and sediment transport on the inner shelf of central California. *Marine Geology* 181, 195-213.
- Styles, R. and S.M. Glenn, 2000. Modeling stratified wave and current bottom boundary layers on the continental shelf. *Journal of Geophysical Research*, 105, 24,119-24,139.

- Styles, R. and S.M.Glenn, 2002. Modeling bottom roughness in the prescence of wave-generated ripples. *Journal of Geophysical Research*, 107, 1 –15.
- Swift, D.J.P., Niederoda, A.W., Christopher, E.V., Hopkins,T.S., 1985. Barrier Island Evolution, Middle Atlantic Shelf, U.S.A. Part I: Shoreface Dynamics. In:G.F. Oertel and S.P. Leatherman (Eds.), *Barrier Islands*. *Marine Geology* 63, 331-361.
- Thieler,E.R., P.T. Gayes, W.C. Schwab, and M.S. Harris, 1999. Tracing sediment dispersal on nourished beaches; two case studies. *Coastal Sediments: Proceedings of the International Symposium on Coastal Engineering and Science of Coastal Sediment Processes*. 4, Vol. 3; Pages 2118-2136. 1999.
- Thieler, R.E. W.C. Schwab, O.H. Pilkey, and W.J. Cleary 2001. Modern sedimentation on the shoreface an inner shelf at Wrightsville Beach, North Carolina. *Journal of Sedimentary Research* 71(6): 958-970.
- Traykovski, P., A. Hay, J.D. Irish, and J.F. Lynch, 1999. Geometry, migration, and evolution of wave orbital ripples at LEO-15. *Journal of Geophysical Research*, 104, 1505-1524.
- Washburn, L., Swenson, M.S., Largier, J.L., Korso, P.M., Ramp, S.R., 1993. Cross-Shelf Sediment Transport by an Anticyclonic Eddy Off Northern California. *Science* vol. 261, 1560-1564.
- Wiberg, P.L., 1995. A theoretical investigation of boundary layer flow and bottom shear stress for smooth, transitional, and rough flow under waves. *Journal of Geophysical Research*, 100, 22,667 – 22,679.
- Wiberg, P.L. and Harris, C.K., 1994. Ripple geometry in wave dominated environments, *Journal of geophysical Research*, 99(C4),775-789.
- Wikramanayake, P.N., 1993. Velocity profiles and suspended sediment transport, Ph.D. thesis, Mass. Inst. of Technol., Cambridge.
- Wikramanayake P.N. and O.S. Madsen, 1992. Calculation suspended sediment transport by combined wave and current flows, *Contract Report* DRP-92, 148pp., US Army Corps of Engineers Coastal Waterway Research Center, Vicksburg, MS.
- Wikramanayake, P.N. and ,O.S. Madsen, 1991. Calculation of moveable bed friction factors, *Technical Report* DACW-39-88-K-0047, 105pp., US Army Corps of Engineers Coastal Engineering Research Center, Vicksburg, MS.
- Williams, J.J., Rose, C.P., 2001. Measured and predicted rates of sediment transport in storm conditions. *Marine Geology* 179, 121-133.

- Wright, L.D., Kim, S.C., Friedrichs, C.T., 1999. Across-shelf variations in bed roughness, bed stress and sediment suspension on the northern California shelf. *Marine Geology* 154, 99-115.
- Wright, L.D., 1995. *Morphodynamics of Inner Continental Shelves*. CRC Marine Science Series, CRC Press, Boca Raton, FL.
- Wright, L.D., J.P. Xu, and O.S. Madsen, 1994. Across-shelf benthic transports on the inner shelf of the Middle Atlantic bight during the “Halloween storm” of 1991. *Marine Geology* 118, 61 – 71.
- Wright L.D., J.D. Boon, S.C. Kim, and J.H. List, 1991. Modes of cross-shore sediment transport on the shoreface of the Middle Atlantic Bight. *Marine Geology*, 96, 19-51.
- Wright L.D., J.D. Boon, M.O. Green, and J.H. List, 1986. Response of the mid-shoreface of the southern mid-Atlantic bight to a ‘Northeater’. *Geol.-marine Lett.*, 6, 153-160.
- Wren, P.A. and Lynn A. Leonard, 2002. Physical processes and sediment transport in Onslow Bay, NC. *Eos Trans. AGU*, 83(47), Fall Meet. Suppl., F690.
- Xie, L., Pietrafesa, L.J., Raman, S., 1997. Interaction between Surface Wind and Ocean Circulation in the Carolina Capes in a Coupled Low-order Model. *Continental Shelf Research* 17, 1483-1511.